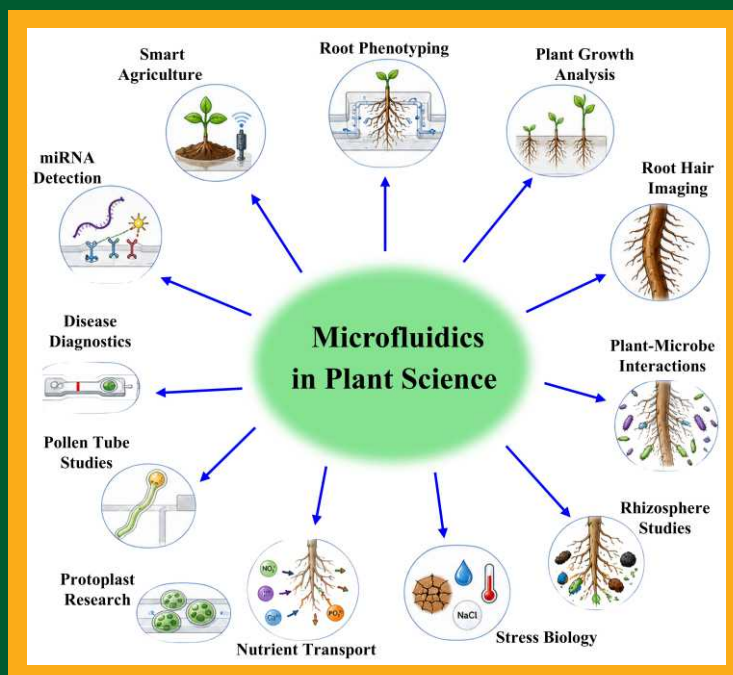


ISSN 0971 - 2976

# JOURNAL OF THE BOTANICAL SOCIETY OF BENGAL



Volume 80  
Number 1, June 2026



AN  
OFFICIAL ORGAN  
OF THE  
**BOTANICAL SOCIETY OF BENGAL**  
Estd. 1935

# BOTANICAL SOCIETY OF BENGAL

(Established in 1935)

Website : [www.botansocbengal.org](http://www.botansocbengal.org)

## Editor-in-Chief

**Subir Bera**, Centre of Advanced Study,  
Department of Botany, University of Calcutta,  
Kolkata, India  
e-mail: [editorjbsb@gmail.com](mailto:editorjbsb@gmail.com)

## Associate Editors

**Usha Chakraborty** (Retired Professor),  
Department of Botany, University of North  
Bengal, Siliguri, India  
e-mail: [ucnbu2012@gmail.com](mailto:ucnbu2012@gmail.com)

**Sandip Mukhopadhyay** (Retired Professor),  
Department of Botany, University of Calcutta,  
Kolkata, India  
e-mail: [sandip135@yahoo.com](mailto:sandip135@yahoo.com)

**Shyamal Kumar Chakraborty** (Retd.), Bidhan  
Nagar Govt. College, Kolkata, India  
e-mail: [skchakraborty040@gmail.com](mailto:skchakraborty040@gmail.com)

## Editorial Board

**Subhendu Mukherji** (Retired Professor),  
Department of Botany, University of Calcutta,  
Kolkata, India

**Radhanath Mukhopadhyay** (Retired  
Professor), Department of Botany, The  
University of Burdwan, Burdwan, India  
e-mail: [rnmburdwan@gmail.com](mailto:rnmburdwan@gmail.com)

**R.R. Rao**, INSA Honorary Scientist, No.328, B-  
4 Block, Kendriya Vihar, Yelahanka,  
Bangalore-560 064, India  
e-mail: [raocimap@gmail.com](mailto:raocimap@gmail.com)

**Arun Kumar Pandey**, Department of Botany,  
University of Delhi, Delhi-110007, India  
e-mail: [arunkpandey@botany.du.ac.in](mailto:arunkpandey@botany.du.ac.in) /  
[arunpandey79@gmail.com](mailto:arunpandey79@gmail.com)

**Ilor Ghosh**, School of Environmental  
Science, Jawaharlal Nehru University, India  
e-mail: [Ighosh@mail.jnu.ac.in](mailto:Ighosh@mail.jnu.ac.in) /  
[iloraghosh17@gmail.com](mailto:iloraghosh17@gmail.com)

**Amita Pal**, Bose Institute, P1/12, CIT Scheme  
VII M, Kankurgachi, Kolkata, India  
e-mail: [amita@jbose.ac.in](mailto:amita@jbose.ac.in)

**Kunal Mukhopadhyay**, Department of  
Bioengineering, Birla Institute of Technology,  
Mesra, Ranchi - 835 215  
e-mail: [kmukhopadhyay@bitmesra.ac.in](mailto:kmukhopadhyay@bitmesra.ac.in)

**Parimal Nag** (Retd.), Syamaprasad College,  
92, Dr. Syamaprasad Mukherjee Road,  
Kolkata-700026  
e-mail: [parimalnag4871@gmail.com](mailto:parimalnag4871@gmail.com)

## Editorial Advisors

**Cheng-Sen Li**, Institute of Botany, Chinese  
Academy of Science, Beijing  
e-mail: [lics@ibcas.ac.cn](mailto:lics@ibcas.ac.cn)

**Angela Bruch**, ROCEEH Research Centre,  
Senckenberg Research Institute, Frankfurt,  
Germany  
e-mail: [angela.bruch@senckenberg.de](mailto:angela.bruch@senckenberg.de)

**Jim Pringle**, Royal Botanical Garden,  
Hamilton, Ontario, Canada  
e-mail: [jpringle@rbg.ca](mailto:jpringle@rbg.ca)

**R.A. Spicer**, School of Environment, Earth and  
Ecosystem Sciences, The Open University,  
UK; Xishuangbanna Tropical Botanical  
Garden, Chinese Academy of Sciences, China  
e-mail: [r.a.spicer@open.ac.uk](mailto:r.a.spicer@open.ac.uk)

**Uma Sankar**, Department of Botany, North-  
Eastern Hill University, Shillong  
e-mail: [arshuma@nehu.ac.in](mailto:arshuma@nehu.ac.in) /  
[arshuma@yahoo.com](mailto:arshuma@yahoo.com)

**S.P. Adhikary**, Ex-Professor & Head, Dept. of  
Biotechnology, Visva-Bharati, Santiniketan,  
West Bengal  
e-mail: [adhikarysp@gmail.com](mailto:adhikarysp@gmail.com)

**D.K. Chauhan**, Department of Botany,  
University of Allahabad, U.P. India  
e-mail: [dkchauhanau@yahoo.com](mailto:dkchauhanau@yahoo.com)

**S.K. Borthakur**, Department of Botany,  
Gauhati University, Guwahati-781014  
e-mail: [skbgu1@gmail.com](mailto:skbgu1@gmail.com)

## Aims and Scope

Journal of the Botanical Society of Bengal has a long history of publishing articles since its inception. It is a peer reviewed, biannual journal. The aim of this journal is to encourage publication of scientific knowledge on any branch of plant science, basic and applied. The topics range from cryptogams to phanerogams,

morphology-anatomy, plant-microbe interaction, genomics and genetics, physiology and biochemistry, palaeobotany-palynology, plant molecular biology and biotechnology, embryology, systematics and other allied fields of plant sciences. Along with full articles, reviewed articles and short communications are also published.

## Copyright and permission

Authors submitting a manuscript for publication in the Journal of the Botanical Society of Bengal do the same on condition that if it is published in the Journal, exclusive copyrights of the paper shall be assigned to the Botanical Society of Bengal. The society will not put any limitation on the personal freedom of the author to use materials published in the paper in his/her furtherwork with due reference.

## Journal Website

[www.botansocbengal.org](http://www.botansocbengal.org)

## Publication Ethics

[www.publicationethics.org](http://www.publicationethics.org)  
<https://authorservices.wiley.com/ethics-guidelines/index.html>

Papers will be accepted only if they abide by the publication ethics and bioethics.

## Subscription Information

All communications should be addressed to the Secretary, Botanical Society of Bengal, Department of Botany, University of Calcutta, 35 Ballygunge Circular Road, Kolkata 700019. The subscription price is Rs.2000.00 per volume (two numbers in a year) in India including ordinary Book Post charge. The subscription for foreign countries is US \$ 500.00 per volume, including air mail charges.

## Office of Publication

Department of Botany, University of Calcutta,  
35, Ballygunge Circular Road, Kolkata 700019,  
West Bengal, India

The figure in the cover page showing : Schematic overview of the applications of microfluidics in plant science in the article by Agarwal *et al.*, *J. Bot. Soc. Bengal*, 80(1): 1-15, 2026

## *Guest Editorial*

### **4th BOTANICAL CONGRESS, 2026**

The 4th Botanical Congress 2026 was successfully organized from 26th to 28th March 2026 by Raja Narendralal Khan Women's College (Autonomous), Gope Palace, Medinipur, in collaboration with the Botanical Society of Bengal. The event aimed to bridge foundational botanical knowledge with cutting-edge advancements in different branches of plant science. The primary objectives of the Congress were 1. To promote interdisciplinary research in plant sciences 2. To provide a platform for the dissemination of recent scientific advancements 3. To encourage the participation of students and young researchers 4. To facilitate collaboration among academic and research institutions 5. To integrate classical and modern approaches in botanical research.



The Congress featured six major thematic areas. Each theme was explored through dedicated technical sessions, including invited keynote lectures, invited lectures, oral presentations, and interactive discussions. • Theme 1: Cryptogamic World, Systematics and Evolution. • Theme 2: Medicinal Plants, Drug Discovery, and Biotechnology. • Theme 3: Genetics, Embryology, and Tissue Culture. • Theme 4: Food Science and Human Nutrition. • Theme 5: Plant–Microbe Interaction, Biogeography, and Climate Change. • Theme 6: Plant Physiology, Biochemistry, and Plant-Based Innovations.

The Congress commenced with a grand inaugural ceremony on 26th March 2026, marking the beginning of a

vibrant three-day academic gathering. The event was graced by eminent dignitaries from the academic fraternity. The Hon'ble Vice-Chancellor of Vidyasagar University, Prof. Dipak Kumar Kar, presided as the Inaugurator, while Prof. Arnab Sen, Hon'ble Vice-Chancellor of Raiganj University, attended as the Chief Guest. Dr. Swapna Ghorai, Principal, Raja Narendralal Khan Women's College (Autonomous), delivered the welcome address and highlighted the core objectives of the Congress, emphasizing its role in fostering academic dialogue, encouraging interdisciplinary research, and promoting innovation in plant sciences. The President of the Botanical Society of Bengal (BSB), Prof. Prabir Kumar Saha, provided a comprehensive overview of the organization's history, achievements, and ongoing initiatives, while the Secretary, Prof. Santanu Paul, highlighted the urgent need to integrate traditional botanical knowledge with modern approaches, including computational biology and molecular techniques. The Convener, Dr. Rashmi Mukherjee, delivered a heartfelt address acknowledging the invaluable contributions of collaborating institutions, delegates, participants, organizing members and funding agencies, expressing sincere gratitude and highlighting the collaborative spirit behind the event.

Series of high-impact technical sessions were inaugurated by eminent speakers and dignitaries. Prof. N.D. Paria Memorial Lecture was delivered by Dr. Sudhansu Sekhar Dash, Scientist – F, Additional Director and the Head of Technical Division, Botanical Survey of India who in his address, emphasized the need to modernize taxonomy through interdisciplinary collaboration. A Thalassemia awareness session by Dr. Ramendu HomChaudhuri, (Eminent Orthopedic Surgeon & District Governor, Rotary International District:3291) which aimed to dispel common myths surrounding thalassemia and provided participants with up-to-date knowledge on management strategies, preventive measures, and lifestyle considerations for the affected individuals. Almost 50 school students from eight institutions, were invited to participate in specially curated outreach programs designed to make botanical science accessible, engaging, and inspiring. Two popular lectures were delivered by Prof. Alok Bhattacharya, Professor (Retd.), Department of Botany, University of Burdwan, and Prof. Debdulal Banerjee, Professor, Department of Botany & Forestry, Vidyasagar University, Midnapore. All the technical sessions of the Botanical Congress featured oral presentations by participants across the respective thematic areas. A separate segment of poster presentations was arranged for postgraduate students, for encouraging their scientific temperament at the onset of their academic journey.

The 4th Botanical Congress, 2026, concluded on a solemn and celebratory note with a formal valedictory session, to reflect upon the key achievements, outcomes, and overall impact of the Congress. Participants, guests and members of the organizing committee shared their observations and experiences, highlighting the academic richness and intellectual diversity that characterized the Congress. Certificates and prizes were distributed to participants, presenters, and young scientists in recognition of their valuable contributions to the success of the Congress. Outstanding oral and poster presentations were specially acknowledged and awarded.

The successful organization of the Congress was made possible through the generous support of funding agencies, including ANRF, BSI, and the Botanical Society of Bengal. Their financial and institutional support ensured the smooth execution of the event and participation of a wide range of delegates. The organizing committee expressed gratitude to all sponsors and collaborators for their valuable contributions. The Congress concluded successfully, leaving a lasting impression on all participants.

**Professor Santanu Paul**  
Secretary  
Botanical Society of Bengal

---

**REVIEW ARTICLE**

---

**Microfluidics in plant science: emerging technologies and applications**

---

**Kaushal Agarwal<sup>1</sup>, Dhruvkumar H. Wankawala<sup>2</sup>, Giridhar Raveendar<sup>2</sup>, Sudha Gupta<sup>3</sup> and Pranab Kumar Mondal<sup>1,2,\*</sup>**

<sup>1</sup>School of Agro and Rural Technology, Indian Institute of Technology Guwahati, Guwahati, 781039, India

<sup>2</sup>Microfluidics and Microscale Transport Processes Laboratory, Department of Mechanical Engineering, Indian Institute of Technology Guwahati, Guwahati, 781039, India

<sup>3</sup>Department of Botany, University of Kalyani, Kalyani-741235, West Bengal, India

---

Received : 14.06.2025

Accepted : 25.06.2026

Published : 30.06.2026

---

Microfluidics, which involves the precise manipulation of fluid volumes ranging from microliters to picoliters within microscale channels has emerged as a transformative technology in plant science research. By enabling accurate control of cellular and environmental conditions, microfluidic platforms provide unprecedented opportunities to investigate plant growth, development, and physiological responses to environmental stimuli. Recent advances have led to the development of specialized microfluidic platforms, including RootChip, RootArray, TipChip, and PlantChip, which offer high-throughput experimental capabilities while addressing several limitations associated with conventional plant cultivation and analysis methods. These platforms have significantly enhanced the study of plant-microbe interactions, chemical signalling, nutrient uptake and transport, as well as plant responses to biotic and abiotic stresses under precisely regulated conditions. Moreover, microfluidic technologies have expanded the scope of plant phenotyping by facilitating real-time monitoring of plant behaviour and enabling the simulation of complex environmental scenarios, such as dynamic flow regimes and microgravity conditions. This review particularly provides a comprehensive overview of microfluidic technologies used in plant science, highlights their major applications and recent developments, and discusses the current challenges and future research directions that must be addressed to fully realize their potential in next-generation agricultural innovation.

**Keywords:** Microfluidics, Plant science, Lab-on-a-chip, Plant-microbe interactions, Root phenotyping, Microscale transport, Stress biology.

---

\*Corresponding author : mail2pranab@gmail.com  
pranabm@iitg.ac.in

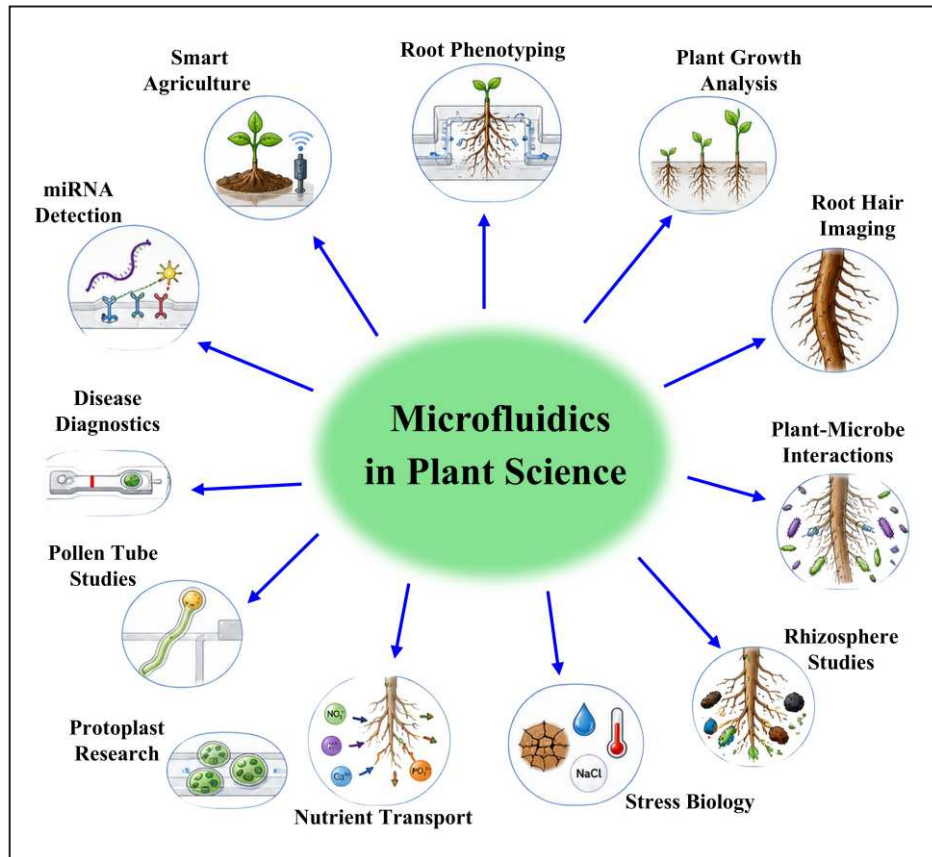
## INTRODUCTION

Microfluidics has emerged as a versatile technology for experimental plant biology, offering unprecedented opportunities over microscale environments and enabling detailed investigation of plant cellular processes and plant-environment interactions (Elitaş *et al.*, 2017; Kaiser *et al.*, 2023; Marczakiewicz-Perera *et al.*, 2026). These systems provide a unique platform for reproducing physiologically relevant microenvironments, allowing real-time observation of plant cells, tissues, and organs under well-defined conditions (Agarwal *et al.*, 2024a; Ali *et al.*, 2020; Alla *et al.*, 2026; Aryal *et al.*, 2024; Cohen *et al.*, 2026; Liu *et al.*, 2022; Mahesh and Vaidya, 2017; Sanati Nezhad, 2014). To address diverse experimental requirements, a wide range of specialized microfluidic platforms has been developed. Systems such as RootChip, RootArray, TipChip, PlantChip, and various other Lab-on-a-Chip (LOC) devices have significantly advanced plant biology research by overcoming many limitations of conventional experimental approaches and enabling high-resolution analysis of plant tissues and developmental processes (Agudelo *et al.*, 2012; Agudelo *et al.*, 2013; Allan *et al.*, 2023, 2024; Fendrych *et al.*, 2018; Ghanbari *et al.*, 2014; Grossmann *et al.*, 2011, 2012; Jiang *et al.*, 2014; Mao *et al.*, 2010; Naghavi, 2014; Parashar and Pandey, 2011; Song *et al.*, 2019; Stanley *et al.*, 2018; Zhao *et al.*, 2026). These platforms have been widely employed for root imaging, root hair characterization, pollen tube growth studies, analysis of plant-microbe interactions, stress response monitoring, protoplast observation, and live-cell imaging under controlled microfluidic conditions (Fig. 1) (Agudelo *et al.*, 2012; Agudelo *et al.*, 2013; Aufrecht *et al.*, 2017, 2018; Bascom *et al.*, 2016; Grossmann *et al.*, 2011, 2012; Khan *et al.*, 2019; Kozgunova and Goshima, 2019; Massalha *et al.*, 2017b; Meier *et al.*, 2010; Vang *et al.*, 2018; Yanagisawa *et al.*, 2021).

Among the numerous advantages offered by microfluidic systems, the ability to generate stable, reproducible, and precisely controlled concentration gradients within microchannels is particularly significant. This capability enables detailed

investigations of plant responses to environmental stimuli, providing valuable insights into the mechanisms by which plants perceive, integrate, and respond to external signals (Amir Sanati Nezhad *et al.*, 2014). Recent studies have demonstrated that fluid flow dynamics and microenvironmental conditions can directly influence root growth, nutrient uptake, and stress adaptation. Microfluidic platforms have therefore become indispensable for examining root responses to hydrodynamic forces, xylem-associated transport processes, and porous environments under well-defined and reproducible conditions (Agarwal *et al.*, 2024a; Kalita *et al.*, 2025; Mandal *et al.*, 2023; Padhi *et al.*, 2024; Panja *et al.*, 2024a). Beyond studying physical and chemical gradients, microfluidic systems also provide a multipurpose framework for evaluating plant responses to changes in nutrient availability, temperature, and biotic/abiotic stress factors. Their capacity for precise environmental control, real-time monitoring, and parallel experimentation enables higher throughput analyses compared with conventional methodologies (Neethirajan *et al.*, 2011, 2018; Noirot-Gros *et al.*, 2020a).

Microfluidic technologies have also greatly advanced the study of plant-microbe interactions (Aufrecht *et al.*, 2018; Gao *et al.*, 2018; Massalha *et al.*, 2017a; Yee *et al.*, 2021). The precise regulation of fluid flow, nutrient availability, and signalling molecules within microfluidic devices enables controlled investigation of chemical signalling and biological processes underlying symbiotic and pathogenic relationships. This facilitates detailed analysis of interaction dynamics under highly reproducible experimental conditions (Meier *et al.*, 2010). In addition to their utility in interaction studies, microfluidic platforms have gained considerable importance for plant phenotyping (Aufrecht *et al.*, 2017; Busch *et al.*, 2012; Chen *et al.*, 2025; Clark *et al.*, 2020; Guichard *et al.*, 2020; Jabusch *et al.*, 2021; Sozzani *et al.*, 2014; Vang *et al.*, 2018; Yanagisawa *et al.*, 2021). For example, devices such as PlantChip have provided efficient and cost-effective framework for phenotyping studies in model plants like *Arabidopsis* (Jiang *et al.*, 2014; Sun *et al.*, 2021). Beyond phenotyping applications, the adaptability of microfluidic systems has enabled the



**Fig. 1.** Schematic overview of the diverse applications of microfluidics in plant science. Microfluidic platforms enable precise control of the plant microenvironment and facilitate investigations across multiple research domains, including root phenotyping, plant growth analysis, root hair imaging, plant-microbe interactions, rhizosphere studies, stress biology, nutrient transport, protoplast research, pollen tube studies, disease diagnostics, microRNAs detection, and smart agriculture.

simulation of specialized environmental conditions, including microgravity conditions, thereby facilitating investigations into plant growth under extreme environmental constraints (Du *et al.*, 2022). Such innovations have expanded the scope of plant research by creating new opportunities in sustainable agriculture and environmental management (Kamat *et al.*, 2023; Zhao *et al.*, 2024).

Recent developments have further broadened the scope of plant microfluidics to encompass sensing, diagnostics, transport studies, and smart agriculture applications. Emerging platforms include nutrient monitoring devices, microRNA (miRNAs) detection systems, plant disease diagnostic tools, soil-on-a-chip technologies, and phytofluidic devices designed to investigate flow mediated plant responses under

controlled environmental setting (Fig. 1) (Agarwal *et al.*, 2024a; Cohen *et al.*, 2026; Gao *et al.*, 2018; Kamat *et al.*, 2023; Kawakatsu *et al.*, 2024; Stanley *et al.*, 2018; Zhao *et al.*, 2024). Moreover, microfluidic systems are increasingly being explored for hydroponic cultivation and sustainable plant production, where controlled flow regimes, intermittent nutrient delivery, and plasma assisted growth environments have been shown to enhance root development and overall plant performance (Padhi *et al.*, 2024; Panja *et al.*, 2024a).

In this review article, we primarily discuss the evolution of microfluidic technologies for plant research, major fabrication approaches and material considerations, and the diverse applications of microfluidic platforms in plant biology. We further

highlight representative microfluidic systems and their contributions to phenotyping, cellular studies, plant-microbe interactions, rhizosphere research, and reproductive biology. Finally, we examine the current challenges, emerging technological developments, and future research opportunities that may shape the continued advancement of plant microfluidics in both fundamental research and agricultural applications.

## SIGNIFICANCE AND POTENTIAL OF MICROFLUIDICS IN PLANT RESEARCH

One of the key strengths of microfluidic platforms is their ability to establish well-defined spatial and temporal gradients of nutrients, hormones, and signalling molecules (Aufrecht *et al.*, 2017; Sakai *et al.*, 2019). Such control enables systematic studies of signal transduction, environmental adaptation, and developmental regulation. These platforms have facilitated real-time imaging and monitoring of root growth, root hair development, calcium signalling, osmotic stress responses, and other dynamic physiological processes (Allan *et al.*, 2023; Aufrecht *et al.*, 2017; Grossmann *et al.*, 2012; Khan *et al.*, 2019; Sun *et al.*, 2021). Microfluidic systems further enhance experimental efficiency through automation and miniaturization. The incorporation of components such as micropumps, microvalves, and programmable control modules allows automated fluid handling while reducing reagent consumption (Song *et al.*, 2024). Consequently, experimental workflows become more efficient, reproducible, and scalable, supporting high-throughput screening in plant research (Agarwal *et al.*, 2024a).

Microfluidic systems also offer opportunities to optimize nutrient delivery in hydroponic cultivation systems. Controlled flow regimes have been shown to improve nutrient transport and support root development under regulated environments (Padhi *et al.*, 2024; Panja *et al.*, 2026). Another important application lies in the study of plant-microbe interactions. Microfluidic platforms provide controlled environments for investigating rhizosphere dynamics, microbial colonization, chemical communication, and root-associated signalling processes (Aufrecht *et al.*, 2018; Gao *et al.*, 2018;

Massalha *et al.*, 2017a; Noirot-Gros *et al.*, 2020a; Yee *et al.*, 2021). The ability to visualize these interactions in real time has improved understanding of both beneficial symbioses and pathogenic interactions (Aufrecht *et al.*, 2018; Massalha *et al.*, 2017a; Walton *et al.*, 2022). In addition, microfluidic technologies have significantly improved plant phenotyping and diagnostics capabilities (Sozzani *et al.*, 2014). Devices such as RootChip enable continuous observation of growth and stress responses, supporting rapid and largescale phenotypic analyses in model plants (Grossmann *et al.*, 2012; Jiang *et al.*, 2014). More recently, microfluidic diagnostic devices have enabled sensitive detection of plant biomarkers, including microRNAs, nutrients, and disease associated signals from plant extracts using minimal sample volumes (Kawakatsu *et al.*, 2024).

Microfluidic technologies are also expanding the scope of plant diagnostics. These platforms provide rapid and sensitive tools for monitoring plant physiological status, stress responses, and molecular biomarkers using minimal sample volumes. Recent advances include portable microfluidic sensing devices for microRNA detection, nutrient analysis, and disease diagnostics, enabling efficient and minimally invasive plant monitoring (Kamat *et al.*, 2023; Kawakatsu *et al.*, 2024; Zhao *et al.*, 2024). Alongside diagnostics, modular microfluidic bioreactors facilitate investigations of cell-cell interactions, metabolic compartmentalization, and other systems level processes (Dubey *et al.*, 2023).

Overall, microfluidic approaches provide a versatile framework for studying plant functions across multiple biological scales. Their ability to combine environmental control, high-resolution observation, automation, and analytical integration positions them as a promising next-generation technology for plant research. These capabilities also support agricultural innovations aimed at improving crop productivity, stress resilience, and sustainable resource management.

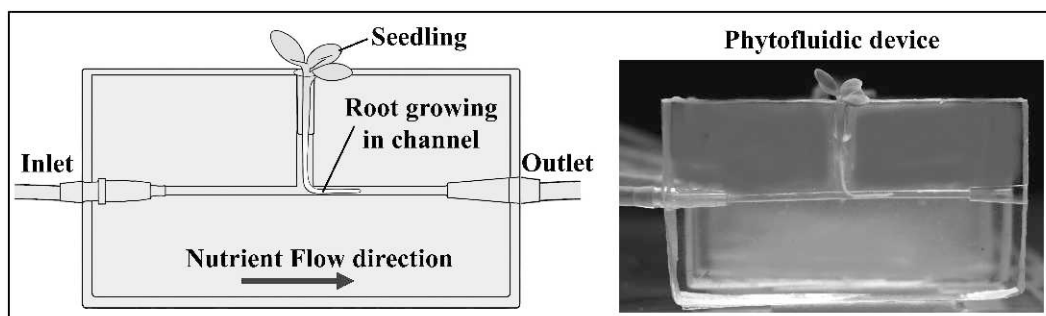
## EVOLUTION OF MICROFLUIDIC TECHNOLOGIES FOR PLANT RESEARCH

Microfluidic technology emerged from advances in microelectromechanical systems (MEMS) and miniaturized analytical devices originally developed for chemical and biomedical applications. These platforms integrate microscale components such as microchannels, reservoirs, valves, and pumps to manipulate extremely small fluid volumes with high precision. Their ability to regulate chemical and physical conditions within confined spaces made them attractive tools for biological research (Mahesh and Vaidya, 2017; Amir Sanati Nezhad *et al.*, 2014). The development of droplet-based microfluidics further expanded the field by enabling compartmentalization of individual cells and biomolecules, thereby supporting high-throughput analysis and screening applications (Seemann *et al.*, 2012). The early success of microfluidics was largely associated with studies involving bacterial, insect, and mammalian cells, while plant-related applications remained relatively limited (Branch *et al.*, 2001; Chang *et al.*, 2003; Leclerc *et al.*, 2004; Leclerc *et al.*, 2003; Walker *et al.*, 2002). Prior to the adoption of microfluidics, plant research relied heavily on conventional cell culture techniques, including feeder layer and nurse cultures. Although effective, these approaches required large volumes of media, extensive laboratory space, and offered limited control over microenvironmental conditions. The emergence of microfluidics provided a more efficient alternative, enabling controlled experimentation with small cell populations under continuous flow conditions and more *in vivo* like environments (Naghavi, 2014).

The first notable applications in plant science focused on isolated plant cells and protoplasts. A landmark study demonstrated the successful culture of *Nicotiana tabacum* protoplasts within PDMS based microchannels under continuous nutrient flow, establishing the feasibility of microfluidic cultivation for plant systems (Ko *et al.*, 2006). These experiments showed that microscale environments could sustain plant cell growth while providing enhanced control over cellular surroundings. Consequently, microfluidics began to attract interest as a platform for

plant physiological and genetic investigations. As the technology matured, researchers extended its use beyond single-cell studies to a broader range of plant processes. Microfluidic devices were adapted for root imaging, pollen tube growth studies, root hair analysis, and live-cell monitoring within microfluidic environments (Agudelo *et al.*, 2012; Agudelo *et al.*, 2013; Aufrecht *et al.*, 2017; Ghanbari *et al.*, 2014; Meier *et al.*, 2010; Vang *et al.*, 2018). Additionally, microfluidic platforms were developed for in-chip seed germination and seedling growth, which helped extending microfluidic investigations from individual cells to whole-plant systems. Early microfluidic studies often employed customized parallel-plate flow chambers coupled with microscopy. While these systems provided valuable insights, their technical complexity and need for specialized expertise restricted widespread adoption. This limitation stimulated the development of dedicated simpler plant oriented microfluidic platforms designed for routine biological studies.

A major transition occurred with the development of dedicated plant microfluidic devices such as RootChip, TipChip, and Lab-on-a-Chip systems (Agudelo *et al.*, 2013; Grossmann *et al.*, 2011; Meier *et al.*, 2010). Their emergence marked a shift from adapting existing microfluidic tools to creating devices specifically tailored for plant biology. Subsequent innovations broadened the scope of plant microfluidics. New platforms facilitated long-term cultivation, moss studies, and advanced protoplast experimentation (Bascom *et al.*, 2016; Kozgunova and Goshima, 2019; Sakai *et al.*, 2019; Yanagisawa *et al.*, 2021). At the same time, device architectures became increasingly sophisticated, allowing investigations of nutrient transport, fluid movement through porous structures, root biomechanics, and responses to abiotic stress (Agarwal *et al.*, 2024a; Kalita *et al.*, 2025; Marczakiewicz-Perera *et al.*, 2026; Nezhad *et al.*, 2014). Recent developments have focused on reproducing environmental complexity more realistically. Dual-flow microfluidic systems now permit independent treatments on either side of a root, providing new opportunities to investigate signalling pathways and localized physiological responses, including calcium mediated processes (Allan *et al.*,



**Fig. 2.** Schematic illustration and corresponding actual photograph of the phytofluidic device (Agarwal *et al.*, 2024b). A seedling is positioned with its root growing inside the microchannel, while nutrient solution flows from the inlet to the outlet under controlled flow conditions.

2023, 2024). In parallel, ecosystem-inspired platforms such as soil-on-a-chip and EcoFAB have incorporated features of natural soil habitats, including microbial interactions and spatial heterogeneity (Gao *et al.*, 2018).

In the latest developments, obstacle-based microfluidic platforms have been developed to examine how roots grow under mechanical constraints, providing insights into plant mechanosensing (Singh *et al.*, 2021; Zhang *et al.*, 2025). More recently, the concept of 'phytofluidic device' has been introduced to describe on-chip microfluidic systems specifically engineered for plant studies (Fig. 2), particularly those examining nutrient flow dynamics and stress responses under controlled hydraulic conditions (Agarwal *et al.*, 2024a). A further key emerging direction in plant microfluidics is the incorporation of artificial intelligence (AI) and machine learning (ML) into microfluidic workflows. These approaches facilitate automated image processing, pattern recognition, and predictive analysis of plant responses, reducing manual intervention while improving analytical efficiency (Dong *et al.*, 2024; Zhou *et al.*, 2025). Simultaneously, the integration of sensing technologies enables continuous tracking of physiological parameters and detect molecular biomarkers such as microRNAs, associated with plant growth, nutrient status, and stress responses within microfluidic environments (Kamat *et al.*, 2023; Kawakatsu *et al.*, 2024). Advances in biofabrication and micro/nanorobotic technologies are further

expanding the functionality of these systems. Such innovations improve operational precision and allow dynamic interactions within microscale experimental conditions (Dong *et al.*, 2024; Zhou *et al.*, 2025).

Overall, plant microfluidics has progressed from simple microscale culture systems to highly specialized experimental platforms. Through continued integration of realistic growth environments, porous media, dual flow architectures, and root-substrate interaction models, microfluidic technology is increasingly supporting investigations that closely reflect natural plant conditions.

## FABRICATION METHODS AND MATERIAL CONSIDERATIONS FOR MICROFLUIDIC DEVICES

The performance and functionality of microfluidic devices depend largely on the fabrication method used to create their microscale features. A variety of manufacturing techniques have been developed to produce channels, chambers, and interconnected networks with precise dimensions and geometries. Among these, soft lithography has become the most commonly employed approach, particularly for research scale applications. This method typically involves generating a patterned master mould through photolithography, followed by casting of polydimethylsiloxane (PDMS) to replicate the desired microstructures. The widespread use of PDMS is attributed to its transparency, flexibility, gas permeability, and compatibility with biological samples. Several alternative fabrication methods are

**Table 1.** Comparison of commonly used fabrication methods for microfluidic devices.

<b>Fabrication method</b>	<b>Advantages</b>	<b>Limitations</b>	<b>Typical applications</b>
Soft lithography	Optical transparency and biocompatibility	Limited scalability and mould dependent fabrication	Most PDMS based plant microfluidic devices
Photolithography	High resolution and precise patterning	Requires cleanroom facilities	Fabrication of complex microstructures
Laser ablation	Rapid prototyping and flexible design modification	Moderate resolution and possible surface roughness	Custom microfluidic device fabrication
Injection moulding	High reproducibility and mass production capability	High initial tooling cost	Commercial scale production of devices
3D printing	Rapid fabrication, design flexibility, and customization	Generally lower resolution than lithographic methods	Rapid prototyping and customized devices

also used depending on the intended application. Photolithography offers excellent spatial resolution and is suitable for producing complex microscale patterns. Laser based fabrication techniques provide rapid design modification and accelerated prototyping. In contrast, injection moulding and thermoplastic processing are better suited for large volume manufacturing as they provide high reproducibility and support industrial scale production.

The emergence of three-dimensional (3D) printing has introduced additional flexibility into microfluidic device fabrication. Unlike conventional mould based approaches, 3D printing enables direct production of customized architectures with reduced fabrication time and lower design constraints. This capability has facilitated the development of complex microfluidic structures tailored to specific biological applications. Recent studies have explored a range of innovative fabrication concepts, including 3D printed root observation systems, paper-based microfluidic platforms, colloidal lithography, modular microfluidic

assemblies, and nanochannel integrated devices (Adamski *et al.*, 2016; Ismayeel *et al.*, 2024; Moussus and Meier, 2021; Zemmour *et al.*, 2025). These approaches aim to improve device customization, imaging performance, flow control, and experimental versatility within plant microfluidics.

Material selection represents another important aspect of device fabrication. Commonly used materials include glass, silicon, PDMS, and various thermoplastics, each offering distinct physical and chemical properties. The choice of material is generally determined by factors such as optical requirements, mechanical durability, chemical compatibility, gas exchange characteristics, and biological suitability. A comparison of commonly used fabrication methods is presented in Table 1. Although soft lithography remains the preferred technique for many plant microfluidic applications because of its simplicity and compatibility with living tissues, recent advances in 3D printing and thermoplastic manufacturing are broadening the options available for rapid prototyping and scalable

Table 2. Representative microfluidic platforms used in plant research.

Platform	Plant species	Key applications	Key features	Major limitations	Reference
RootChip	<i>Arabidopsis thaliana</i>	Root imaging and chemical stimulation studies	Controlled chemical delivery and live imaging	Limited environmental realism	(Grossmann <i>et al.</i> , 2011)
RootArray	<i>Arabidopsis thaliana</i>	Root phenotyping and growth analysis	Parallel root cultivation, high-throughput screening	Primarily developed for model plants	(Busch <i>et al.</i> , 2012)
PlantChip	<i>Arabidopsis thaliana</i>	Plant growth monitoring and phenotyping	Automated cultivation and continuous monitoring	Limited suitability for long-term cultivation	(Jiang <i>et al.</i> , 2014)
TipChip	<i>Lilium longiflorum</i> , <i>Nicotiana tabacum</i>	Pollen tube and tip-growing cell studies	Precise control of guidance cues and confined growth environments	Restricted to tip-growing cells	(Carlos G. Agudelo <i>et al.</i> , 2013)
Dualflow RootChip	<i>Arabidopsis thaliana</i>	Localized stimulation and signalling studies	Independent treatment of opposite root sides	Complex device fabrication, operation	(C. Stanley <i>et al.</i> , 2018)
RMIChip	<i>Arabidopsis thaliana</i>	Root-microbe interaction studies	Live imaging of microbial colonization and rhizosphere interactions	Simplified representation of rhizosphere conditions	(Massalha <i>et al.</i> , 2017)
EcoFAB	<i>Brachypodium distachyon</i> , <i>Arabidopsis thaliana</i>	Plant-microbe and ecosystem studies	Controlled ecosystem and microbiome studies	Limited ecological complexity	(Gao <i>et al.</i> , 2018)
Moss imaging platform	<i>Physcomitrium patens</i>	Moss growth and cellular imaging	Long-term cultivation and high-resolution microscopy	Species-specific application	(Kozgunova and Goshima, 2019)
Root hair microfluidic platform	<i>Arabidopsis thaliana</i>	Root hair development and stress response studies	High-resolution imaging of root hair dynamics	Limited applicability to whole-plant analyses	(Aufrecht <i>et al.</i> , 2017)
Synthetic soil platform	<i>Arabidopsis thaliana</i>	Root-soil interaction studies	Soil-like porous architecture	Limited representation of soil complexity	(Orebaugh <i>et al.</i> , 2026)
PRFD (Phytofluidic device)	<i>Brassica juncea</i> , <i>Oryza sativa</i>	Nutrient flow mediated stress and root response studies	Controlled flow environment and real-time root monitoring	Early stage development with limited validation	(Agarwal <i>et al.</i> , 2024a; Panja <i>et al.</i> , 2026)

device production.

## APPLICATIONS OF MICROFLUIDIC TECHNOLOGIES IN PLANT RESEARCH

Microfluidic technologies have facilitated advances across multiple domains of plant biology, from phenotyping and cellular studies to ecological interactions and stress physiology. To address different biological questions, numerous plant microfluidic platforms have been developed with distinct designs and functionalities. These devices vary in terms of plant species studied, target tissues, experimental objectives, and analytical capabilities. Table 2 summarizes representative plant microfluidic platforms, highlighting their principal applications, key features, limitations, and selected references. The major application areas and representative case studies associated with these platforms are discussed in the following sections.

### Plant-microbe interactions and environmental response

Microfluidic platforms have provided new opportunities to investigate plant-associated microbial communities under predefined experimental conditions that mimic natural systems such as the rhizosphere and xylem. By recreating microscale habitats surrounding plant tissues, these systems enable direct observation of microbial establishment, movement, and persistence in the vicinity of roots. Such capabilities have improved understanding of how microorganisms colonize plant surfaces and interact with host tissues over time (Meier *et al.*, 2010; Neethirajan *et al.*, 2011). Several studies have employed microfluidic devices to visualize root associated microbial behaviour in real time. These investigations have revealed patterns of bacterial attachment, biofilm formation, microbial competition, and metabolite mediated interactions within rhizosphere-like environments that are difficult to resolve using conventional approaches (Aufrecht *et al.*, 2018; Massalha *et al.*, 2017a; Noiro-Gros *et al.*, 2020b). For example, microfluidic imaging systems have enabled direct observation of bacterial colonization processes under controlled chemical gradients, providing insights into microbial responses

to localized environmental cues (Noiro-Gros *et al.*, 2020a).

Microfluidic technologies have also been applied to examine plant responses to environmental heterogeneities such as nutrient gradients, drought, salinity, and temperature variation. These capabilities enable systematic investigation of plant stress responses at both cellular and whole-plant levels, improving our understanding of plant adaptation and resilience. Devices incorporating porous matrices, confined channels, and structured growth media have further facilitated investigations of root navigation, substrate exploration, and adaptation to physical constraints (Kalita *et al.*, 2025; Panja *et al.*, 2024). On and above biological interactions, microfluidic systems have contributed to studies of transport processes relevant to plant function. Investigations on xylem inspired architectures and electrohydrodynamic phenomena have provided useful models for examining fluid movement, and transport pathways in plant related systems (Dbouk and Drikakis, 2024; Kalita *et al.*, 2025).

### Microfluidics platforms for rhizosphere and ecosystem studies

Microfluidic platforms have increasingly been employed to recreate simplified plant associated ecosystems under controlled laboratory conditions. Devices such as EcoFAB and soil-on-a-chip integrate plant roots, microbial communities, and defined physicochemical environments within a single experimental framework, enabling systematic investigation of rhizosphere processes (Gao *et al.*, 2018). These platforms have facilitated direct observation of microbial colonization, microbial community dynamics, and metabolite exchange in the vicinity of plant roots (Massalha *et al.*, 2017b; Noiro-Gros *et al.*, 2020). To improve ecological relevance, researchers have developed synthetic soil systems, porous media platforms, and specialized growth chambers that more closely mimic the structural complexity of natural rhizosphere environments. These systems support studies of microbial interactions, spatial heterogeneity, root-substrate relationships, and nutrient distribution under controlled yet biologically meaningful conditions

(Behera *et al.*, 2025; Gao *et al.*, 2018; Orebaugh *et al.*, 2026; Yee *et al.*, 2021). More recent developments have further enhanced the ability to investigate plant-microbiome assembly at high spatial resolution. For example, the Arabidopsis Root Microbiome Microfluidic (ARMM) device enables simultaneous high-resolution imaging of microbial community assembly and root morphogenesis, offering new insights into the dynamic interactions between plants and their associated microbiota.

### Reproductive biology and future implications

Compared with other areas of plant research, the application of microfluidics to reproductive biology remains at an early stage. Nevertheless, these technologies have provided useful experimental platforms for examining key reproductive events, particularly pollen germination and pollen tube development. Several studies have demonstrated successful cultivation and tracking of pollen tubes within microfluidic devices, revealing growth patterns comparable to those observed under conventional experimental conditions (Agudelo *et al.*, 2012; Ghanbari *et al.*, 2014; Naghavi, 2014; Nezhad *et al.*, 2014). The microscale architecture of these systems allows precise positioning of pollen grains and controlled delivery of chemical gradient, facilitating investigations of elongation dynamics, guidance mechanisms, and mechanical properties of tip-growing cells. Additional studies have examined how pollen tubes respond to spatial constraints and mechanical obstacles (Agudelo *et al.*, 2012; Ghanbari *et al.*, 2014; Yanagisawa *et al.*, 2018). Such studies have provided insights into the adaptive behaviour of tip-growing cells during navigation through restricted environments. Moreover, advanced microfluidic platforms have enabled simultaneous analysis of multiple pollen tubes, supporting quantitative assessment of guidance behaviour and force generation with improved experimental throughput (Shamsudhin *et al.*, 2016).

Although current applications are concentrated primarily on pollen biology, the versatility of microfluidic systems suggests broader opportunities for reproductive research. Future developments may

focus on the investigations of pollen-pistil interactions, fertilization processes, reproductive signalling, and reproductive responses to environmental stress.

### CHALLENGES AND LIMITATIONS

Despite considerable progress, several challenges continue to limit the wider implementation of microfluidic technologies in plant research. One major concern is the strong reliance on a small number of model species, particularly *Arabidopsis thaliana*. Consequently, the applicability of many existing platforms to agriculturally important crops remains insufficiently explored. Another important limitation is the lack of standardized device architectures, operating protocols, and performance metrics. Differences in platform design and experimental conditions often make comparisons among studies difficult and can hinder reproducibility across laboratories. Greater standardization will be essential for establishing broadly applicable methodologies and accelerating technology adoption. Biological constraints also remain significant. Maintaining healthy plant growth within confined microscale environments for extended periods can be challenging due to changes in root architecture, biomass accumulation, and long-term physiological requirements. Integrating larger plants and more complex root systems into microfluidic devices therefore remains an important area for future development.

From a technical perspective, material related limitations continue to affect device performance. For example, PDMS, one of the most commonly used fabrication materials can absorb certain small molecules, potentially influencing the delivery and availability of experimental treatments. In addition, issues such as air bubble formation, channel fouling, and biofilm development may compromise fluid flow and experimental reliability during prolonged studies. A further challenge lies in bridging the gap between simplified laboratory systems and natural environments. Although recent advances have improved environmental realism, many microfluidic devices still cannot fully capture the physical,

chemical, and biological complexity of field conditions. Translating findings from microscale platforms to greenhouse or field environments therefore requires careful validation.

Thus, future research should focus on developing robust, scalable, and accessible microfluidic systems that support long-term cultivation, accommodate diverse plant species, and integrate advanced sensing and automation technologies. Addressing these challenges will be critical for expanding the role of microfluidics in both fundamental plant science and agricultural applications.

### **FUTURE DIRECTIONS AND RESEARCH OPPORTUNITIES**

The continued advancement of plant microfluidics will depend on the development of systems that more effectively connect microscale experimentation with biologically relevant plant processes. Although substantial progress has been achieved, many current platforms remain optimized for specific experimental questions and model species. Future efforts should therefore emphasize adaptable device architectures that can accommodate diverse plant types, developmental stages, and experimental objectives. Achieving this goal will require parallel advances in both device fabrication and analytical integration. Advances in scalable fabrication technologies, particularly 3D printing and thermoplastic manufacturing are expected to improve the reproducibility, affordability, and wider accessibility of microfluidic devices. At the same time, the incorporation of advanced sensing and imaging tools, including biosensors, fluorescence-based imaging, and mass spectrometry, will strengthen the capability of these platforms to monitor plant physiological and biochemical processes in real time. Future microfluidic systems are likely to integrate intelligent sensing, automated fluid control, diagnostic modules, and artificial intelligence assisted data analysis, enabling more comprehensive assessment of plant responses to changing environmental conditions (Dong *et al.*, 2024; Zhao *et al.*, 2024; Zhou *et al.*, 2025).

An important research opportunity lies in extending microfluidic studies beyond short-term observations toward complete developmental trajectories. The ability to monitor plants across longer timescales would facilitate investigations of growth transitions, developmental plasticity, reproductive processes, and stress memory under precisely controlled conditions. Such capabilities could provide a more comprehensive understanding of plant responses throughout the life cycle. Another promising direction involves the integration of multiple biological scales within a single platform. Future devices may combine cellular, tissue-level, organ-level, and whole-plant analyses, enabling researchers to link molecular events with physiological outcomes. This multiscale approach could improve understanding of how local responses are translated into whole-plant behaviour. A further effort is needed toward expanding applications beyond traditional model systems. The development of crop-oriented platforms capable of supporting agriculturally important species would enhance the relevance of microfluidic technologies for breeding, crop management, and stress resilience research. Comparative studies across species will further reveal conserved and species-specific response mechanisms. From an application perspective, future progress will depend on improving accessibility and interoperability. Modular device designs, standardized operating procedures, and open source development strategies could facilitate broader adoption across laboratories and research disciplines.

Overall, we believe plant microfluidics is moving toward increasingly integrated, scalable, and biologically relevant platforms. Continued collaboration among plant biologists, engineers, material scientists, and computational researchers will be essential for realizing the full potential of these technologies in both fundamental research and sustainable agriculture.

### **CONCLUSION**

Microfluidic technologies have evolved from simple microscale culture systems to advanced platforms capable of investigating plant growth, development, plant-microbe interactions, and environmental

responses with high precision. Through improved regulation of microscale environments, these platforms have enabled advances in phenotyping, single-cell studies, reproductive biology, stress physiology, and rhizosphere research. More recent developments, including sensing integrated devices, ecosystem inspired platforms, and phytofluidic devices have further broadened the scope of plant microfluidics and its applications in plant science. However, the wider adoption of these technologies will depend on overcoming challenges related to standardization, long-term cultivation, species diversity, and the translation of laboratory-based systems into practical applications.

## DISCLAIMER

The author(s) declare no conflict of interest in the work.

## REFERENCE

- Adamski, K., Kubicki, W. and Walczak, R. 2016. Inkjet 3D printed microfluidic devices. *MIXDES-Proceedings of the 23rd International Conference Mixed Design of Integrated Circuits and Systems*, 504-506.
- Agarwal, K., Mehta, S.K. and Mondal, P.K. 2024a. Unveiling nutrient flow-mediated stress in plant roots using an on-chip phytofluidic device. *Lab on a Chip*, **24**(16): 3775-3789.
- Agudelo, C.G., Sanati, A., Ghanbari, M., Packirisamy, M. and Geitmann, A. 2012. A microfluidic platform for the investigation of elongation growth in pollen tubes. *Journal of Micromechanics and Microengineering*, **22**(11): 115009.
- Agudelo, Carlos G., Nezhad, A.S., Ghanbari, M., Naghavi, M., Packirisamy, M. and Geitmann, A. 2013. TipChip: A modular, MEMS-based platform for experimentation and phenotyping of tip-growing cells. *Plant Journal*, **73**(6): 1057-1068.
- Ali, S., Ozturk, A., Wondimu, A. and Asmatulu, E. 2020. Microfluidics-based Learning and Analysis for Plant Cell Studies. *ASEE Midwest Section Conference*, 1-9.
- Alla, S.K., Ramana, C.H.V.V., Ratnaraju, M., Naidu, C.H. G., Thomas, S., Sharma, A., Gangwar, A. and Das, T. 2026. Next-generation microfluidics for sustainable detection systems. *Sustainable Analytical Chemistry: Methods, Materials, and Applications*, 435-480.
- Allan, C., Sun, Y., Whisson, S.C., Porter, M., Boevink, P.C., Nock, V. and Meisrimler, C.N. 2024. Observing root growth and signalling responses to stress gradients and pathogens using the bi-directional dual-flow RootChip. *Lab on a Chip*, **24**(24): 5360-5373.
- Allan, C., Tayagui, A., Hornung, R., Nock, V. and Meisrimler, C.N. 2023. A dual-flow RootChip enables quantification of bi-directional calcium signaling in primary roots. *Frontiers in Plant Science*, **13**: 1040117.
- Aryal, P., Hefner, C., Martinez, B. and Henry, C.S. 2024. Microfluidics in environmental analysis: Advancements, challenges, and future prospects for rapid and efficient monitoring. *Lab on a Chip*, **24**(5): 1175-1206.
- Aufrecht, J.A., Ryan, J.M., Hasim, S., Allison, D.P., Nebenführ, A., Doktycz, M.J. and Retterer, S.T. 2017. Imaging the root hair morphology of arabidopsis seedlings in a two-layer microfluidic platform. *Journal of Visualized Experiments*, **126**: 55971.
- Aufrecht, J.A., Timm, C.M., Bible, A., Morrell-Falvey, J.L., Pelletier, D.A., Doktycz, M.J. and Retterer, S.T. 2018. Quantifying the spatiotemporal dynamics of plant root colonization by beneficial bacteria in a microfluidic habitat. *Advanced Biosystems*, **2**(6):1800048.
- Bascom, C.S., Wu, S.Z., Nelson, K., Oakey, J. and Bezanilla, M. 2016. Long-term growth of moss in microfluidic devices enables subcellular studies in development. *Plant Physiology*, **172**(1): 28-37.
- Behera, P.P., Mehta, S.K., Arun, R.K. and Mondal, P.K. 2025. Pore-scale immiscible interfacial transport facilitates low-cost droplet generation. *Soft Matter*, **21**(35): 6891-6909.
- Branch, D.W., Wheeler, B.C., Brewer, G.J. and Leckband, D.E. 2001. Long-term stability of grafted polyethylene glycol surfaces for use with microstamped substrates in neuronal cell culture. *Biomaterials*, **22**(10): 1035-1047.
- Busch, W., Moore, B.T., Martsberger, B., MacE, D.L., Twigg, R.W., Jung, J., Pruteanu-Malinici, I., Kennedy, S.J., Fricke, G.K., Clark, R.L., Ohler, U. and Benfey, P.N. 2012. A microfluidic device and computational platform for high-throughput live imaging of gene expression. *Nature Methods*, **9**(11): 1101-1106.
- Chang, W.J., Akin, D., Sedlak, M., Ladisch, M.R. and Bashir, R. 2003. Poly(dimethylsiloxane) (PDMS) and silicon hybrid biochip for bacterial culture. *Biomedical Microdevices*, **5**(4): 281-290.

- Chen, J., Fu, L., Xiang, R., Luo, S., Huang, X., Yu, H. and Sun, L. 2025. Artificial intelligence-assisted microfluidic bio-Imaging—From sensors to applications: A Review. *IEEE Sensors Journal*, **25**(2): 2056-2072.
- Clark, N.M., Van Den Broeck, L., Guichard, M., Stager, A., Tanner, H.G., Blilou, I., Grossmann, G., Iyer-Pascuzzi, A.S., Maizel, A., Sparks, E.E. and Sozzani, R. 2020. Novel imaging modalities shedding light on plant biology: Start small and grow Big. *Annual Review of Plant Biology*, **71**(1): 789-816.
- Cohen, L.D., Moratto, E. and Stanley, C.E. 2026. 20 years of microfluidic technology for advancing plant sciences. *Lab on a Chip*, **26**(5):1273-1298.
- Dbouk, T. and Drikakis, D. 2024. Flow and plants. *Physics of Fluids*, **36**(11).
- Dong, H., Lin, J., Tao, Y., Jia, Y., Sun, L., Li, W.J. and Sun, H. 2024. AI-enhanced biomedical micro/nanorobots in microfluidics. *Lab on a Chip*, **24**(5): 1419-1440.
- Du, J., Zeng, L., Yu, Z., Chen, S., Chen, X., Zhang, Y. and Yang, H. 2022. A magnetically enabled simulation of microgravity represses the auxin response during early seed germination on a microfluidic platform. *Microsystems and Nanoengineering*, **8**(1): 11.
- Dubey, S.M., Fendrych, M. and Serre, N.B.C. 2023. Relative membrane potential measurements using DISBAC<sub>2</sub>(3) fluorescence in *Arabidopsis thaliana* primary roots. *Bio-Protocol*, **13**(14).
- Elitaş, M., Yüce, M. and Budak, H. 2017. Microfabricated tools for quantitative plant biology. *Analyst*, **142**(6): 835-848.
- Fendrych, M., Akhmanova, M., Merrin, J., Glanc, M., Hagihara, S., Takahashi, K., Uchida, N., Torii, K. U. and Friml, J. 2018. Rapid and reversible root growth inhibition by TIR1 auxin signalling. *Nature Plants*, **4**(7): 453–459.
- Gao, J., Sasse, J., Lewald, K.M., Zhalnina, K., Cornmesser, L.T., Duncombe, T.A., Yoshikuni, Y., Vogel, J.P., Firestone, M.K. and Northen, T.R. 2018. Ecosystem fabrication (EcoFAB) protocols for the construction of laboratory ecosystems designed to study plant-microbe interactions. *Journal of Visualized Experiments*, **134**: 57170.
- Ghanbari, M., Nezhad, A.S., Agudelo, C.G., Packirisamy, M. and Geitmann, A. 2014. Microfluidic positioning of pollen grains in lab-on-a-chip for single cell analysis. *Journal of Bioscience and Bioengineering*, **117**(4): 504-511.
- Grossmann, G., Guo, W.J., Ehrhardt, D.W., Frommer, W.B., Sit, R.V., Quake, S.R. and Meier, M. 2011. The Rootchip: An integrated microfluidic chip for plant Science. *Plant Cell*, **23**(12): 4234-4240.
- Grossmann, G., Meier, M., Cartwright, H.N., Sosso, D., Quake, S.R., Ehrhardt, D.W. and Frommer, W.B. 2012. Time-lapse fluorescence imaging of arabidopsis root growth with rapid manipulation of the root environment using the RootChip. *Journal of Visualized Experiments*, **65**: 4290.
- Guichard, M., de Olalla, E.B.G., Stanley, C.E. and Grossmann, G. 2020. Microfluidic systems for plant root imaging. *Methods in cell biology*, **160**: 381-404.
- Ismayeel, M., Mehta, S.K. and Mondal, P.K. 2024. Maximizing blue energy via densely grafted soft layers in nanopores. *Langmuir*, **40**(48): 25495-25508.
- Jabusch, L.K., Kim, P.W., Chiniquy, D., Zhao, Z., Wang, B., Bowen, B., Kang, A.J., Yoshikuni, Y., Deutschbauer, A.M., Singh, A.K. and Northen, T.R. 2021. Microfabrication of a chamber for high-resolution, in situ imaging of the whole root for plant–microbe interactions. *International Journal of Molecular Sciences*, **22**(15): 7880.
- Jiang, H., Xu, Z., Aluru, M.R. and Dong, L. 2014. Plant chip for high-throughput phenotyping of Arabidopsis. *Lab on a Chip*, **14**(7): 1281-1293.
- Kaiser, C.F., Perilli, A., Grossmann, G. and Meroz, Y. 2023. Studying root-environment interactions in structured microdevices. *Journal of Experimental Botany*, **74**(13): 3851-3863.
- Kalita, J., Mehta, S.K. and Mondal, P.K. 2025. Unveiling mysteries of micro-porous structures in xylem vascular of plants: characterising nutrient transport using electro-hydrodynamics. *Flow*, **5**: E38.
- Kamat, V., Burton, L., Venkadesh, V., Jayachandran, K. and Bhansali, S. 2023. Enabling smart agriculture through sensor-integrated microfluidic chip to monitor nutrient uptake in plants. *ECS Sensors Plus*, **2**(4): 043201.
- Kawakatsu, Y., Okada, R., Hara, M., Tsutsui, H., Yanagisawa, N., Higashiyama, T., Arima, A., Baba, Y., Kurotani, K.I. and Notaguchi, M. 2024. Microfluidic device for simple diagnosis of plant growth condition by detecting miRNAs from filtered plant extracts. *Plant Phenomics*, **6**: 0162.
- Khan, Z., Karamahmutoğlu, H., Elitaş, M., Yüce, M. and Budak, H. 2019. THROUGH THE LOOKING GLASS: Real-time imaging in brachypodium roots and osmotic stress analysis. *Plants*, **8**(1): 14.

- Ko, J.M., Ju, J., Lee, S.H. and Cha, H.C. 2006. Tobacco protoplast culture in a polydimethylsiloxane-based microfluidic channel. *Protoplasma*, **227**(2): 237-240.
- Kozgunova, E. and Goshima, G. 2019. A versatile microfluidic device for highly inclined thin illumination microscopy in the moss *Physcomitrella patens*. *Scientific Reports*, **9**(1): 15182.
- Leclerc, E., Sakai, Y. and Fujii, T. 2004. Perfusion culture of fetal human hepatocytes in microfluidic environments. *Biochemical Engineering Journal*, **20**(2-3): 143-148.
- Leclerc, Eric, Sakai, Y. and Fujii, T. 2003. Cell culture in 3-dimensional microfluidic structure of PDMS (polydimethylsiloxane). *Biomedical Microdevices*, **5**(2): 109-114.
- Liu, C., Lin, H., Li, B., Dong, Y. and Qiu, Y. 2022. Screening endophyte with capability to improve phytoremediation efficiency from hyperaccumulators: A novel and efficient microfluidic method. *Chemosphere*, **286**: 131723.
- Mahesh, K. and Vaidya, S. 2017. Microfluidics: A boon for biological research. *Current Science*, **112**(10): 2021-2028.
- Mandal, D., Datta, S., Raveendar, G., Mondal, P.K. and Nag Chaudhuri, R. 2023. RAV1 mediates cytokinin signaling for regulating primary root growth in *Arabidopsis*. *Plant Journal*, **113**(1): 106-126.
- Mao, X., Huang, T.J. and Ho, C.-M. 2010. The lab-on-a-chip approach for molecular diagnostics. *Molecular Diagnostics: Techniques and Applications for the Clinical Laboratory*, Academic Press, 21-34.
- Marczakiewicz-Perera, P., Köhler, J.M. and Cao, J. 2026. Application of microfluidics in plant physiology and development studies. *Applied Sciences*, **16**(1): 464.
- Massalha, H., Korenblum, E., Malitsky, S., Shapiro, O.H. and Aharoni, A. 2017a. Live imaging of root-bacteria interactions in a microfluidics setup. *Proceedings of the National Academy of Sciences*, **114**(17): 4549-4554.
- Meier, M., Lucchetta, E.M. and Ismagilov, R.F. 2010. Chemical stimulation of the *Arabidopsis thaliana* root using multi-laminar flow on a microfluidic chip. *Lab on a Chip*, **10**(16): 2147-2153.
- Moussus, M. and Meier, M. 2021. A 3D-printed *Arabidopsis thaliana* root imaging platform. *Lab on a Chip*, **21**(13): 2557-2564.
- Naghavi, M. 2014. Studying the cytomorphic aspects of pollen tube growth behavior using Lab-On-Chip technology. PhD thesis. *Université de Montréal, Canada*.
- Neethirajan, S., Kobayashi, I., Nakajima, M., Wu, D., Nandagopal, S. and Lin, F. 2011. Microfluidics for food, agriculture and biosystems industries. *Lab on a Chip*, **11**(9): 1574-1586.
- Neethirajan, S., Ragavan, V., Weng, X. and Chand, R. 2018. Biosensors for sustainable food engineering: Challenges and perspectives. *Biosensors*, **8**(1): 23.
- Noirot-Gros, M.F., Shinde, S.V., Akins, C., Johnson, J.L., Zerbs, S., Wilton, R., Kemner, K.M., Noirot, P. and Babnigg, G. 2020a. Functional imaging of microbial interactions with tree roots using a microfluidics setup. *Frontiers in Plant Science*, **11**: 408.
- Orebaugh, J., Carrell, A.A., York, L.M., Cregger, M.A. and Del Valle Kessra, I. 2026. Synthetic soils for ecological and synthetic biology applications. *FEMS Microbiology Reviews*, **50**: fuag012.
- Padhi, P., Mehta, S.K., Agarwal, K. and Mondal, P.K. 2024. Intermittent flow influences plant root growth: A phytofluidics approach. *Physics of Fluids*, **36**(4): 043602.
- Panja, S., Mehta, S.K., Kalita, J., Panchal, D., Zhang, X. and Mondal, P.K. 2026. How plasma activated water promotes plant root growth through interfacial modulation of nitrogen uptake. *Journal of Colloid and Interface Science*, **715**: 140281.
- Panja, S., Mehta, S.K., Kalita, J., Prasad, M.K. and Mondal, P.K. 2024a. Soft plant root structure-media flow interactions: Exploring the adverse effect of lead contamination in North-Eastern Indian rice. *Physics of Fluids*, **36**(11): 111914.
- Parashar, A. and Pandey, S. 2011. Plant-in-chip: Microfluidic system for studying root growth and pathogenic interactions in *Arabidopsis*. *Applied Physics Letters*, **98**(26): 263703.
- Sakai, K., Charlot, F., Saux, T. Le, Bonhomme, S., Nogué, F., Palauqui, J.C. and Fattaccioli, J. 2019. Design of a comprehensive microfluidic and microscopic toolbox for the ultra-wide spatio-temporal study of plant protoplasts development and physiology. *Plant Methods*, **15**(1): 79.
- Sanati Nezhad, A. 2014. Microfluidic platforms for plant cells studies. *Lab on a Chip*, **14**(17): 3262-3274.
- Sanati Nezhad, Amir, Ghanbari, M., Agudelo, C.G., Naghavi, M., Packirisamy, M., Bhat, R.B. and Geitmann, A. 2014. Optimization of flow assisted entrapment of pollen grains in a microfluidic platform for tip growth analysis. *Biomedical Microdevices*, **16**(1): 23-33.

- Seemann, R., Brinkmann, M., Pfohl, T. and Herminghaus, S. 2012. Droplet based microfluidics. *Reports on Progress in Physics*, **75**(1): 016601.
- Shamsudhin, N., Laeubli, N., Atakan, H.B., Vogler, H., Hu, C., Haerberle, W., Sebastian, A., Grossniklaus, U. and Nelson, B.J. 2016. Massively parallelized pollen tube guidance and mechanical measurements on a lab-on-a-chip platform. *PLoS ONE*, **11**(12): e0168138.
- Singh, G., Pereira, D., Baudrey, S., Hoffmann, E., Ryckelynck, M., Asnacios, A. and Chabouté, M.E. 2021. Real-time tracking of root hair nucleus morphodynamics using a microfluidic approach. *Plant Journal*, **108**(2): 303-313.
- Song, Y., Zhou, Y., Zhang, K., Fan, Z., Zhang, F. and Wei, M. 2024. Microfluidic programmable strategies for channels and flow. *Lab on a Chip*, **24**(19): 4483-4513.
- Song, Z.X., Chai, H.H., Chen, F., Yu, L. and Fang, C. 2019. A foldable chip array for the continuous investigation of seed germination and the subsequent root development of seedlings. *Micromachines*, **10**(12): 884.
- Sozzani, R., Busch, W., Spalding, E.P. and Benfey, P.N. 2014. Advanced imaging techniques for the study of plant growth and development. *Trends in Plant Science*, **19**(5): 304-310.
- Stanley, C.E., Shrivastava, J., Brugman, R., Heinzelmann, E., van Swaay, D. and Grossmann, G. 2018. Dual-flow-RootChip reveals local adaptations of roots towards environmental asymmetry at the physiological and genetic levels. *New Phytologist*, **217**(3): 1357-1369.
- Stanley, C., Shrivastava, J., Brugman, R., Heinzelmann, E., Frajs, V., Bühler, A., van Swaay, D. and Grossmann, G. 2018. Fabrication and use of the dual-flow-RootChip for the imaging of Arabidopsis roots in asymmetric microenvironments. *Bio-Protocol*, **8**(18): e3010-e3010.
- Sun, C., Zhang, Y., Liu, L., Liu, X., Li, B., Jin, C. and Lin, X. 2021. Molecular functions of nitric oxide and its potential applications in horticultural crops. *Horticulture Research*, **8**: 71.
- Vang, S., Seitz, K. and Krysan, P.J. 2018. A simple microfluidic device for live-cell imaging of arabidopsis cotyledons, leaves, and seedlings. *BioTechniques*, **64**(6): 255-261.
- Walker, G.M., Ozers, M.S. and Beebe, D.J. 2002. Insect cell culture in microfluidic channels. *Biomedical Microdevices*, **4**(3): 161-166.
- Walton, C.L., Khalid, M., Bible, A.N., Kertesz, V., Retterer, S.T., Morrell-Falvey, J. and Cahill, J.F. 2022. In situ detection of amino acids from bacterial biofilms and plant root exudates by liquid microjunction surface-sampling probe mass spectrometry. *Journal of the American Society for Mass Spectrometry*, **33**(9): 1615-1625.
- Yanagisawa, N., Kozgunova, E., Grossmann, G., Geitmann, A. and Higashiyama, T. 2021. Microfluidics-based bioassays and imaging of plant cells. *Plant and Cell Physiology*, **62**(8): 1239-1250.
- Yanagisawa, N., Sugimoto, N., Higashiyama, T. and Sato, Y. 2018. Development of microfluidic devices to study the elongation capability of tip-growing plant cells in extremely small spaces. *Journal of Visualized Experiments*, **135**: 57262.
- Yee, M.O., Kim, P., Li, Y., Singh, A.K., Northen, T.R. and Chakraborty, R. 2021. Specialized plant growth chamber designs to study complex rhizosphere interactions. *Frontiers in Microbiology*, **12**: 625752.
- Zemmour, C., Torchinsky, I., Breiman, N., Oginets, A., Vakahi, A. and Benny, O. 2025. Enhanced control of particle distribution in colloidal lithography for Janus metal-capped nanoparticles. *Colloids and Surfaces A: Physicochemical and Engineering Aspects*, **710**: 136203.
- Zhang, H., Yan, X., Zhang, M., Zhao, Y., Jiang, S., Jiang, Y., Wei, Y., Zhang, Y. and Sun, L. 2025. Behavior study of plant roots under physical obstacles based on a root obstacle microfluidic chip. *Journal of Agricultural and Food Chemistry*, **73**(48): 30895-30903.
- Zhao, X., Zhai, L., Chen, J., Zhou, Y., Gao, J., Xu, W., Li, X., Liu, K., Zhong, T., Xiao, Y. and Yu, X. 2024. Recent advances in microfluidics for the early detection of plant diseases in vegetables, fruits, and grains caused by bacteria, fungi, and viruses. *Journal of Agricultural and Food Chemistry*, **72**(28): 15401-15415.
- Zhao, Y., Jiang, Y., Niu, M., Zhu, Y., Jiang, S., Wei, Y., Zhang, Y. and Sun, L. 2026. The applications of microfluidic chip systems in plant research. *Analytical Chemistry*, **98**(14): 10264-10284.
- Zhou, C., Liu, C., Liao, Z., Pang, Y. and Sun, W. 2025. AI for biofabrication. *Biofabrication*, **17**(1): 012004.

---

**FULL LENGTH ARTICLE**

---

**Effect of vermicompost on growth and yield of four selected ornamental flowering plants**

---

**Subodh Hansda<sup>1</sup>, Sourav Gorai<sup>1</sup>, Ankit Kumar Ghorai<sup>2</sup> and Subrata Raha<sup>1\*</sup>**

<sup>1</sup>Department of Botany, Sidho-Kanho-Birsha University, Purulia, West Bengal, India .

<sup>2</sup>Assistant Director Agriculture, Bagmundi, Purulia, India.

---

Received : 01.08.2025

Accepted : 02.03.2026

Published : 30.06.2026

---

The present investigation was undertaken during 2020-21 and 2021-22 to examine the effect of different doses of vermicompost application on growth parameters of *Antirrhinum majus* (Snapdragon), *Gazania rigens* (Gazania), *Verbena X hybrida* (Verbena), and *Catharanthus roseus* (Vinca). The effect on growth parameters viz., numbers of leaves, numbers of branches/plant, plant height (cm), root length (cm) and leaf area (cm<sup>2</sup>) and yield parameters viz., days to flower bud initiation, number of flowers plant<sup>-1</sup>, flowering period (days), fresh weight of flower(g) and dry weight of flower(g) were documented for these flowers. Treatment T<sub>3</sub> (30% vermicompost, 70% base medium, and NPK) demonstrated the most significant favourable impact on the growth and yield of *Antirrhinum majus*, *Verbena X hybrida*, and *Gazania rigens*. However, *Catharanthus roseus* responded positively to treatment T<sub>4</sub> (40% vermicompost + 60% base medium + NPK). The experiment was laid out in completely randomised block design with seven treatments for each flowering plant, each replicated thrice. The findings indicate that combinations of vermicompost and base medium can markedly improve the growth of diverse ornamental plants, while the ideal treatment may differ among species.

**Keywords:** Vermicompost, *Antirrhinum majus*, *Verbena X hybrida*, *Catharanthus roseus*, *Gazania rigens*.

---

## INTRODUCTION

Floriculture plays a significant part in the Indian economy by generating jobs, marketing of flowers and foliage. India has the second largest total area under flower crop production in the world, followed by China. India produces 2910 thousand MT of flowers annually on an area of roughly 303 thousand hectares. Tamil Nadu, Karnataka, Madhya Pradesh, West Bengal, Uttar Pradesh, Gujarat, Chhattisgarh, and Assam are the states in India that produce most of the

country's floriculture crops (Horticulture statistics at a glance, 2018).

Fertilizers are one of the elements influencing crop yields, but their extensive use, particularly when coupled with improper management techniques like burning plant waste, substantially lowers soil organic matter. Additionally, prolonged use of chemical fertilizers causes groundwater contamination and leaching (Esmaeili *et al.* 2022). Scientists have determined that alternative cultivation, such as natural or organic farming, will be necessary for Indian agriculture following the Green Revolution of India. Organic farming makes it possible to preserve the

---

\*Corresponding author : subrata-raha@skbu.ac.in

quality of agricultural goods for the benefit of human health and society (Rani *et al.*, 2023). Several factors influence plant growth, and one of the most crucial ones for the development and production of high-quality flowers is the growing medium. The perfect medium supports the plant, provides water and other vital nutrients, and allows oxygen to diffuse to the roots (El-Sayed *et al.*, 2018 and Padhiyar *et al.*, 2017). Growing media's excellent water-holding capacity, aeration, and increased nutrient uptake have all been shown to increase horticulture crop yields. For a variety of decorative crops to have abundant flowering and lush vegetative growth, high-quality growing media is essential (Kaushal and Kumari, 2020). Vermicomposting is the process of turning any biodegradable material, *viz.*, farm, kitchen, market, animal, and biowastes from the agricultural sectors into a nutrient-rich soil supplement by passing it through the worms' stomachs. Vermicompost fulfills the plant's requirements for nutrition because it contains macronutrients like phosphate, nitrogen, and potassium in addition to micronutrients like certain organic and amino acid sources (Adhikary, 2012). In this context, Manna and Biswas (1996) reported application of vermicompost not only adds macro and micro nutrients and growth regulators to the soil but also increases soil water retention, microbial population, humic substances of the soil, mineralization and release of nutrients. Presently, scant information is available on the recommended dose of vermicompost for optimal growth and production of *Antirrhinum majus* (Snapdragon), *Gazania rigens* (Gazania), *Verbena X hybrida* (Verbena), and *Catharanthus roseus* (Vinca). Hence, the present investigation was undertaken with the main objective of evaluating the effect of vermicompost on the growth and productivity of the selected four ornamental flowering plants.

## MATERIALS AND METHODS

### Experimental site and conditions

On field experiments were conducted at Sidho-Kanho-Birsha University, Purulia, West Bengal. The experimental site (23.36°N, 86.33°E, average elevation of 241 metres above mean sea level) is

located in the red and lateritic zone (agroclimatic zone 6) with hot and dry sub-humid rainfed conditions as prevailing climatic conditions. The experiments were conducted from October 2020 to January 2021 and from October 2021 to January 2022.

### Experimental setup

Growing media was prepared by mixing soil and vermicompost in different proportions as mentioned in Table 1. Soil was collected from paddy fields (depth: 0-15 cm) near Sidho-Kanho-Birsha University. Soil was air-dried by spreading it over a polypropylene sheet under the sun, preferably in the shade, well away from rain. Pot experiments were conducted with these growing media in earthen pots (height: 10 inches, diameter: 10 inches). The seedlings *Antirrhinum majus* (Snapdragon), *Gazania rigens*

**Table 1.** Treatment details

Treatment	Composition
T <sub>0</sub> (Control)	100% Base medium +NPK
T <sub>1</sub>	10% Vermicompost + 90% Base medium +NPK
T <sub>2</sub>	20% Vermicompost + 80% Base medium +NPK
T <sub>3</sub>	30% Vermicompost + 70% Base medium +NPK
T <sub>4</sub>	40% Vermicompost + 60% Base medium +NPK
T <sub>5</sub>	50% Vermicompost + 50% Base medium +NPK
T <sub>6</sub>	60% Vermicompost + 40% Base medium +NPK

(*Gazania*), *Verbena X hybrida* (Verbena), and *Catharanthus roseus* (Vinca) were purchased from a nursery and transplanted into these clay pots. The experiment details of the four selected ornamental flowers are provided in Table 2. The inorganic fertilizer (120:90:60 kg/ha NPK) was applied 30 days after plantation, and pots were watered at regular intervals. The experiment was conducted with 7 treatments, including a control treatment in triplicate, planted with one plant per pot.

**Table 2.** Experiment details of four selected ornamental flowers

Flowers	Variety	Company	Family
<i>Antirrhinum majus</i> (Snapdragon)	Madame Butterfly MIX	Syngenta Flowers	Scrophulariaceae
<i>Gazania rigens</i> (Gazania)	Frosty Kiss Flame	Syngenta Flowers	Asteraceae
<i>Verbena X hybrida</i> (Verbena)	Verbena Hybrida Tuscany Mix	Syngenta Flowers	Verbenaceae
<i>Catharanthus roseus</i> (Vinca)	Vinca Sunstorm Formula Mix	Syngenta Flowers	Apocynaceae

### Analysis of nutrient status of growing media

The physico-chemical parameters of the growing media have been analysed using various methods. The pH of the growing media was determined in a growing media and water ratio of 1:2.5 (w/v) with the help of a glass electrode pH meter following the method outlined by Jackson (1973). Electrical conductivity of growing media suspensions (growing media: water: 1:2.5) was measured at room temperature (25°C) by using a direct reading conductivity meter (Jackson, 1973). Oxidizable organic carbon (OC) of the growing media was determined following the method of Walkley and Black (1934). In this method, 0.5 g of growing media was wet oxidized by 10 ml of 1(N) K<sub>2</sub>Cr<sub>2</sub>O<sub>7</sub> and 20 ml concentrated H<sub>2</sub>SO<sub>4</sub>. The digested material was kept in a dark place for 30 min, followed by titration with 0.5 N ferrous ammonium sulphate after the addition of 200 ml of water and 10 ml of orthophosphoric acid. The total Nitrogen (N) of the soils was estimated using the hot alkaline potassium permanganate method as suggested by Subbiah and Asija (1956). The available phosphorus of the soil was extracted by Olsen reagent (0.5 M NaHCO<sub>3</sub>; pH 8.5) (Olsen *et al.*, 1954) and the extracted phosphorus was estimated using a spectrophotometer at 760 nm following the L-ascorbic acid method as described by Murphy and Riley (1962). Available potassium of the soil sample was extracted with neutral normal ammonium acetate, as described by Jackson (1973). The extracted potassium was estimated with the help of a Flame photometer.

### Analysis of growth and yield attributes

The plant growth parameters, *viz.*, number of leaves plant<sup>-1</sup>, number of branches plant<sup>-1</sup>, plant height (cm), root length (cm) and leaf area (cm<sup>2</sup>) were recorded following protocols (Evans, 1972). The yield parameters, *viz.*, analysis days to flower bud initiation, number of flowers plant<sup>-1</sup>, flowering period (days), fresh weight of flower(g) and dry weight of flower(g) were recorded as per Mehmood *et al.* (2013).

### STATISTICAL ANALYSIS

One-way ANOVA was performed to compare the effects of different doses of vermicompost on growth and yield parameters of the flowering plants by adopting a completely randomised block design (Gomez and Gomez, 1984). Critical differences (p = 0.05) levels were computed for comparison of treatment means in cases where the results were significant.

### RESULTS AND DISCUSSION

#### Soil nutrient status before plantation

The pH in the pots across the treatments ranged from 5.6 to 6.3, with a mean of 5.95, which indicated slightly acidic conditions of the growth media in these pots. The electrical conductivity varied from 0.17 to 0.59 with a mean of 0.35, which indicates neutral conditions. The organic carbon content varied from low (0.42 %) to high (1.9 %) across the pots. The total

**Table 3.** Physicochemical parameters of treatment set

Treatment	pH		EC dsm-1		OC (%)		Total N (Kg ha-1)		Total P <sub>2</sub> O <sub>5</sub> (Kg ha-1)		Total K <sub>2</sub> O (Kg ha-1)	
T <sub>0</sub> (Control)	5.6	SA	0.17	N	0.42	L	235	L	55	M	323	M
T <sub>1</sub>	5.6	SA	0.17	N	0.42	L	235	L	55	M	323	M
T <sub>2</sub>	5.9	SA	0.26	N	0.92	H	552	H	192	H	538	H
T <sub>3</sub>	5.9	SA	0.45	N	1.90	H	540	H	137	H	551	H
T <sub>4</sub>	6.3	SA	0.36	N	1.35	H	810	H	239	H	564	H
T <sub>5</sub>	6.2	SA	0.49	N	1.35	H	810	H	366	H	538	H
T <sub>6</sub>	6.2	SA	0.59	N	1.42	H	852	H	50	M	564	H

SA- Slightly Acidic, L-Low, M-Medium, N-Neutral/Normal

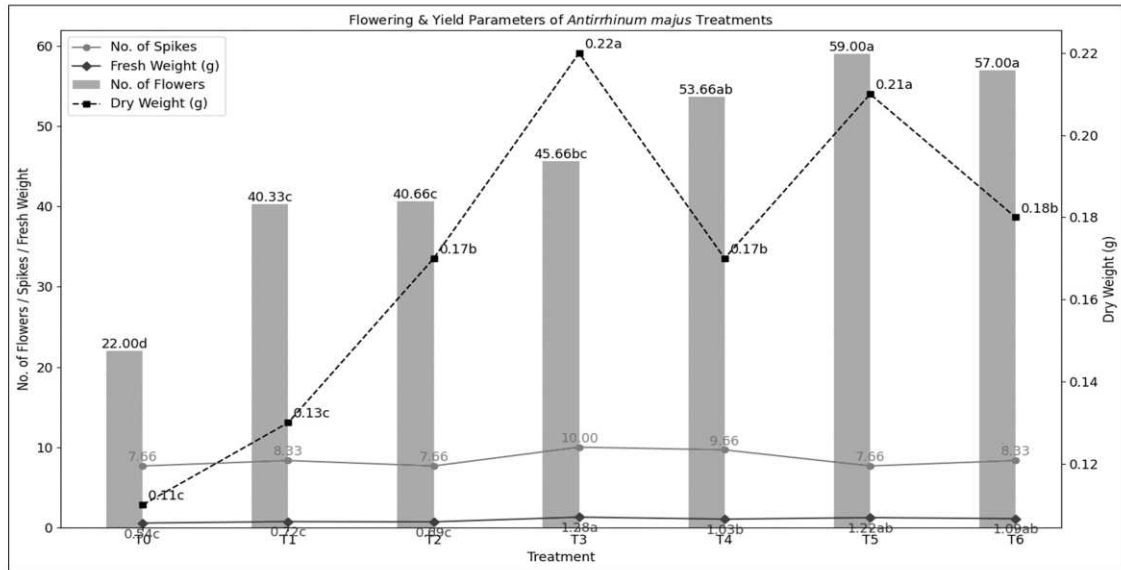
Nitrogen (N) in the growth media among the pots ranged from 235 kg ha<sup>-1</sup> to 810 kg ha<sup>-1</sup>. The total Phosphorus (P<sub>2</sub>O<sub>5</sub>) ranged from medium (55 Kg ha<sup>-1</sup>) to high (366 Kg ha<sup>-1</sup>). The total potassium (K<sub>2</sub>O) ranged from medium (323 Kg ha<sup>-1</sup>) to high (564 Kg ha<sup>-1</sup>). The physicochemical parameters have been summarised in Table 3.

#### Vermicompost's effect on the growth and yield of *Antirrhinum majus*

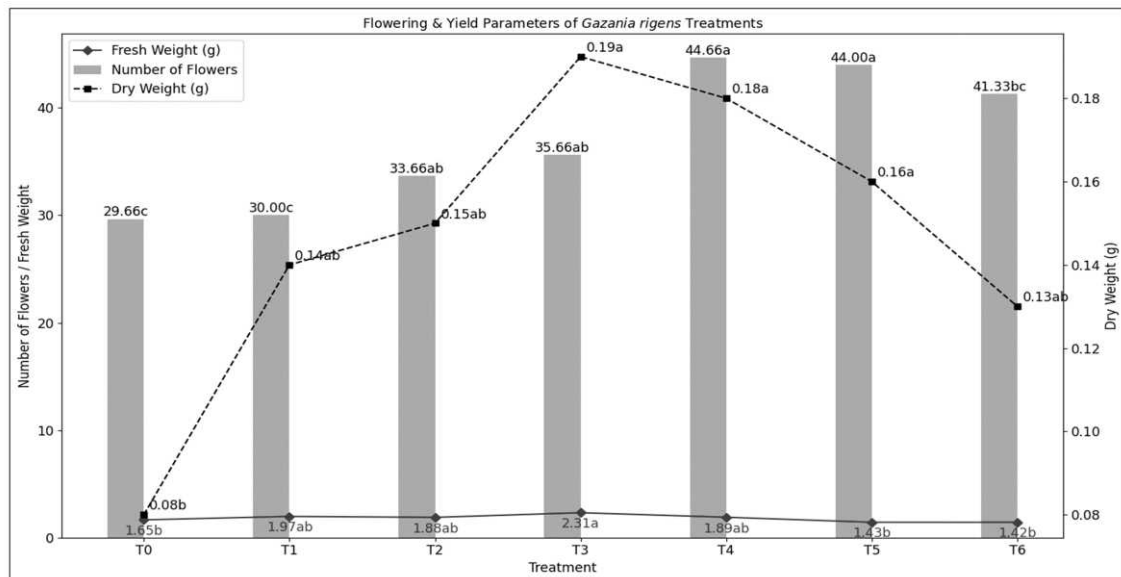
Growth parameters like average number of leaves plant<sup>-1</sup>, number of branches, root length (cm) and leaf area (cm<sup>2</sup>) were recorded at the time of flower bud initiation, and the pertaining data are summarised in Table 4 and represented in Fig. 1. Number of leaves plant<sup>-1</sup> (381) was maximum in T<sub>5</sub> set (50% Vermicompost + 50% Basal medium + NPK), followed by T<sub>6</sub> and T<sub>3</sub>, which were statistically at par with each other. The minimum number of leaves plant<sup>-1</sup> was observed in the T<sub>1</sub> (235.33), followed by the control, T<sub>0</sub> (229). Among the applications of different treatments, the plant exhibited the maximum number of branches (16.66) in the T<sub>3</sub> set (30% Vermicompost + 70% Basal medium + NPK); however, the mean number of branches across the treatments was not significantly different. The plant height was significantly higher in the sets T<sub>3</sub>, T<sub>5</sub> and T<sub>6</sub> (27 cm) as compared to the other treatments. The root length

recorded highest in T<sub>3</sub> and T<sub>1</sub> (12.66 cm), however, did not vary significantly across the treatments. The leaf area was observed to be significantly higher in T<sub>5</sub> (10.83 cm<sup>2</sup>) and was at par with the treatments T<sub>6</sub>, T<sub>2</sub> and T<sub>1</sub>.

Yield or floral parameters, viz., minimum days to flower bud initiation, number of spikes, number of flowers plant<sup>-1</sup>, flowering period (days), and fresh and dry weight of flower (g) were recorded and have been summarised in Table 4. There were significant differences among the treatments concerning the number of flowers per plant. The maximum number of flowers was recorded in T<sub>5</sub> (59) and T<sub>6</sub> (57), which were significantly different from other treatments. T<sub>6</sub> shows the highest median and the widest range. T<sub>5</sub> and T<sub>4</sub> also perform well, with high medians and tight consistency. In comparison to other treatments, the T<sub>3</sub> set (30% Vermicompost + 70% Base medium + NPK) recorded a mean minimum of 46.33 days to flower bud initiation; however, the treatments did not differ significantly. The mean number of spikes ramped up to 10 in T<sub>3</sub>, followed by 9.66 in T<sub>4</sub> and the least in control (T<sub>0</sub>) and T<sub>1</sub>. Days to flowering showed no significant differences across the treatments, which ranged from 7.33 to 9.66. Significantly higher fresh weight of flowers was obtained from T<sub>3</sub> (1.28 g), followed by T<sub>5</sub> (1.22 g), T<sub>6</sub> (1.09 g) and T<sub>4</sub> (1.03 g) as compared to the rest treatments. Consequently, maximum dry weight



**Fig.1.** Graphical representation of the effect of different vermicompost treatments on four key flowering and yield parameters of *A. majus*. Data marked by common letters are not statistically different according to the DMRT.



**Fig.2.** Graphical representation of the effect of different vermicompost treatments on four key flowering and yield parameters of *Gazania rigens*. Data marked by common letters are not statistically different according to the DMRT.

**Table 4.** Vermicompost effect on growth and yield of *Antirrhinum majus*

Treatment	Growth Parameters						Yield					
	Numbers of Leaf plant <sup>-1</sup>	Numbers of Branches plant <sup>-1</sup>	Plant Height (cm)	Root Length (cm)	Leaf Area (cm <sup>2</sup> )	Days to flower bud initiation	Nos of Spikes	Number of flowers plant <sup>-1</sup>	Flowering Period (Days)	Fresh weight of Flower(g)	Day weight of Flower(g)	
<b>T<sub>0</sub></b> <b>(Control)</b>	229 <sup>c</sup>	13.66	14 <sup>c</sup>	11.66	6 <sup>b</sup>	70	7.66	22 <sup>d</sup>	8.33	0.54 <sup>c</sup>	0.11 <sup>c</sup>	
<b>T<sub>1</sub></b>	235.33 <sup>bc</sup>	12.66	20 <sup>bc</sup>	12.66	10 <sup>a</sup>	60.66	8.33	40.33 <sup>c</sup>	8.33	0.72 <sup>c</sup>	0.13 <sup>c</sup>	
<b>T<sub>2</sub></b>	280 <sup>b</sup>	12.33	21.66 <sup>b</sup>	10.66	9.16 <sup>a</sup>	66.66	7.66	40.66 <sup>c</sup>	9.33	0.69 <sup>c</sup>	0.17 <sup>b</sup>	
<b>T<sub>3</sub></b>	339.33 <sup>a</sup>	16.66	27 <sup>a</sup>	12.66	8.33 <sup>ab</sup>	46.33	10	45.66 <sup>bc</sup>	9.66	1.28 <sup>a</sup>	0.22 <sup>a</sup>	
<b>T<sub>4</sub></b>	258 <sup>bc</sup>	13.33	19 <sup>bc</sup>	11.33	8.33 <sup>ab</sup>	50.33	9.66	53.66 <sup>ab</sup>	9.33	1.03 <sup>b</sup>	0.17 <sup>b</sup>	
<b>T<sub>5</sub></b>	381 <sup>a</sup>	14.33	27 <sup>a</sup>	12	10.83 <sup>a</sup>	62.66	7.66	59 <sup>a</sup>	8.33	1.22 <sup>ab</sup>	0.21 <sup>a</sup>	
<b>T<sub>6</sub></b>	378.33 <sup>a</sup>	12.33	27 <sup>a</sup>	11.66	10.6 <sup>a</sup>	55	8.33	57 <sup>a</sup>	7.33	1.09 <sup>ab</sup>	0.18 <sup>b</sup>	
<b>CD</b> <b>(p&lt;0.05)</b>	44.82	NS	1.62	Ns	0.83	NS	NS	8.43	NS	1.19	0.02	
<b>SEM</b>	14.54	1.43	0.52	0.67	2.56	5.24	0.92	2.73	0.84	0.06	0.007	
<b>F-test</b>	20.41*	1.14	39.82*	1.078	4.42*	3.07	1.13	20.45*	0.91	16.08*	30.87*	

Note: Data marked by common letters are not statistically different according to the DMRT at  $p < 0.05$ . NS represents non-significant differences among the treatments. \*represents that the F test was significant at  $p < 0.05$ . CD represent the critical difference, and SEM represents the standard error of the mean.

was recorded in T<sub>3</sub> (0.22 g) and T<sub>5</sub> (0.21 g). This indicates strong performance in terms of flower mass as an effect of T<sub>3</sub>.

Snapdragon (*Antirrhinum*) is a flowering plant widely used in the global cut flower market but primarily grown in India for ornamental purposes in rock gardens, beds, and pots. Its terminal spikes bear vibrant flowers in various colours except blue, which are valued as cut flowers in India. Recent studies further conducted by Kumar *et al.* (2023) confirm that a balanced combination of snapdragon's growth and flowering was enhanced by a mixture of cocopeat, vermicompost, and vermiculite at a ratio of 2:1:1. In our study, the medium compositions significantly ( $p < 0.05$ ) affected the number of leaves plant<sup>-1</sup>, plant height and leaf area. Our study on snapdragon's vegetative growth and flowering parameters showed that among the 11 recorded traits, treatment T<sub>3</sub> (30% Vermicompost + 70% Base medium + NPK) significantly enhanced eight parameters, while T<sub>5</sub> benefited the remaining three. Therefore, T<sub>3</sub> may be recommended for achieving economically higher yields in snapdragon cultivation. Thus, incorporating vermicompost into snapdragon cultivation practices can significantly improve both vegetative and reproductive performance.

#### **Effect of vermicompost on the growth and yield of *Gazania rigens***

Growth parameters of *Gazania rigens* (L.) var. Frosty Kiss Flame, *viz.*, average numbers of leaves plant<sup>-1</sup>, root length (cm) and leaf area (cm<sup>2</sup>) were recorded at the time of flower bud initiation, and the pertaining data are summarised in Table 5. The average number of leaves per plant (105.66) was highest in the T<sub>3</sub> treatment (30% Vermicompost + 70% Base medium + NPK), followed by T<sub>4</sub> (104), which was comparable to one another and significantly different from T<sub>0</sub>, T<sub>1</sub>, T<sub>2</sub> and T<sub>6</sub>. The plant height exhibited an increasing trend with significant variations until T<sub>3</sub> (15 cm), but subsequently decreased with larger dosages of vermicompost in T<sub>4</sub>, T<sub>5</sub>, and T<sub>6</sub>. The maximum root length was recorded in T<sub>3</sub> (22.6 cm) and T<sub>4</sub> (22.33 cm), greatly exceeding the results of the other treatments. The leaf area expansion of *G. rigens* exhibited

significant variation among the treatments, reaching a maximum in T<sub>5</sub> and moderate levels in T<sub>6</sub> (22.67 cm) and T<sub>3</sub> (22.33 cm).

The yield in terms of floral parameters, including minimum days to flower bud initiation, number of flowers per plant, flowering duration (days), and fresh and dried weight of flowers (g), was documented and summarized in Table 5 and number of flowers, fresh and dry weight of flowers are presented in Fig. 2. The effect of vermicompost doses on flowering showed an increasing trend till T<sub>4</sub> and then declined to a certain extent in T<sub>6</sub>. There were substantial differences across the treatments for the number of flowers per plant. The highest number of flowers per plant was recorded in T<sub>4</sub> (44.66), followed by and at par with T<sub>5</sub> (44). The minimum days to flower bud initiation were observed in T<sub>3</sub> (56.33) followed by T<sub>4</sub> (56), significantly lower than other treatments. Number of days to flowering showed no significant differences across the treatments, ranging from 7.33 to 9.33. Significantly higher fresh weight of flowers was obtained from T<sub>3</sub> (2.31 g), followed by moderately low in T<sub>1</sub> (1.97 g), T<sub>4</sub> (1.89 g) and T<sub>2</sub> (1.88 g) as compared to the rest of the treatments. The maximum dry weights were seen in T<sub>3</sub> (0.19 g), T<sub>4</sub> (0.18 g), and T<sub>5</sub> (0.16 g), which exhibited significant differences from the dry weights recorded in the other treatments.

*Gazania rigens* is a South African Asteraceae blooming plant. It can be seeded annually in cold climates or perennially in temperate climates. Due to its attractive and medicinal properties, home producers have been interested in this plant in recent years. Flowering occurs on sunny days and dormancy on foggy nights. Orange, yellow, and red capitula are vivid, while the petals' bases are white, blue, brown, or black (Moustafa *et al.*, 2007). Studies have demonstrated that the application of vermicompost significantly enhances the growth and yield of *G. rigens* (African daisy). In a 2018 study, various concentrations of vermicompost and vermiwash were applied to *G. rigens*, resulting in notable improvements in morphological and physiological traits. The optimal treatment combination of 40% vermicompost and 200 mg/l vermiwash yielded the highest number of flowers, increased plant height, and

**Table 5.** Vermicompost effect on growth and yield of *Gazania rigens*

Treatment	Growth Parameters						Yield				
	Numbers of Leaf/plant	Plant Height (cm)	Root Length (cm)	Leaf Area (cm <sup>2</sup> )	Days to flower bud initiation	Number of flowers/Plant	Flowering Period (Days)	Fresh weight of Flower(g)	Day weight of Flower(g)		
<b>T<sub>0</sub></b>	81 <sup>c</sup>	12 <sup>b</sup>	18 <sup>d</sup>	13.33 <sup>c</sup>	68.33 <sup>b</sup>	29.66 <sup>c</sup>	8.33 <sup>a</sup>	1.65 <sup>b</sup>	0.08 <sup>b</sup>		
<b>T<sub>1</sub></b>	88.66 <sup>bc</sup>	12 <sup>b</sup>	19 <sup>cd</sup>	15.66 <sup>c</sup>	62.33 <sup>ab</sup>	33.66 <sup>ab</sup>	7.33 <sup>a</sup>	1.88 <sup>ab</sup>	0.15 <sup>ab</sup>		
<b>T<sub>2</sub></b>	89.33 <sup>bc</sup>	12.66 <sup>b</sup>	20 <sup>bc</sup>	18 <sup>bc</sup>	61.33 <sup>ab</sup>	33.66 <sup>ab</sup>	7.33 <sup>a</sup>	1.88 <sup>ab</sup>	0.15 <sup>ab</sup>		
<b>T<sub>3</sub></b>	105.66 <sup>a</sup>	15 <sup>a</sup>	22.66 <sup>a</sup>	22.33 <sup>ab</sup>	56.33 <sup>a</sup>	35.66 <sup>ab</sup>	9.33 <sup>a</sup>	2.313 <sup>a</sup>	0.19 <sup>a</sup>		
<b>T<sub>4</sub></b>	104 <sup>a</sup>	13 <sup>b</sup>	22.33 <sup>a</sup>	16 <sup>c</sup>	56 <sup>a</sup>	44.66 <sup>a</sup>	9 <sup>a</sup>	1.893 <sup>ab</sup>	0.18 <sup>a</sup>		
<b>T<sub>5</sub></b>	105.33 <sup>a</sup>	12.66 <sup>b</sup>	20.33 <sup>bc</sup>	24.5 <sup>a</sup>	65.33 <sup>ab</sup>	44 <sup>a</sup>	8 <sup>a</sup>	1.426 <sup>b</sup>	0.16 <sup>a</sup>		
<b>T<sub>6</sub></b>	96 <sup>ab</sup>	11.33 <sup>b</sup>	21.33 <sup>ab</sup>	22.67 <sup>ab</sup>	59.33 <sup>ab</sup>	41.33 <sup>bc</sup>	8.33 <sup>a</sup>	1.423 <sup>b</sup>	0.13 <sup>ab</sup>		
<b>CD (p&lt;0.05)</b>	9.89	1.79	1.62	5.39	5.2	7.32	NS	0.56	NS		
<b>SEM</b>	3.2	0.58	0.52	1.75	3.17	2.37	0.57	0.18	146.12		
<b>F-test</b>	8.26*	4.1*	9.68*	6.50*	2.34*	6.54*	0.37	3.4*	2.1		

Note: Data marked by common letters are not statistically different according to the DMRT at p < 0.05. NS represents non-significant differences among the treatments. \* represents that the F test was significant at p < 0.05. CD represent critical difference, and SEM represents standard error of the mean.

enhanced chlorophyll content. These findings suggest that integrating vermicompost into the cultivation of *G. rigens* can effectively boost both vegetative growth and flowering performance (Esmaili *et al.*, 2022). Our investigation into the effect of growth media on the vegetative growth and flowering characteristics of *G. rigens* revealed that treatment T<sub>3</sub> (30% Vermicompost + 70% Basal medium + NPK) significantly improved six of the nine recorded traits: number of leaves per plant, plant height, root length, flowering duration, fresh weight of flowers, and dry weight of flowers. T<sub>4</sub> enhanced two parameters: the number of flowers per plant and the days to flower bud initiation. Treatment T<sub>3</sub> alone promoted the enlargement of leaf area. Consequently, T<sub>3</sub> may be advised for attaining economically superior yields in *G. rigens* production.

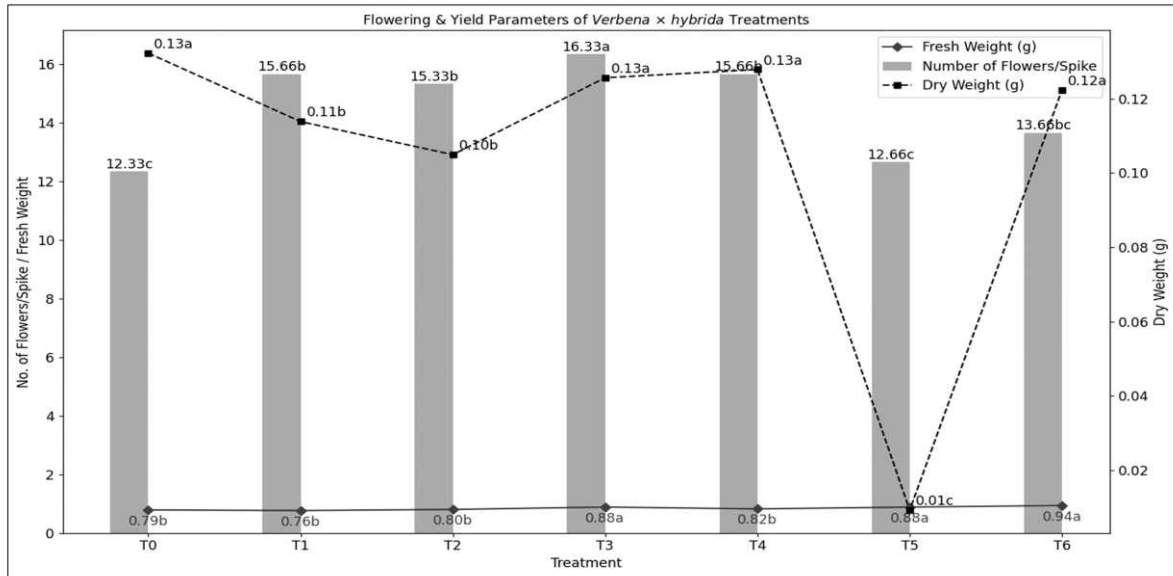
#### **Effect of vermicompost on the growth and yield of *Verbena X hybrida***

Growth parameters of *Verbena X hybrida* var. *Verbena Hybrida* Tuscan Mix. *viz.*, average numbers of leaves plant<sup>-1</sup>, root length (cm) and leaf area (cm<sup>2</sup>) were recorded at the time of flower bud initiation and the pertaining data are summarised in Table 6. The average number of leaves per plant (90.33) was highest in the T<sub>2</sub> treatment (20% Vermicompost + 80% Base medium + NPK), followed by T<sub>3</sub> (84), which was comparable to each other and significantly different from T<sub>0</sub>, T<sub>1</sub>, T<sub>3</sub>, T<sub>5</sub> and T<sub>6</sub>. The number of branches per plant exhibited considerable variation throughout the treatments, with a maximum recorded in T<sub>3</sub> (11.66 cm). The plant height recorded the highest in T<sub>3</sub> and T<sub>4</sub> (18.66 cm), but was at par with the plant heights recorded from other treatments. The maximum root length was recorded in T<sub>3</sub> (22.33 cm) and T<sub>6</sub> (22 cm), greatly exceeding the results of the other treatments. The leaf area of *Verbena* showed no significant variation among the treatments, reaching a maximum in T<sub>5</sub> (6.33 cm).

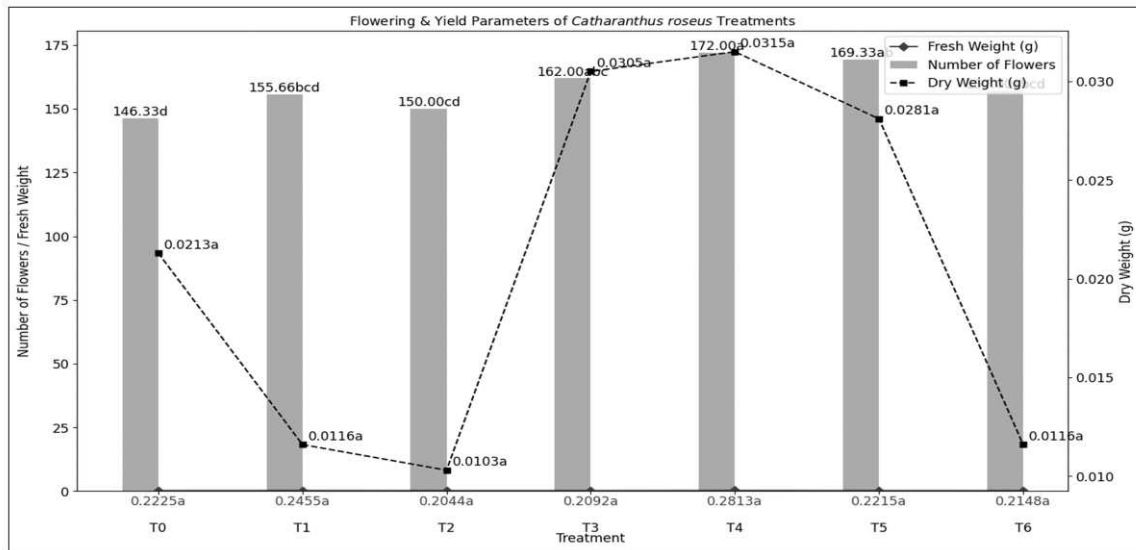
The yield in terms of floral parameters, including minimum days to flower bud initiation, number of flowers per plant, flowering duration (days), and fresh and dried weight of flowers (g), is documented and summarized in Table 6 and flowers number as well as fresh and dry weight of flowers is given in Fig. 3. The

minimum days to flower bud initiation were observed in T<sub>3</sub> (54), followed by T<sub>2</sub> (60.33), significantly lower than other treatments. The effect of vermicompost doses on flowering showed an increasing trend till T<sub>3</sub> and then declined to a certain extent in T<sub>5</sub>. The highest number of flowers per plant was recorded in T<sub>3</sub> (16.33). Number of days to flowering showed no significant differences across the treatments, ranging from 4.66 (T<sub>5</sub>) to 6.33 (T<sub>3</sub>). The highest fresh weight of flowers was obtained from T<sub>6</sub> (0.9365 g), followed by moderately low in T<sub>3</sub> (0.8836 g) and T<sub>5</sub> (0.8834 g) as compared to the rest treatments. The maximum dry weights were seen in T<sub>0</sub> (0.13 g), T<sub>4</sub> (0.13 g), and T<sub>3</sub> (0.12 g), which were comparatively higher than the other treatments.

It is generally referred to as Garden Verbena or Verbena. Verbenas are hybrid plants belonging to the Verbenaceae family, typically cultivated as annuals, with most species originating from the tropical and subtropical regions of the Americas. It is utilized as a medicinal plant for alleviating fever, headaches, and intestinal issues, and is commonly employed for bedding, edging, or in rock gardens due to its enduring flowers and capacity to attract butterflies. Specific studies on the effects of vermicompost on *Verbena X hybrida* (*Garden verbena*) are limited. A study by Tepecik *et al.* (2023) examined the impact of sewage sludge on garden verbena (*Verbena hybrida*), focusing on plant nutrients and heavy metal levels. The findings indicated that sewage sludge applications influenced plant growth and soil properties, suggesting potential benefits for ornamental plant cultivation. Additionally, research by Marchese *et al.* (2006) explored the use of river waste and Argentinean peat as alternative substrates for plug production of *Verbena X hybrida*. The study found that these locally produced substrates could be viable substitutes for traditional peat, affecting germination and early growth stages. While direct comparisons between different composts are limited, the research suggests that organic amendments like sewage sludge and alternative substrates can positively impact plant growth and yield. Our research into the effect of growth media on the vegetative growth and flowering characteristics of *Verbena X hybrida* revealed that treatment T<sub>3</sub> (30% Vermicompost + 70% Base



**Fig. 3.** Graphical representation of the effect of different vermicompost treatments on four key flowering and yield parameters of *Verbena X hybrida*. Data marked by common letters are not statistically different according to the DMRT.



**Fig. 4.** Graphical representation of the effect of different vermicompost treatments on four key flowering and yield parameters of *Catharanthus roseus*. Data marked by common letters are not statistically different according to the DMRT.

**Table 6.** Vermicompost effect on growth and yield of *Verbena X hybrida*

Treatment	Growth Parameters						Flowering					
	Numbers of Leaf/plant	Numbers of Branches/plant	Plant Height (cm)	Root Length (cm)	Leaf Area (cm <sup>2</sup> )	Days to flower bud initiation	Nos. of Spikes	Number of flower/Spikes	Flowering Period (Days)	Fresh weight of Flower(g)	Day weight of Flower(g)	
T <sub>0</sub>	66.33 <sup>bc</sup>	7.66 <sup>c</sup>	16.16 <sup>a</sup>	17.33 <sup>c</sup>	4.5 <sup>a</sup>	70 <sup>a</sup>	12.33 <sup>a</sup>	12.33	6	0.7859	0.1322	
T <sub>1</sub>	71 <sup>bc</sup>	9.66 <sup>abc</sup>	15.33 <sup>a</sup>	19.33 <sup>bc</sup>	4.66 <sup>a</sup>	60 <sup>bc</sup>	25.66 <sup>b</sup>	15.66	5.66	0.7644	0.1138	
T <sub>2</sub>	90.33 <sup>a</sup>	8.66 <sup>bc</sup>	14.66 <sup>a</sup>	18.33 <sup>c</sup>	5.66 <sup>a</sup>	60.33 <sup>c</sup>	24.33 <sup>b</sup>	15.33	5	0.8033	0.1049	
T <sub>3</sub>	84 <sup>a</sup>	11.66 <sup>a</sup>	18.66 <sup>a</sup>	22.33 <sup>a</sup>	5.66 <sup>a</sup>	54 <sup>c</sup>	32 <sup>b</sup>	16.33	6.33	0.8836	0.1256	
T <sub>4</sub>	79.66 <sup>ab</sup>	11 <sup>ab</sup>	18.66 <sup>a</sup>	21 <sup>ab</sup>	4.5 <sup>a</sup>	58.66 <sup>bc</sup>	31.33 <sup>b</sup>	15.66	5	0.8216	0.1278	
T <sub>5</sub>	56.33 <sup>c</sup>	8.33 <sup>c</sup>	17.66 <sup>a</sup>	21 <sup>ab</sup>	6.33 <sup>a</sup>	65.66 <sup>ab</sup>	27.33 <sup>b</sup>	12.66	4.66	0.8834	0.0093	
T <sub>6</sub>	66 <sup>bc</sup>	11 <sup>ab</sup>	16 <sup>a</sup>	22 <sup>a</sup>	4.83 <sup>a</sup>	66.66 <sup>a</sup>	24 <sup>b</sup>	13.66	5.66	0.9365	0.1223	
<b>CD (p&lt;0.05)</b>	13.86	2.13	NS	1.92	NS	6.21	8.66	NS	NS	NS	NS	
<b>SEM</b>	4.49	0.69	2.48	0.62	0.59	2.02	2.80	1.41	0.75	0.65	0.08	
<b>F-test</b>	9.00	3.96	1.126	8.07	3.396	7.78	5.69	1.51	0.67	0.4	1.31	

*Verbena X hybrida*

Note: Data marked by common letters are not statistically different according to the DMRT at  $p < 0.05$ . NS represents non-significant differences among the treatments. \* represents that the F test was significant at  $p < 0.05$ . CD represent the critical difference, and SEM represents the standard error of the mean.

**Table 7.** Vermicompost effect on growth and yield of *Catharanthus roseus*

Treatment	Growth Parameters						Flowering				
	Numbers of Leaf/plant	Numbers of Branches/plant	Plant Height (cm)	Root Length (cm)	Leaf Area (cm <sup>2</sup> )	Days to flower bud initiation	Number of flowers/pot or Plant	Flowering Period (Days)	Fresh weight of Flower(g)	Day weight of Flower(g)	
T <sub>0</sub>	117 <sup>f</sup>	9.66 <sup>a</sup>	48.26 <sup>d</sup>	11.16 <sup>a</sup>	11.16 <sup>a</sup>	61 <sup>a</sup>	146.33 <sup>d</sup>	6 <sup>a</sup>	0.2225 <sup>a</sup>	0.0213 <sup>a</sup>	
T <sub>1</sub>	129 <sup>c</sup>	13.66 <sup>a</sup>	47.413 <sup>d</sup>	11.66 <sup>bcd</sup>	12.83 <sup>a</sup>	62 <sup>a</sup>	155.66 <sup>bcd</sup>	6.33 <sup>a</sup>	0.2455 <sup>a</sup>	0.0116 <sup>a</sup>	
T <sub>2</sub>	136.66 <sup>d</sup>	12.66 <sup>a</sup>	53.34 <sup>c</sup>	12.5 <sup>ab</sup>	10.33 <sup>a</sup>	56.66 <sup>a</sup>	150 <sup>cd</sup>	6.66 <sup>a</sup>	0.2044 <sup>a</sup>	0.0103 <sup>a</sup>	
T <sub>3</sub>	148 <sup>c</sup>	11.33 <sup>a</sup>	58.2 <sup>bc</sup>	12.5 <sup>ab</sup>	13.33 <sup>a</sup>	60.66 <sup>a</sup>	162 <sup>abc</sup>	6.33 <sup>a</sup>	0.2092 <sup>a</sup>	0.0305 <sup>a</sup>	
T <sub>4</sub>	152.66 <sup>c</sup>	14.33 <sup>a</sup>	58.42 <sup>ab</sup>	12.66 <sup>a</sup>	11.5 <sup>a</sup>	53.66 <sup>a</sup>	172 <sup>a</sup>	7.66 <sup>at</sup>	0.2813 <sup>a</sup>	0.0315 <sup>a</sup>	
T <sub>5</sub>	172.33 <sup>a</sup>	11.66 <sup>a</sup>	59.33 <sup>a</sup>	12.33 <sup>abc</sup>	15.5 <sup>a</sup>	53.66 <sup>a</sup>	172 <sup>a</sup>	7.66 <sup>a</sup>	0.2813 <sup>a</sup>	0.0315 <sup>a</sup>	
T <sub>6</sub>	160.33 <sup>b</sup>	13.33+a	54.53 <sup>c</sup>	11.5 <sup>cd</sup>	12.66 <sup>a</sup>	63.33 <sup>a</sup>	157 <sup>abc</sup>	6.33 <sup>a</sup>	0.2148 <sup>a</sup>	0.0116 <sup>a</sup>	
CD (p<0.05)	6.64	NS	3.31	0.30	NS	NS	15.33	NS	NS	NS	
SEM	2.15	1.31	1.07	0.94	1.27	2.09	4.97	0.44	0.02	0.01	
F-test	87.54*	5.62*	13.85*	4.00*	1.8	2.05	4.25*	1.79	1.59	2.14	

Note: Data marked by common letters are not statistically different according to the DMRT at p < 0.05. NS represents non-significant differences among the treatments. \*represents that the F test was significant at p < 0.05. CD represent the critical difference, and SEM represents the standard error of the

significantly improved eight of the eleven recorded traits. These traits included the number of branches per plant, the height of the plant, the length of the roots, the number of days until the flower bud initiation, the number of flowers per spike, the flowering duration, the flowering duration, and the fresh weight of the flowers. Therefore, T<sub>3</sub> might be recommended to achieve economically superior yields in the production of *Verbena X hybrida* in farmers' fields.

### Effect of vermicompost on the growth and yield of *Catharanthus roseus*

Growth parameters of *Catharanthus roseus* var. Vinca Sunstorm Formula Mix *viz.*, average numbers of leaves plant<sup>-1</sup>, root length (cm) and leaf area (cm<sup>2</sup>) were recorded at the time of flower bud initiation and the pertaining data is summarised in Table 7 and number of flowers and fresh and dry weight of flowers is given in Fig. 4. The average number of leaves per plant showed a rising tendency and was determined to be highest in T<sub>3</sub> (172.33) and subsequently dropped in T<sub>6</sub> (160.33). The largest number of branches per plant was recorded in T<sub>4</sub> (14.33 cm); however, there were no significant differences among the treatments overall. The tallest plant height was observed in T<sub>3</sub> (59.33 cm), followed by T<sub>4</sub> (58.42 cm) and T<sub>5</sub> (58.2 cm). The highest root length was seen in T<sub>4</sub> (12.66 cm), significantly deviating from the results of the other treatments. The leaf area of *C. roseus* exhibited no significant variation among the treatments, attaining a maximum of 15.55 cm<sup>2</sup> in T<sub>5</sub>.

The yield of floral parameters, such as minimum days to flower bud initiation, number of flowers per plant, flowering duration (days), and fresh and dried weight of flowers (g), was recorded and reported in Table 7. The shortest duration for flower bud initiation was recorded in T<sub>4</sub> (53.66), succeeded by T<sub>2</sub> (56.66), both lower than the other treatments. The impact of vermicompost doses on flowering resulted in the highest number of flowers per plant in T<sub>3</sub> (172), with significant variation among the treatments. The duration of flowering exhibited no significant variations across the treatments, ranging from 7.66 days (T<sub>4</sub>) to 6 days (T<sub>3</sub>). The maximum fresh weight of flowers was recorded in T<sub>4</sub> (0.28 g), followed by T<sub>1</sub>

(0.24 g) and T<sub>5</sub> (0.20 g), which were moderately lower than the other treatments. The highest dry weights were seen in T<sub>4</sub> (0.31 g), T<sub>3</sub> (0.30 g), and T<sub>5</sub> (0.28 g), which were relatively superior to the other treatments.

Commonly referred to as Vinca or Madagascar periwinkle, it is a member of the Apocynaceae family. Vinca is esteemed not only for its aesthetic appeal but also for its versatility, flourishing in diverse situations ranging from full sun to partial shade. Research indicates that vermicompost significantly improves several growth parameters in *C. roseus*. A study by Sheikh (2018) demonstrated that the direct application of 80% vermiwash to soil improved seed germination and seedling growth in *C. roseus*, as measured by seedling traits (branch length, root length). Similarly, a field experiment by Sangeetha *et al.* (2012) assessed the impact of various organic sources, including vermicompost, on the growth and yield of *C. roseus*. The results showed that the combined application of recommended doses of inorganic fertilizers and vermicompost at 5 tons per hectare significantly increased plant height, number of branches per plant, shoot length, and root length compared to the control group. Our study on *C. roseus* vegetative growth and flowering parameters showed that among the 10 recorded traits, treatment T<sub>4</sub> (40% Vermicompost + 60% Base medium + NPK) significantly enhanced six parameters: number of branches per plant, root length, number of flowers per plant, flowering period, fresh weight and dry weight. Therefore, T<sub>4</sub> might be recommended to achieve economically superior yields in the production of *C. roseus* in farmers' fields.

### CONCLUSION

The current study was conducted in the red and lateritic zone of West Bengal, particularly at Purulia. Applying vermicompost to specific flowering plants improves soil fertility and enhances flower plant growth and yield parameters, including plant height, number of leaves, root length, leaf area, number of leaves, days to flower bud initiation, number of flowers, flowering periods, and fresh and dry weight of flowers. Our present investigation highlighted that treatment T<sub>3</sub> (30% vermicompost, 70% base medium, and NPK) was most effective in promoting the growth and yield of *Antirrhinum majus*, *Verbena X hybrida*,

and *Gazania rigens*. In contrast, *Catharanthus roseus* showed a more favourable response to treatment T<sub>4</sub> (40% vermicompost + basal media + NPK). These findings suggest that specific combinations of vermicompost and base media can significantly enhance the growth of various ornamental plants, though the optimal treatment may vary between species.

## DISCLAIMER

The authors declared that there is no conflict of interest while performing the work and preparation of the manuscript.

## REFERENCE

- Adhikary, S. 2012. Vermicompost: The story of organic gold: A review. *Agricultural Sciences*, **3**: 905-917.
- El-Sayed, A.A., El-Leithy, A.S., Bazraa, W.M. and Abdel-Latef, M.S. 2018. Effect of growing media, bio and organic fertilization on the flowering and chemical constituents of *Calendula officinalis* L. *Plants. Bioscience Research*, **15**(3): 2029-2040.
- Esmaili, M., Kalatejari, S., Fatehi, F. and Diyanat, M. 2022. Evaluation of biological fertilizers on growth of African daisies (*Gazania rigens* L.). *Journal of Soil Management and Sustainable Production*, **12**(2): 107-125.
- Esmaili, M., Kalatejari, S., Fatehi, F. and Diyanat, M. 2022. Evaluation of biological fertilizers of vermicompost and vermiwash application on growth of African daisies (*Gazania rigens* L.). *Journal of Soil Management and Sustainable Production*, **12**(2): 107-125.
- Evans, G.C. 1972. *The Quantitative Analysis of Plant Growth*. Berkeley, University of California Press.
- Gomez, K.A. and Gomez, A.A. 1984. *Statistical Procedures for Agricultural Research* (2nd ed.). John Wiley & Sons.
- Jackson, M.L. 1973. *Soil Chemical Analysis*. Prentice Hall Pvt. Ltd.
- Kaushal, S. and Kumari, P. 2020. Growing media in floriculture crops. *Journal of Pharmacognosy and Phytochemistry*, **9**(2): 1056-1061.
- Kumar, R., Singh, A.K., Tomar, K.S., Kanawjia, A. and Ojha, G. 2023. Studies on effect of different soil-based and soil-less growing media on growth and flowering of snapdragon (*Antirrhinum majus* L.). *Journal of Ornamental Horticulture*, **26**(1 and 2): 90-97.
- Manna, M.C. and Biswas, T.K. 1996. Effect of vermicompost on soil properties and productivity of greengram. *In Proceedings of the National Symposium on Soil Biology and Ecology*. Indian Society of Soil Science, 56-58.
- Marchese, N., Benedetto, A.D. and Lavado, R. 2006. The possibilities of river waste and Argentinean peat as a plug growing media for *Verbena x hybrida*. *International Journal of Agricultural Research*, **1**: 142-150.
- Mehmood, T., Ahmad, W., Ahmad, K.S., Shafi, J., Shehzad, M.A. and Sarwar, M.A. 2013. Comparative effect of different potting media on vegetative and reproductive growth of floral shower (*Antirrhinum majus* L.). *Universal Journal of Plant Science*, **1**(3): 104-111.
- Ministry of Agriculture and Farmers Welfare 2018. *Horticulture statistics at a glance. Department of Agriculture, Cooperation and Farmers Welfare, Government of India*.
- Moustafa, A.M.Y. and Khodair, A.I. 2007. Phytochemical investigation and a-cellulose content determination of *Gazania splendens* Moore. *Research Journal of Phytochemistry*, **1**: 21-32.
- Murphy, J.A.M.E.S. and Riley, J.P. 1962. A modified single solution method for the determination of phosphate in natural waters. *Analytica Chimica Acta*, **27**: 31-36.
- Olsen, S.R. 1954. Estimation of available phosphorus in soils by extraction with sodium bicarbonate (No. 939). US Department of Agriculture.
- Padhiyar, B.M., Bhatt, D.S., Desai, K.D., Patel, V.H. and Chavda, J.R. 2017. Influence of different potting media on growth and flowering of pot chrysanthemum var. Ajina purple. *International Journal of Chemical Studies*, **5**(4): 1667-1669.
- Rani, M., Kaushik, P., Bhayana, S. and Kapoor, S. 2023. Impact of organic farming on soil health and nutritional quality of crops. *Journal of the Saudi Society of Agricultural Sciences*, **22**(8): 560-569.
- Sheikh, S. and Dakhane, P.V. 2018. Effects of vermiwash on seed germination and seedling growth in *Catharanthus roseus* – a potent biofertilizer. *International Journal of Researches in Biosciences, Agriculture and Technology*, **3**: 105-109.

- Subbiah, B.V. and Asija, G.L. 1956. A rapid procedure for the estimation of available nitrogen in soils. *Current Science*, **25**: 259-260.
- Tepecik, M., Ongun, A.R., Kayıkcıoğlu, H.H., Delibacak, S., Birişçi, T., Aktaş, E., Önaç, A.K. and Balık, G. 2023. Effects of sewage sludge on marigold (*Tagetes erecta* L.) garden verbena (*Verbena hybrida*) plants and soil nutrient elements and heavy metal. *KSU Journal of Agriculture and Nature*, **26**(1): 161-171.
- Walkley, A. and Black, I.A. 1934. An examination of the Degtjareff method for determining soil organic matter, and a proposed modification of the chromic acid titration method. *Soil Science*, **37**(1): 29-38.

---

**FULL LENGTH ARTICLE**

---

**Chitosan and Aloe leaf gel extract based composite biofilm production using bagasse - microcrystalline cellulose as reinforcement**

---

Mithu Biswas<sup>1\*</sup>, Anusree Das<sup>1</sup>, Srabanti Rana<sup>1</sup>, Swastik Guha<sup>2</sup>

<sup>1</sup>Department of Botany, Asutosh College, Affiliated to University of Calcutta.

<sup>2</sup>Department of Environmental Studies, University of Delhi, North Campus.

---

Received : 30.10.2025

Accepted : 27.02.2026

Published : 30.06.2026

---

Next-generation composite biofilms or bioplastics, tailored with fiber reinforcements and additives for varied applications, has been the thrust area of research due to their sustainability, biodegradability or compostability. Chitosan biopolymer has gained significance in medical, pharmaceutical and food industries due to its unique film forming property, non-toxicity, antimicrobial activity and high gas barrier quality. The present study was performed by incorporating sugarcane bagasse - microcrystalline cellulose (BG-MCC) as reinforcement and Aloe leaf gel extract as an additive to chitosan matrix, to overcome the limitations of pure chitosan biofilms, such as hydrophilicity and poor mechanical properties. Glycerol (0.9%) is used as plasticizer in fabricating the biofilms. The BG-MCC composite biofilm showed improved water resistant property, acid and alkali tolerance, good flexibility, higher melting point (215°C) with delayed decomposition time of (3–4) weeks in active compost soil. Aloe leaf gel extract significantly enhanced the antioxidant property of chitosan biofilm by increasing the DPPH radical scavenging rate to 91%, showing immense potential for its application in active food packaging, medical and pharmaceutical sectors.

**Keywords:** Composite; reinforcement; sustainability; compostability; bagasse; antioxidant; antimicrobial; *Aloe barbadensis* Mill.

---

## INTRODUCTION

Plastics are mainly composed of synthetic polymers which are derived from petrochemicals. The diverse group of synthetic plastics due to their versatility, durability and low cost, have made their application ubiquitous and indispensable (Shen *et al.*, 2020; Reddy *et al.*, 2023). Plastics are non-biodegradable, non-compostable and often, carcinogenic chemicals or xenobiotic compounds can leach out from plastics into groundwater or rivers affecting the entire ecosystem (IUCN, 2025). Recent studies have focused

on developing biodegradable and compostable plastics being derived from natural polymers such as starch, cellulose, chitosan, and proteins, thereby reducing the hazardous environmental impact (Muneer *et al.*, 2021). The field of bio-based polymers from various animal wastes, agro-residues and/or food waste products or microbial sources has shown promising results in developing materials capable of forming biofilms / bioplastics with antimicrobial properties that contribute to the food, agriculture, biomedical and pharmaceutical industries (Román-Doval *et al.*, 2023; Moeini *et al.*, 2020; Wang *et al.*, 2021; Flórez *et al.*, 2022; Qureshi *et al.*, 2022; Dutta and Sit, 2024).

---

\*Corresponding author : mithu.biswas@asutoshcollege.in

### Green composite or composite biofilm/bioplastic

Composite consists of one (or more) harder and stronger discontinuous phases termed as 'reinforcement' that remains embedded in a continuous phase termed as the 'matrix' (Owonubi *et al.*, 2019). Recently, green composite science has received considerable attention for the development of composite biofilm/bioplastic owing to their eco-friendliness, sustainability, versatility and durability (Admase *et al.*, 2025). Biocomposite / green composite in the form of biofilm/bioplastic are fabricated out of natural plant or animal based biopolymers as matrix and natural cellulosic fibers/crystallites (micro or nano) as reinforcements (Samickannu *et al.*, 2022). Biopolymers, e.g., a) natural polymers: polysaccharides- starch, cellulose, chitosan, seaweed cell polysaccharides and proteins – collagen, casein, gluten, silk, etc. b) chemically synthesized polymers using renewable bio-based monomers: Polylactic acid (PLA), Polyglycolic acid (PGA) c) polymers produced by microorganisms or genetically modified bacteria: bacterial cellulose and polyhydroxyalkanoates (PHA) (Biswas, 2025), used singly or in combination are important in the development of composite biofilm/bioplastics. Biofilm/bioplastics prepared from different sources exhibit varied stiffness, brittleness, deformability and moisture sensitivity when compared to conventional synthetic plastics. Mechanical and thermal properties of biofilm/bioplastics can be improved with the addition of natural lignocellulosic fibers in the form of micro-crystalline cellulose / nano-crystalline cellulose, as reinforcements (Ventura-Cruz and Tecante, 2021). The use of composite technology with natural polymers, plasticizers and reinforcement materials is under development and a thrust area of research for future generation biofilm/bioplastic production (Kong *et al.*, 2023).

### Chitosan (CS) as a biopolymer matrix

Chitosan is a cationic polysaccharide obtained by chitin deacetylation. Chitin is a chief component of crustacean exoskeleton, a major waste product of the seafood processing industries all over the world (Varun *et al.*, 2017). Chitosan exhibits excellent cross-

linking and chelating properties due to the presence of reactive groups, ionic conductivity, and formation of intermolecular hydrogen bonds (Heo *et al.*, 2023). Its biocompatibility and non-toxicity makes it an attractive material for numerous applications, particularly in biomedical and pharmaceutical sector (Souza *et al.*, 2020; Aranaz *et al.*, 2021; Zhou *et al.*, 2023).

Various strategies have been applied to improve the mechanical properties of chitosan, using plasticizers like glycerol, sorbitol and cross-linkers such as glutaraldehyde, genipin, and tripolyphosphate (TPP). These cross-linkers enhance the mechanical strength and stability of chitosan by forming chemical or ionic bonds between chitosan chains (Woźniak and Biernat, 2022). Cross-linking the polymers with reinforcements such as micro or nano crystalline cellulose, fibers, fillers and whiskers, are newer attempts to enhance their mechanical properties (Priyadarshi and Rhim, 2020). Researchers are working on various types of antibacterial chitosan films, including chitosan films with metal nanoparticles, metal oxide nanoparticles, graphene, fullerene and its derivatives to expand the antioxidant and antimicrobial properties of the polymer matrix of the chitosan film (Khubiev *et al.*, 2023). The polymers are even blended with additives such as herbal extracts, essential oils, and also with other natural and synthetic polymers to tailor the product for specific end uses (Kumar *et al.*, 2023; Stefanowska *et al.*, 2023).

### Composite biofilm production using Chitosan as natural biopolymer matrix

Different research workers attempted to make biofilms fabricated out of different biopolymers. Biofilms are made out of chitosan and banana peel concentrate (*Musa paradisiaca*) using glycerol and sorbitol as plasticizer resulting in tensile strength of 46.4201 Mpa and 31.4228 MPa, respectively (Sofiah *et al.*, 2019). Antibacterial properties of edible film, fabricated out of chitosan, banana stem fiber MCC and glycerol was reported by Nurhaliza *et al.*, 2022. Biofilm was fabricated out of chitosan, glycerol and nanocellulose, derived from *Parthenium*

*hysterophorus*, an invasive plant species (Reddy *et al.*, 2023).

### **Aloe leaf gel extract as additive biopolymer**

*Aloe barbadensis* Mill. is a succulent, xerophytic plant of immense medicinal importance. Aloe leaf gel is used worldwide in cosmetics, food and pharmaceutical industry (Kumara *et al.*, 2021). Hyaluronic acid, heparin and acemannan are the main mucopolysaccharides found in Aloe, of which acemannan is the most unique and abundant. Moreover, such polysaccharides can reinforce gel formation through the synergistic interplay of ion-induced crosslinking and salting out in the presence of univalent or bivalent cations (Mensah *et al.*, 2025). Chitosan biofilms with *Aloe barbadensis*, *Cissus quadrangularis* and *Curcuma longa* plant extracts showed significant antibacterial activity against *Escherichia coli* and *Staphylococcus aureus* (Ganesan *et al.*, 2023). The rheological and antioxidant properties of the chitosan-based biofilm improved with the inclusion of *Aloe vera* leaf gel. A significant reduction in microbial growth was found in fruits coated with such biofilm, even after 28 days of cold storage (Kaur *et al.*, 2024).

### **Microcrystalline Cellulose (MCC) from sugarcane bagasse as reinforcement**

Cellulose fibers, cellulose whiskers, cellulose crystals, microcrystalline cellulose (MCC) nanocrystalline cellulose (NCC), monocystals, microcrystals are all cellulose derivatives commonly extracted from natural lignocellulosic resources (Samraj *et al.*, 2022). MCC is obtained by digesting the amorphous part of cellulose of lignocellulosic plant material and is characterized by a high degree of crystallinity, with values ranging from 55% to 80% (Xiang *et al.*, 2016). MCC is generally used as reinforcement in thermoset, thermoplastic and bio-based polymer matrices to increase the mechanical strength of the biocomposite (Jethoo, 2019). Sugarcane bagasse, a major lignocellulosic waste of sugar industry, is used as a raw material for MCC extraction in the present work.

Composite films have the potential to crosslink two

distinct types of biopolymers. When combined with other additives like nano-particles, metal ions, antibiotics, and other plant extracts, these biopolymer-derived films can have enormous applications in wider areas of science. Poor mechanical properties of chitosan-based biofilms have led to the development of reinforced chitosan-based biofilms. Fabrication of composite biofilm from chitosan (biopolymer) and Aloe leaf gel extract, as matrices, reinforced with bagasse-MCC and using glycerol as plasticizer, was investigated in the present work. A novel combination of composite biofilm was successfully fabricated and characterized. This study focuses on the process optimization in fabricating the biofilm and characterization of the biodegradability of biofilm and other physico-chemical properties for its application in medical and pharmaceutical sector or food packaging industries.

## **MATERIALS AND METHODS**

### **Materials**

Materials used for the experiment were chitosan (MW-1250 kDa, SRL), glycerol (molecular biology, SRL), de-ionized water, glacial acetic acid, bagasse from local market and fresh Aloe leaf (white gel part extracted from fresh leaf and homogenized into a paste in mixer).

### **Methods**

#### **Methods of MCC extraction from sugarcane bagasse and estimation of percent yield recovery of MCC**

Sugarcane bagasse (BG) was cut into small pieces, washed thoroughly in water, sun-dried and ground into coarse powder. MCC extraction was done following modified chlorination and alkaline method by Nigam *et al.*, 2021. The BG-powder was treated in NaOH solution (5 % w/v) in a ratio 1:20 (w/v) for 2 h at 80°C, washed thoroughly till neutral pH and then dried in oven at 60°C for 3 h. Dried fiber was then treated with 4% Sodium hypochlorite (NaClO) solution with continuous stirring at 80°C for 2 h while maintaining a fiber / liquid ratio of 1:20 (w/v). Bleached fiber was washed thoroughly and oven-dried at 60°C for 3 h.

the sample with 2.5 N HCl for 1 h at 50°C in a ratio 1:60 (w/v) under continuous stirring. Cold water was added to stop the reaction. The diluted suspension was then centrifuged at 4000 RCF for 10 min to obtain precipitation of white crystalline cellulose which was further dried and sieved to collect size below 100 µm. The sieved crystalline fiber was coded as BG-MCC (Bagasse-Microcrystalline Cellulose). Gravimetric method was used to estimate the percent yield recovery (wt%) of MCC.

Percent Yield Recovery (wt%) = (Final weight of recovered BG-MCC / Initial dry weight of Bagasse taken for chemical pretreatment) x 100.

### **Fabrication of biofilm**

Solvent casting method was followed for producing chitosan biofilms (Hasan *et al.*, 2022). Chitosan was dissolved in 50 ml of 1% acetic acid @ 2% (w/v), stirred for 1 h at 350 rpm using a magnetic stirrer at 50°C. Glycerol (30%) - 1.5 ml (equivalent to 0.9% v/v of reaction mixture) was added under continuous stirring process and the stirrer was set at 1000 rpm for 1h. The solution was casted in equal amount on two glass petriplates (4.5 cm diameter) and kept in an oven at 45°C for 24 h to dry and form a solid film. Biofilm fabricated out of only chitosan (biopolymer) and glycerol (plasticizer) was taken as control Sample A – (Chitosan + glycerol as plasticizer).

Sample B – (Chitosan + BG-MCC+ glycerol): Aqueous mixture of MCC (1 % w/v) was prepared by continuous stirring for 1 h at 350 rpm using a magnetic stirrer. MCC- 10 ml was added to 40 ml of 2% chitosan solution (as prepared in sample A) and stirred for 30 min at 1000 rpm and 70°C. Glycerol (30%) - 1.5 ml was added under continuous stirring process for another 1h. The solution was casted similarly on petri plates and kept in oven at 45°C for 24 h to get the biofilm.

Sample C – (Chitosan + Aloe gel + BG-MCC+ glycerol): MCC (1 %) - 10 ml was added to 30 ml of 2% chitosan solution and stirred for 30 min at 1000 rpm and 70°C. Fresh Aloe gel – 10 ml was added and stirred for another 30 min under same condition.

Glycerol (30%) - 1.5 ml was added under continuous stirring process for another 1h. The solution was casted similarly on petriplates and kept in oven at 45°C for 24 h to get the biofilm. A process flow diagram showing BG-MCC production and biofilm fabrication is given in Fig. 1.

### **Optimization of wt% of MCC in biofilm production and analyzing the thickness and flexibility of the fabricated biofilm**

MCC (wt%) in biofilm fabrication was optimized by adding 0.05 %, 0.1 % and 0.2 % respectively, in three separate sets and the quality of finished biofilms were assessed by its flexibility and thickness test (Jethoo, 2019). After 1 week of the biofilm production, a weight of 200g was placed over folded biofilm and kept for 24 h and the physical changes were observed thereafter.

The thickness test of biofilm was measured using a micrometer scrap (accuracy of 0.01 mm). Thickness was measured at five points to obtain an average value. Measurement was taken 3 times. Plastic thickness values are obtained using the formula:

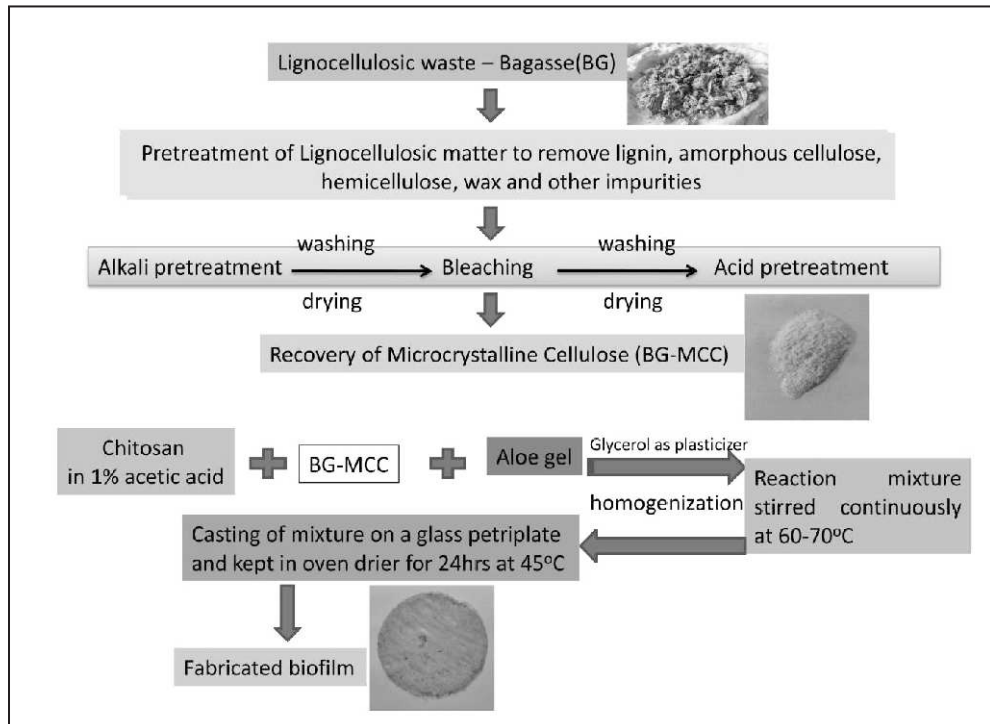
$$\text{Average thickness} = (\text{point 1} + \text{point 2} + \text{point 3} + \text{point 4} + \text{point 5}) / 5$$

### **Determination of melting point of biofilm**

Differential scanning calorimeter (DSC) was used to analyze the melting point of biodegradable plastics. DSC is a method to analyze the physical and chemical changes of materials due to phase transformation and exothermic or endothermic reaction (Vyazovkin, 2002).

### **Water hydration property of biofilm**

Small pieces of sample A, B and C were taken and initial weight of individual sample was measured. Samples were immersed in distilled water, and kept in waterbath at a constant temperature of 50°C for 24 h. The samples were removed after 24 h, surface dried and weighed again to determine the amount of water absorbed. The amount of water absorbed was



**Fig.1.** Process flow diagram showing BG-MCC production and biofilm fabrication

calculated in percentage. The following equation was used to measure the water absorption percentage:

$$WA\% = [(W_f - W_0)/W_0] \times 100 \dots\dots\dots W_0 = \text{Initial weight (g)}; W_f = \text{Final weight (g) after 24 h. (Nazrin et al., 2025).$$

**DPPH radical scavenging test for total antioxidant activity evaluation**

The free radical scavenging activity of biofilm samples (Control-Sample A, Sample B and Sample C) were measured by the DPPH (2,2-Diphenyl-1-picrylhydrazyl) scavenging method (Gulcin and Alwaseel, 2023). A 0.1mM solution of DPPH in methanol was prepared and 2 ml of this solution was added to 0.2g of each of the three samples (in triplicates). The reaction mixtures were kept in dark for 30 min. A control set-up with only methanolic DPPH solution was also kept under same condition. The absorption was measured at 517 nm in UV-VIS Spectrophotometer after 30 min of reaction. The DPPH radical scavenging activity was calculated

according to the following equation:

$$\% \text{ of DPPH scavenging activity} = \{1 - (AbS/AbC)\} \times 100$$

Where, AbC is the absorbance of the control (0.1mM DPPH in methanol) and AbS is the absorbance of the test samples using methanol as blank.




**Alkali and acid tolerance test**

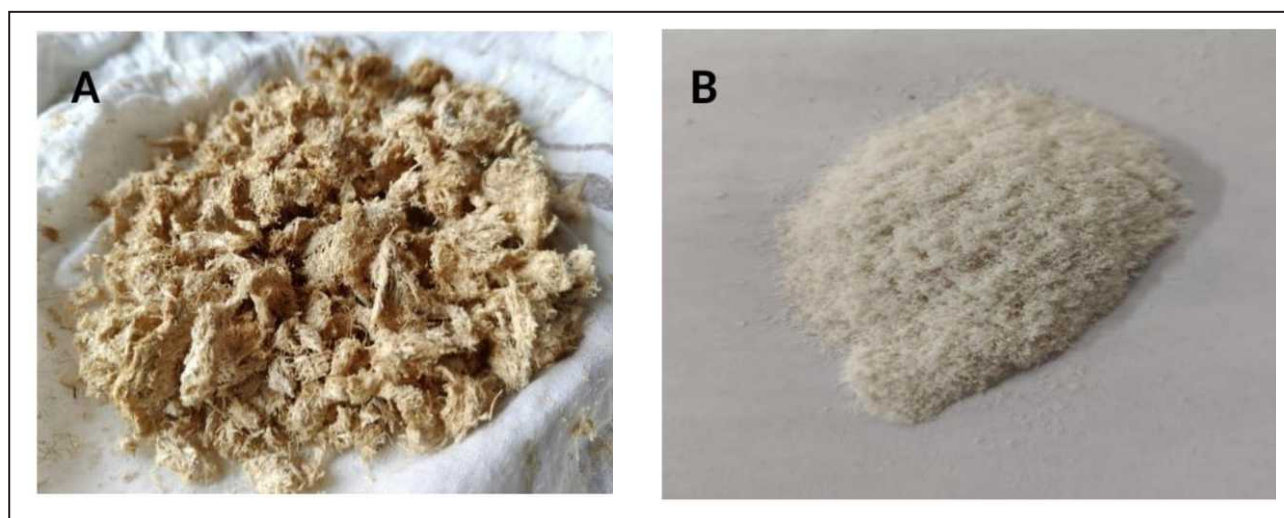
Biofilm degradation in acidic or alkaline conditions was typically tested by immersing samples in solutions of a specific strength for a given period of time, then analyzing their physical changes (Samraj et al., 2022).

**Soil burial degradability test of biofilm**

Biofilm samples of 1 sq cm size were cut and initial weights were measured. They were buried in active compost soil at a depth of 7.5 cm, and then incubated for 30 days with sampling time every 7 days. After

**Table 1.** Biofilm produced in different experimental set-ups

Experimental set-up	Chitosan @25% in 1% acetic acid solution	BG-MCC and/or Aloe gel	0.9% Glycerol as plasticizer	Total volume of reaction mixture	Homogenization of reaction mixture on magnetic hot plate at 1000 rpm at 70°C  Observation after 48 h of oven drying at 45°C	Photograph of biofilm produced
<b>Control A</b> Chitosan + glycerol	50 ml	-	1.5 ml	51.5 ml	Transparent and delicate biofilm	
<b>Sample B</b> Chitosan+ BG-MCC+ glycerol	40 ml	10 ml MCC @ 0.1%	1.5 ml	51.5 ml	Opaque and flexible biofilm	
<b>Sample C</b> Chitosan+ BG-MCC+ Aloe gel + glycerol	30 ml	10 ml MCC @ 0.1% + 10 ml fresh Aloe lea gel extract	1.5 ml	51.5 ml	Opaque, glossy and flexible biofilm	

**Fig.2.** Bagasse as raw material (A) and recovered microcrystalline cellulose from bagasse (B)

every 7 days, the buried samples were taken out, cleaned to remove surface dirt and soil and then re-weighed. Experiments were done in triplicates. Similar such biofilm samples were kept in normal room condition with relative humidity ~ 88% and temperature 35°C to 37°C. The weight loss of the biofilm samples was calculated using following equation:

$$\% \text{ Weight change} = (W_0 - W_f) / W_0 \times 100$$

$W_0$  = Initial weight (g);  $W_f$  = Final weight (g) (Nissa *et al.*, 2019)

## RESULTS AND DISCUSSION

### Estimation of percent yield recovery of MCC

BG-MCC of 17.69g was recovered from 30g of dried sugarcane bagasse, which accounts for a yield recovery of 58.96%. The cellulose, hemicellulose and lignin contents of sugarcane bagasse are (32% to 45%), (20% to 32%) and (17% to 32%), respectively with 1.0–9.0% ash and some extractives (Alokika *et al.*, 2021). Due to high cellulose content, the yield or percent recovery rate of BG-MCC was also high (58.96%). The recovery rate of MCC from sugarcane bagasse varies depending on the specific process and pretreatment methods used. A maximum of 80% recovery was achieved from bagasse, using chemical catalysts (Katakojwala and Venkata Mohan, 2020). The pretreatment process helped in removing the lignin, amorphous part of cellulose, wax, moisture and other impurities leaving behind, white particles of microcrystalline cellulose (Fig. 2).

The crystallinity and the microstructure of crystalline cellulose have profound effect on the thermal and mechanical properties of biofilm. Addition of pretreated fibers, micro or nanocrystalline cellulose can further enhance their interaction with the biopolymer matrix leading to enhancement of flexibility of composite biofilm (Biswas, 2025).

### Fabrication of biofilm

A modified protocol was followed for fabricating chitosan biofilm using solvent casting method, Table 1. It was observed that chitosan biofilm (Control

Sample-A) was transparent, soft and delicate, which was not easy to handle. The biofilms produced with the application of MCC in both Sample B and C, were opaque and more flexible. The MCC reinforcement might have enhanced its mechanical properties. The MCC crystals during homogenization spread uniformly as observed in the biofilms. Sample C with Aloe gel was glossier but less flexible than Sample B might be due to the higher water content of the fresh Aloe gel.

### Optimization of wt% of MCC in biofilm production and analyzing the thickness and flexibility of the fabricated biofilm

Data in Table 2 revealed that 0.1 wt% of BG-MCC was optimum because the biofilm produced was smooth, firm, flexible and self-supporting. Similar thicknesses of films were reported using different starch sources and chitosan, either singly or in combination (Das and Chowdhury, 2016). BG-MCC (0.5wt %), produced soft and pliable biofilm which was not firm. Though the thickness of biofilm increased with the increase in concentration of BG-MCC (0.2 wt%), it made the biofilm grainy and brittle. MCC has high compressibility and when added in optimum amount, strengthens the biofilm (Boey *et al.*, 2022). There were no signs of crack or any other visible changes even after keeping the biofilm folded under the applied weight.

### Determination of melting point of biofilm

The melting point of naturally occurring polymer derived from chitosan, is generally in the range of 200°C to 250°C. However, the exact melting point can vary based on factors like source and purity. The melting point of biofilms varies significantly depending on the specific type and composition. For example, starch biofilms can have a melting point ranging from 57°C to 201°C, while composite biofilms melt within 50°C to 210°C, in some cases might reach upto 303°C. Some biofilms like bio-PET have a melting point between 250–260°C. Others, like polybutylene succinate (PBS), have a melting point of 90–120°C (Dheana and Ekawardhani, 2022). Sample-B biofilm showed a high melting point of 215°C, Table 3. Generally fiber reinforcement in biofilms lead to an

**Table 2.** Thickness and flexibility test of biofilm samples

Sl. No.	Samples	Thickness ( $\mu\text{m}$ )			Average Thickness ( $\mu\text{m}$ )	Observation (texture and flexibility of biofilm)
		(i)	(ii)	(iii)		
1	0.05% MCC	76	83	88	82	Soft and pliable
2	0.1% MCC	150	156	161	158	Smooth, firm and flexible
3	0.2% MCC	248	256	258	254	Grainy texture with increase in brittleness

**Table 3.** Comparison of melting points of standard synthetic and biofilms

Category of synthetic polymers with standard value of melting point ( $^{\circ}\text{C}$ )			Category of biofilms with reported range of melting point ( $^{\circ}\text{C}$ )		Experimental biofilms with observed value of melting point ( $^{\circ}\text{C}$ )		
High Density Polythene	Polyvinyl chloride	Polyvinyl fluoride	Starch biofilms	Composite biofilms	Control sample-A (Chitosan +glycerol)	Sample-B (Chitosan-BG-MCC+ glycerol)	Sample-C (Chitosan BG-MCC+ Aloe gel+ glycerol)
130	160	200	57-201	50-210	210	<b>215</b>	200

increase in the biofilm's melting point ( $T_m$ ). This is because the fibers can act as barriers to the movement of polymer chains, making it harder for the material to melt at lower temperatures (Amin *et al.*, 2019). Application of microcrystalline or nanocrystalline cellulose is therefore more effective in fabricating biofilm of improved qualities. Sample-C contained fresh Aloe gel with high water content and added in volume replacement of chitosan, which might have caused the lowering of melting point than control Sample-A.

#### Water hydration property of biofilm

An interesting result was observed after 24h hydration of biofilm samples in water, Table 4. In control Sample

A, the weight increased by 22.51%, might be due to absorption of water by un-crosslinked part of chitosan molecules primarily through interactions between water molecules and the hydrophilic functional groups (hydroxyl and amino groups) present in the chitosan structure. In Sample B and Sample C, the weight increased nominally by 1.15% and 4.29%, respectively. The reason might be due to the varying degrees of cross-linking in both the samples. The cross-linking process with the crystalline cellulose might have resulted in surface modification, resulting in water and chemical resistance. The modified surface layer acts as a barrier to water migration (Wei *et al.*, 2019).

**Table 4.** Water hydration property of biofilm

Sample	Initial weight (mg)	Final weight (mg)	Average (%) weight change after 24 h
Control Sample-A	205	252	22.51%
	200	242	
	208	257	
Sample-B	203	205	1.15%
	202	204	
	205	208	
Sample-C	202	207	4.29%
	200	210	
	204	215	


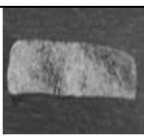
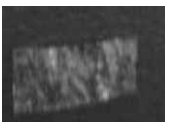
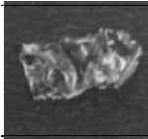
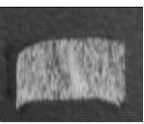
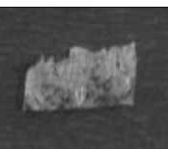
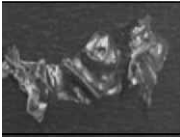




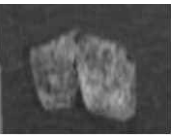
**DPPH radical scavenging test for total antioxidant activity evaluation**

The DPPH radical is a stable free radical that appears as a deep violet solution, commonly used for assessment of antioxidant activity. Presence of antioxidant compound in the reaction mixture neutralizes the DPPH radical thereby causing the colour of the solution to fade from violet to yellow. The higher the concentration of effective antioxidants the greater the percentage of DPPH inhibition as measured by the change in absorbance (AbS) (Gulcin and Alwasel, 2023). In Table 5, pure chitosan biofilm showed minimum scavenging activity with 15% inhibition. Sample-B resulted in 63% inhibition which

**Table 5.** Antioxidant property of biofilm showing % inhibition

Sl. No.	Sample	Average AbS at 517 nm	Standard Deviation (std) and Coefficient of Variation (CV)	% inhibition
Control 1	2 ml (0.1 mM) DPPH in methanol	0.035	$\pm 0.002$ std 5.71 % CV	No inhibition
Control 2				
Control 3				
A1	2 ml DPPH solution in sample A	0.030	$\pm 0.003$ std 9.71 % CV	15%
A2				
A3				
B1	2 ml DPPH solution in sample B	0.013	$\pm 0.0005$ 3.84 % CV	63%
B2				
B3				
C1	2 ml DPPH solution in sample C	0.003	$\pm 0.00017$ 5.66 % CV	91%
C2				
C3				

**Table 6.** Physical changes observed after alkali treatment

Sample in varying concentrations of NaOH	Control A Physical changes observed after 48 h incubation time	Pictures of Control A after alkali treatment	Sample B Physical changes observed after 48 h incubation time	Pictures of Sample B after alkali treatment	Sample C Physical changes observed after 48 h incubation time	Pictures of Sample C after alkali treatment
0.5[N]	folded		no change		folded	
1[N]	shrinked		folded		folded	
2.5[N]	shrinked crumbled		folded		shrinked	
5[N]	shrinked crumbled		folded		shrinked	

can be attributed to the functional groups of BG-MCC in cross-linked biopolymer. Maximum scavenging activity was observed in Sample-C containing Aloe gel, resulting in 91% inhibition. Since fresh Aloe gel was used in the process, the presence of polysaccharides, vitamins and phenolic contents might have induced increased inhibition. Hence, such biofilms have immense importance in biomedical and pharmaceutical industry.

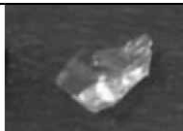


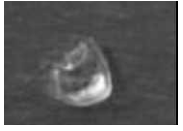



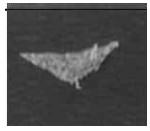




#### Alkali and acid tolerance test

The alkali test results in Table 6 revealed that the biofilms survived the harsh alkaline (NaOH) treatment before getting crumbled or degraded at higher concentrations of 5[N] NaOH. The brittleness increased with the increasing concentrations of alkali. The control Sample-A was affected most at above

1[N] NaOH concentration. Since chitosan gel is a weak base, strong alkali further shifted it into an even more alkaline range, which might have impacted its stability and strength. Sample B was less affected due to presence of microcrystalline cellulose. The pH of Aloe gel is naturally acidic, thus alkali treatment might have induced neutralizing effect and thus Sample C was not much affected.

The acid test results in Table 7 revealed that the biofilms survived the harsh acidic (HCl) treatment before getting crumbled or degraded at higher concentrations of 5[N] HCl. The brittleness increased with increasing concentrations of acid. Since chitosan gel is a weak base, the control Sample-A was not much affected with acid treatment for its neutralizing effect. Sample B was less affected due to presence of microcrystalline cellulose. Sample C was affected

**Table 7.** Physical changes observed after acid treatment

Sample in varying concentrations of HCl	Control A Physical changes observed after 48 h incubation time	Pictures of Control A after acid treatment	Sample B Physical changes observed after 48 h incubation time	Pictures of Sample B after acid treatment	Sample C Physical changes observed after 48 h incubation time	Pictures of Sample C after acid treatment
0.5[N]	folded		folded		folded	
1[N]	folded		folded		folded	
2.5[N]	shranked		shranked		shranked, browning	
5[N]	crumbled		crumbled		shranked, browning	

**Table 8.** Degradation (% weight change) of biofilm with time

Number of days Sample buried under soil	Control A % Weight change (Average)	Control B % Weight change (Average)	Control C % Weight change (Average)
Day 0	0	0	0
Day 9	44.28% ± 5.03	28.57% ± 2.89	33.33% ± 3
Day 18	(-) 42.85% ± 4.16	(-) 31.42% ± 3.02	(-) 38.33% ± 4.2
Day 27	(-) 37.14% ± 3.05	(-) 34.28% ± 3.7	(-) 40% ± 4.10

most at above 1[N] HCl concentration. The pH of Aloe gel is naturally acidic, but strong acids can further shift it into an even more acidic range, which might have impacted its stability and strength.

### Soil burial biofilm degradability test

The initial increase in weight in all the samples was due to absorption of water from the soil. The degradation was initiated by the decomposers in the soil with the action of hydrolytic enzymes. Data in Table 8 revealed that 9<sup>th</sup> day onwards, the weight started decreasing indicating biodegradation in all the samples. The time taken for biofilms to fully degrade in soil varies, but generally ranges from a few weeks to several months, and even longer in some cases (Nissa *et al.*, 2019). Several factors influence this, including the type of biofilm, soil conditions (moisture, temperature, microbial activity), and the size of the biofilm material. Sample B showed a positive result because it lasted for a month before being degraded completely and the rate of degradation was slower in comparison to other two samples. Water hydration data also revealed the water resistance nature of Sample-B. The samples kept in normal room condition, with high relative humidity (~88% RH), started degrading after 45 days. The result indicated that the composite biofilms can be used in food packaging in low moisture environments.

### CONCLUSION

Development of future composite biofilms or bioplastics as an alternative to conventional plastics, customized with fiber reinforcements and different additives, has gained immense research impetus due to their sustainability, biodegradability or compostability. Much emphasis is still needed to work on its thermal and mechanical properties. The present study aimed to develop a durable and flexible composite biofilm in active packaging, pharmaceutical or medical applications. The application of bagasse microcrystalline cellulose (BG-MCC) has improved the mechanical strength of the fabricated biofilm. Moreover, the biofilm developed out of natural polymers is of food grade quality with natural ingredients to compete with conventional non-biodegradable synthetic food packaging materials. Biofilm showed water resistant property, acid and

alkali tolerance, good flexibility, high melting point with delayed decomposition time. Addition of fresh leaf gel extract from the medicinal plant *Aloe barbadensis*, showed promising results with high antioxidant property but concentrated Aloe gel could have given improved mechanical strength of biofilm. The antioxidant properties can be correlated with its antimicrobial activity to further extend its significance in bioactive food packaging or in drug delivery system.

### ACKNOWLEDGEMENT

The author would like to thank the anonymous reviewers, co-authors and acknowledge the support from the Institution, to accomplish this work.

### DISCLAIMER

The authors declared that there is no conflict of interest while performing the work and preparation of the manuscript.

### REFERENCE

- Admase, A.T., Gesese, T.N., Fenta, S.W. and Eshete, B.G. 2025. Synthesis and characterization of bio-based eco-friendly biofilm composites reinforced with waste eggshell powder. *Scientific Reports*, **15**(1): 31617. <https://doi.org/10.1038/s41598-025-00398-4>
- Alokika, Anu, Kumar, A., Kumar, V. and Singh, B. 2021. Cellulosic and hemicellulosic fractions of sugarcane bagasse: Potential, challenges and future perspective. *International Journal of Biological Macromolecules*, **169**: 564-582. <https://doi.org/10.1016/j.ijbiomac.2020.12.175>
- Amin, Md. R., Chowdhury, Md. A. and Kowser, Md. A. 2019. Characterization and performance analysis of composite biofilms synthesized using titanium dioxide nanoparticles with corn starch. *Heliyon*, **5**(8): e02009. <https://doi.org/10.1016/j.heliyon.2019.e02009>.
- Biswas, M. 2025. A Review: Bioprospecting natural fibers from Invasive Alien Plant species (IAPs) for application in biocomposites. *Journal of Plant Science Research*, **41**(3): 1-10. <https://doi.org/10.32381/JPSR.2025.41.03.5>
- Boey, J.Y., Leem C.K. and Tay, G.S. 2022. Factors Affecting Mechanical Properties of Reinforced Biofilms: A review, *Polymers*, **14**(18): 3737. <https://doi.org/10.3390/polym14183737>

- Das, M. and Chowdhury, T. 2016. Heat sealing property of starch based self-supporting edible films. *Food Packaging and Shelf Life*, **9**: 64-68. <https://doi.org/10.1016/j.fpsl.2016.05.002>
- Dheana, W. and Ekawardhani, Y.A. 2022. Exploration of Interior Material Based on Plastic Waste. *Proceeding of International Conference on Business, Economics, Social Sciences, and Humanities*, **3**: 510-517. DOI:10.34010/icobest.v3i.180
- Dutta, D. and Sit, N. 2024. Review: A comprehensive review on types and properties of biopolymers as sustainable bio-based alternatives for packaging. *Food Biomacromolecules*, **1**(2): 58-87. <https://doi.org/10.1002/fob2.12019>.
- Flórez, M., Guerra-Rodríguez, E., Cazón, P. and Vázquez M. 2022. Chitosan for food packaging: Recent advances in active and intelligent films. *Food Hydrocolloids*, **124**: 107328. <https://doi.org/10.1016/j.foodhyd.2021.107328>
- Ganesan, P. 2023. Biodegradable curative film for medical application. *Indian Journal of Fibre & Textile Research*, **48**: 52-60.
- Gulcin, İ. and Alwasel, S.H. 2023. DPPH Radical Scavenging Assay. *Processes*, **11**(8): 2248. <https://doi.org/10.3390/pr11082248>
- Hasan, S., Boddu, V.M., Viswanath, D.S. and Ghosh, T.K. 2022. Application of Chitosan in the Medical and Biomedical Field. In: Hasan, S., Boddu, V.M., Viswanath, D.S., Ghosh, T.K., editors. *Chitin and Chitosan: Science and Engineering*. Springer International Publishing; Cham, Switzerland: 2022. pp. 291-321. [Google Scholar]
- Heo, J.W., Chen, J., Kim, M.S., Kim, J.W., Zhang, Z., Jeong, H. and Kim, Y.S. 2023. Ecofriendly and facile preparation of chitosan-based biofilms of novel acetoacetylated lignin for antioxidant and UV-shielding properties. *International Journal of Biological Macromolecules*, **225**(2023): 1384-1393. <https://doi.org/10.1016/j.ijbiomac.2022.11.196>.
- IUCN 2025 as downloaded on June 2025 [www.iucn.org/resources/issuesbrief/plastic-pollution](http://www.iucn.org/resources/issuesbrief/plastic-pollution)
- Jethoo, A.S. 2019. Effect of fiber reinforcement on tensile strength and flexibility of corn starch-based biofilm. *IOP Conference Series: Materials Science and Engineering*, **652**: 012035. DOI:10.1088/1757-899X/652/1/012035
- Katakajwala, R. and Venkata Mohan, S. 2020. Microcrystalline cellulose production from sugarcane bagasse: Sustainable process development and life cycle assessment. *Journal of Cleaner Production*, **249**: 119342. <https://doi.org/10.1016/j.jclepro.2019.119342>.
- Kaur, N., Somasundram, C., Razali, Z., Mourad, A-HI., Hamed, F. and Ahmed, Z.F.R. 2024. *Aloe vera*/Chitosan-Based Edible Film with Enhanced Antioxidant, Antimicrobial, Thermal, and Barrier Properties for Sustainable Food Preservation. *Polymers*, **16**(2): 242. <https://doi.org/10.3390/polym16020242>
- Khubiev, O.M., Egorov, A.R., Kirichuk, A.A., Khrustalev, V.N., Tskhovrebov, A.G. and Kritchenkov, A.S. 2023. Chitosan-Based Antibacterial Films for Biomedical and Food Applications. *International Journal of Molecular Sciences*, **24**(13): 10738. <https://doi.org/10.3390/ijms241310738>
- Kong, U., Mohammad Rawi, N.F. and Tay, G.S. 2023. The Potential Applications of Reinforced Biofilms in Various Industries: A Review. *Polymers*, **15**(10): 2399. <https://doi.org/10.3390/polym15102399>
- Kumara, G.U.A. and Wadimuna, Pushpakumari W. 2021. Pharmaceutical, Nutritional and Cosmetic Applications of *Aloe vera* Plant. *International Journal of Herbal Medicine*, **9**(4): 32-36. <http://www.florajournal.com/>
- Kumar, H., Ahuja, A., Kadam, A.A. and Rastogi, V.K. 2023. Antioxidant Film Based on Chitosan and Tulsi Essential Oil for Food Packaging. *Food Bioprocess Technology*, **16**: 342-355. <https://doi.org/10.1007/s11947-022-02938-6>
- Mensah, E.O., Adadi, P., Asase, R.V., Kelvin, O., Mozdehi, F.J., Amoah, I. and Agyei, D. 2025. *Aloe vera* and its byproducts as sources of valuable bioactive compounds: Extraction, biological activities, and applications in various food industries. *PharmaNutrition*, **31**: 100436. <https://doi.org/10.1016/j.phanu.2025.100436>.
- Moeini, A., Pedram, P., Makvandi, P., Malinconico, M. and Gomez d'Ayala, G. 2020. Wound healing and antimicrobial effect of active secondary metabolites in chitosan-based wound dressings: A review. *Carbohydrate Polymers*, **233**: 115839. DOI: 10.1016/j.carbpol.2020.115839
- Muneer, F., Nadeem, H., Arif, A. and Zaheer, W. 2021. Biofilms from biopolymers: an eco-friendly and sustainable solution of plastic pollution. *Polymer Science, Series C*, **63**: 47-63. DOI:10.1134/S1811238221010057

- Nazrin, A., Ilyas, R.A., Rajeshkumar, L., Hazrati, K.Z., Tarique, Jamal, Mahardika, M., Aisyah, H.A., Atiqah, A. and Radzi, A.M. 2025. Lignocellulosic fiber-reinforced starch thermoplastic composites for food packaging application: A review of properties and food packaging abetted with safety aspects. *Food Packaging and Shelf Life*, **47**: 101431. <https://doi.org/10.1016/j.fpsl.2025.101431>
- Nigam, S., Das, A.K. and Patidar, M.K. 2021. Valorization of *Parthenium hysterophorus* weed for cellulose extraction and its application for bioplastic preparation. *Journal of Environmental Chemical Engineering*, **9**(4): 105424. DOI:10.1016/j.jece.2021.105424
- Nissa, R.C., Fikriyyah, A.K., Abdullah, A.H.D. and Pudjiraharti, S. 2019. Preliminary study of biodegradability of starch-based biofilms using ASTM G21-70, dip-hanging, and Soil Burial Test methods. *IOP Conference Series: Earth and Environmental Science*, **277**: 012007. DOI 10.1088/1755-1315/277/1/012007
- Nurhaliza, Y., Nurulhaq, F., Yudhanto, S.M. and Suryanti, V. 2022. Edible film from microcrystalline cellulose (MCC) of waste banana (*Musa paradisiaca*) stem and chitosan. *Journal of Physics: IOP Conference Series*, **2190** (2022) 012027. <https://doi.org/10.1088/1742-6596/2190/1/012027>
- Owonubi, S., Agwuncha, S., Anusionwu, C., Revaprasadu, N. and Sadiku, R. 2019. Fiber-Matrix Relationship for Composites Preparation. In: Composites from Renewable and Sustainable Materials. *IntechOpen*. <https://doi.org/10.5772/intechopen.84753>
- Priyadarshi, R. and Rhim, J-W. 2020. Chitosan-based biodegradable functional films for food packaging applications. *Innovative Food Science & Emerging Technologies*, **62**: 102346. <https://doi.org/10.1016/j.ifset.2020.102346>
- Qureshi, D., Pattanaik, S., Mohanty, B., Anis, A., Kulikouskaya, V., Hileuskaya, K., Agabekov, V., Sarkar, P., Maji, S. and Pal, K. 2022. Preparation of novel poly(vinyl alcohol)/chitosan lactate-based phase-separated composite films for UV-shielding and drug delivery applications. *Polymer Bulletin*, **79**(1): 3253–3290. DOI:10.1007/s00289-021-03653-6
- Reddy, N.R., Gomathi, V., Sathya Moorthy, P., Thirumalairajan, S. and Ramalakshmi, A. 2023. *Parthenium*-derived nano biodegradable films: A green alternative to plastic packaging. *The Pharma Innovation Journal*, **12**(9): 2283–2286. [www.thepharmajournal.com](http://www.thepharmajournal.com)
- Román-Doval, R., Torres-Arellanes, S.P., Tenorio-Barajas, A.Y., Gómez-Sánchez, A. and Valencia-Lazcano, A.A. 2023. Chitosan: Properties and Its Application in Agriculture in Context of Molecular Weight. *Polymers*, **15**(13): 2867. <https://doi.org/10.3390/polym15132867>
- Samickannu, O.P., Sahu, P., Mohankumar, M. and Santhosh, A. 2022. A Review on Natural Fibre-Reinforced Biopolymer Composites: Properties and Applications. *International Journal of Polymer Science*, **3**: 1-15. <https://doi.org/10.1155/2022/7820731>
- Samraj, S., Senthilkumar, K., Induja, P., Venkata Ratnam, M., Aatral, G.V. and Ramakrishna, G.V.S. 2022. Extraction of Microcrystalline Cellulose and Silica from Agriculture Waste and Its Application in Synthesis of Wheat Gluten and Fish Scales Derived Biofilm. *International Journal of Biomaterials*, **2022**(1): 2297364. <https://doi.org/10.1155/2022/2297364>
- Shen, M., Song, B., Zeng, G., Zhang, Y., Huang, W., Wen, X. and Wangwang, T. 2020. Are biodegradable plastics a promising solution to solve global plastic pollution? *Environmental Pollution*, **263**: 114469. <https://doi.org/10.1016/j.envpol.2020.114469>
- Stefanowska, K., Woźniak, M., Dobrucka, R. and Ratajczak, I. 2023. Chitosan with Natural Additives as a Potential Food Packaging. *Materials*, **16**(4): 1579. <https://doi.org/10.3390/ma16041579>
- Sofiah Aznury, Y.M. Melianti. 2019. Mechanical Properties of Biofilms Product from *Musa Paradisica* Concentrate with Plasticizer Variables. *Journal of Physics: Conference Series*, **1167** (2019) 012048. DOI:10.1088/1742-6596/1167/1/012048
- Souza, V.G.L., Pires, J.R.A., Rodrigues, C., Coelho, I.M. and Fernando, A.L. 2020. Chitosan Composites in Packaging Industry—Current Trends and Future Challenges. *Polymers*, **12**: 417. <https://doi.org/10.3390/polym12020417>
- Varun, T.K., Senani, S., Jayapal, N., Chikkerur, J., Roy, S., Tekulapally, V.B., Gautam, M. and Kumar, N. 2017. Extraction of chitosan and its oligomers from shrimp shell waste, their characterization and antimicrobial effect. *Veterinary World*, **10**(2): 170-175. <https://doi.org/10.14202/vetworld.2017.170-175>
- Ventura-Cruz, S. and Tecante, A. 2021. Nanocellulose and microcrystalline cellulose from agricultural waste: Review on isolation and application as reinforcement in polymeric matrices. *Food*

- Hydrocolloids*, **118**: 106771.  
<https://doi.org/10.1016/j.foodhyd.2021.106771>
- Vyazovkin, S. 2002. Thermal analysis. *Analytical Chemistry*, **74**(12): 2749-2762.  
<https://pubs.acs.org/doi/10.1021/ac020219r>
- Wang, H., Ding, F., Ma, L. and Zhang, Y. 2021. Edible films from chitosan-gelatin: Physical properties and food packaging application. *Food Bioscience*, **40**, 100871. DOI:10.1016/j.fbio.2020.100871
- Wei, X., Linde, E. and Hedenqvist, M. 2019. Plasticiser loss from plastic or rubber products through diffusion and evaporation. *npj Materials Degradation*. **3**, 18. <https://doi.org/10.1038/s41529-019-0080-7>
- Woźniak, A. and Biernat, M. 2022. Methods for crosslinking and stabilization of chitosan structures for potential medical applications. *Journal of Bioactive and Compatible Polymers*, **37**(3): 151-167. <https://doi.org/10.1177/08839115221085738>
- Xiang, L.Y., Mohammed, M.A.P. and Baharuddin, A.S. 2016. Characterisation of microcrystalline cellulose from oil palm fibres for food applications. *Carbohydrate Polymers*, **148**: 11-20. <https://doi.org/10.1016/j.carbpol.2016.04.055>.
- Zhou, Z., Liu, Y., Jiang, X., Zheng, C., Luo, W., Xiang, X., Qi, X. and Shen, J. 2023. Metformin modified chitosan as a multi-functional adjuvant to enhance cisplatin-based tumor chemotherapy efficacy. *International Journal of Biological Macromolecules*, **224**: 797-809. DOI: 10.1016/j.ijbiomac.2022.10.167

---

FULL LENGTH ARTICLE

---

## Characterization of plant growth promoting bacteria from sugarcane Rhizosphere in Vidarbha Region, India

---

A. Banerjee, S. Maity, S. Roy, S. Chandra, B. Chatterjee\* and A.K. Mitra

Department of Microbiology, St. Xavier's College (Autonomous), Park Street, Mullick Bazar, Park Street Area, Kolkata, West Bengal 700016.

---

Received : 31.12.2025

Accepted : 19.05.2026

Published : 30.06.2026

---

Sugarcane, (*Saccharum officinarum*) member of the Poaceae family is a very economical cash crop that serves as an excellent bioresource in the production of alcohol and sugar. In India, around 60 million farmers are dependent on sugarcane cultivation thereby promoting a socio-economic development in the country especially in the rural areas. The major sugarcane producing states in India are Uttar Pradesh, Tamil Nadu, Maharashtra and Andhra Pradesh to name a few. This paper elucidates the characteristic properties of sugarcane rhizospheric soil obtained from the Vidarbha region of Maharashtra, India. Qualitative analysis of the soil sample like pH, electrical conductivity and organic carbon content were conducted. In addition, micro element and macro element contents in the soil were also measured. Isolation of three different bacterial isolates were obtained from the soil sample. They were characterised using Gram staining and Hichrome media. SGW2 tested positive for various plant growth promoting rhizobacterial properties such as nutrient sequestration which includes nitrogen solubilization, phosphate solubilization, potassium solubilization and zinc solubilisation. The bacterial isolate SGW2 also tested positive for siderophore production and agriculturally important enzyme like cellulase. The bacterial isolates SGW1 and SGW3 produced indole acetic acid (IAA) in presence and absence of tryptophan. However, SGW2 only produced IAA in the absence of tryptophan. The Kirby- Bauer Disk Diffusion Susceptibility test revealed the bacterial isolates were antibiotic sensitive. Thus, the bacterial isolates can be further studied for agricultural application in the field in the form of a biofertilizer.

**Keywords:** Sugarcane rhizosphere, plant growth promoting rhizobacteria, physico chemical soil parameters, siderophore.

---

### INTRODUCTION

Sugarcane is an essential crop which acts as an excellent bioresource in the production of alcohol. The dry fibrous part which is left after using the crop is termed as bagasse. This bagasse or sugarcane waste can be returned to the soil & used as an organic

fertilizer after being decomposed. Bagasse residues are typically disposed of in the soil which hosts a variety of Plant Growth Promoting Rhizobacteria (PGPR) species. PGPR refer to the microorganisms present in soil that inhabit the plant rhizosphere and remain in close associations with the roots of the plants. Studies have shown the benefits of using PGPR in sugarcane waste to increase the availability of nutrients, and productivity and also facilitate seed germination (Santos *et al.*, 2020).

---

\*Corresponding author : bidishachatterjee06@gmail.com

PGPR are found in various ecological niches that includes wetlands, deserts, mangrove, forests, and agricultural soils to name a few. Hence their high prevalence in nature shows how well they can adapt in different ecological conditions thereby supporting the growth of the plants and soil balance (Zhang *et al.*, 2024). Furthermore, PGPR can also exhibit systemic resistance in plants, thereby strengthening defence response in plants against various pathogenic bacteria and virus associated infections. PGPRs have also gained importance due to their high salt tolerance ability and their survival under high saline conditions (Kamila *et al.*, 2022).

There are many bacteria playing the role of PGPR in nature for plant growth and they're recognized for being successful at it. Many species like *Azospirillum* sp., *Bacillus* sp. and *Pseudomonas* sp., are found in the sugarcane waste acting as PGPR which are highly recognized for their Indole Acetic Acid (IAA) production and fixing Nitrogen (Mehnaz *et al.*, 2011). The ability of these bacteria to produce siderophores and various phytohormones like cytokinin, Indole Acetic acid (IAA), has been used to prove their PGP activity by stimulating the growth of the plants as well as elongation of roots and germination of seeds.

In this study, bacterial isolates isolated from the rhizospheric soil were tested for various plant growth promoting characteristics such as nutrient sequestration, hormone production like IAA (with and without tryptophan) and metal uptake along with agriculturally important enzymes like cellulase. The antibiotic sensitivity assay was also carried out to avoid the re-release of potentially pathogenic organism back into the soil. The main objectives of this study were to isolate PGPR species from Vidarbha region, India for future application in the agricultural field as biofertilizer.

## MATERIALS AND METHODS

### Sampling and soil characterization

The soil sample was collected from the Vidarbha area, Maharashtra, India. The physical characteristics of the soil sample like pH, Electrical Conductivity (EC) and Organic Carbon were analysed. Macro elements like

Nitrogen, Phosphorus and Potassium along with micronutrients like Iron, Manganese, Copper, Boron, Zinc, Magnesium, Sulphur and Calcium was measured using standard protocol (Kamila *et al.*, 2022).

### Isolation of bacterial colonies from the soil sample

Serial dilution of the soil sample was carried out on freshly prepared Nutrient Agar plates. Bacterial colony count was performed after incubating the plates at 37°C for 24 hours. (David *et al.*, 2014).

### Hichrome Agar characterization of bacterial isolates

The isolated colonies were characterised using Hichrome Agar. The freshly inoculated plates were incubated at 37°C for 24 hours. (Kamila *et al.*, 2022).

### Test for Nitrogen, Phosphate and Potassium (NPK) solubilizing bacteria

Nutrient sequestration potential of the bacterial isolates was tested using Jensen Agar medium, Pikovskaya Agar medium and Aleksandrow Agar medium for nitrogen, phosphate and potassium solubilizing bacteria (Kamila *et al.*, 2022).

### Test for zinc solubilizing bacteria

Zinc solubilizing media was prepared to identify the Zinc solubilizing bacteria (Kamila *et al.*, 2022).

### Indole-acetic acid (IAA) assay

Test for the production of Indole Acetic Acid (IAA) (Sarkar *et al.*, 2013) was performed. The test for IAA was separately performed with and without Tryptophan and absorbance was measured at 530 nm. (Gang *et al.*, 2018).

### Siderophore assay

Siderophores are low-weight, high-affinity iron chelating molecules produced in response to iron deficiency by Gram-positive and Gram-negative

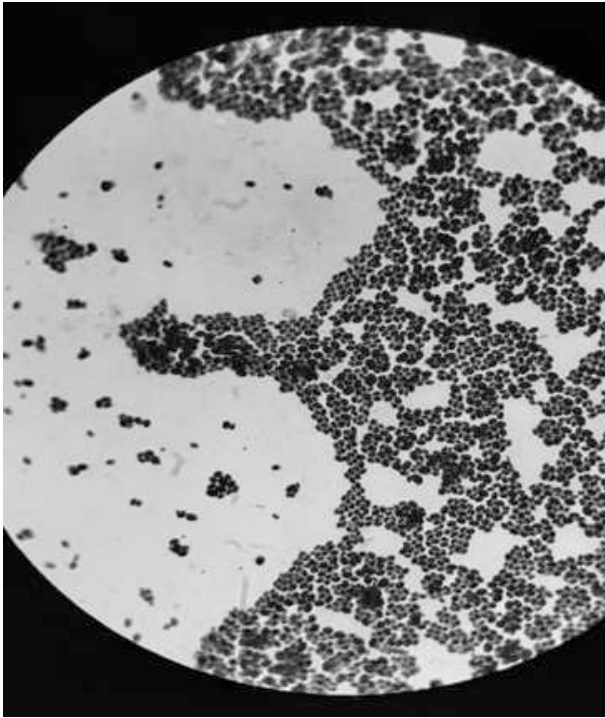


Fig. 1

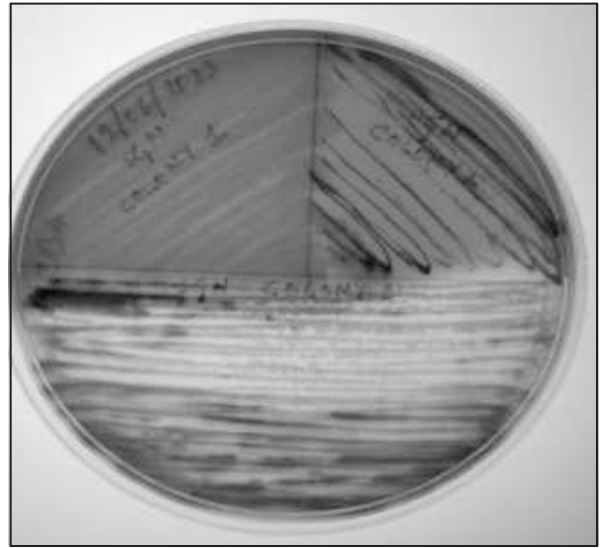


Fig. 2

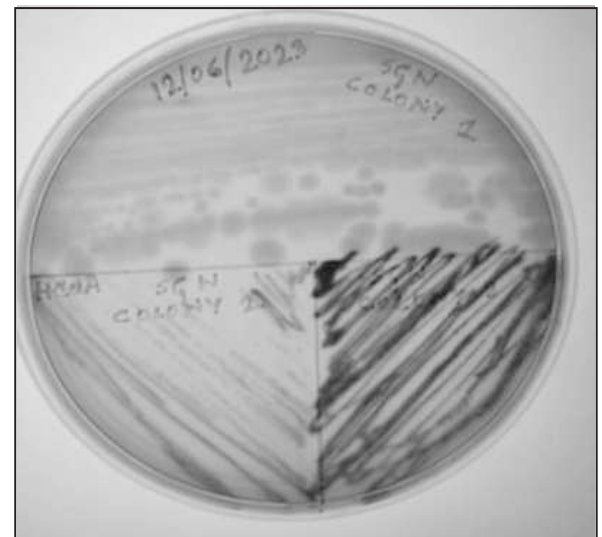


Fig. 3

**Table 1.** The table represents the physico-chemical characteristics of the soil sample

Soil Parameters	Values
pH	7.5
Electrical conductivity	1082 $\mu\text{scm}^{-1}$
Organic Carbon	0.38%
Nitrogen	224kg/hectare
Phosphorus	>160kg/hectare
Potassium	466kg/hectare
Iron	9.2mg/kg
Manganese	4.88mg/kg
Copper	Sufficient
Boron	7mg/kg
Zinc	4.32mg/kg
Magnesium	1.51mg/kg
Sulphur	9.63mg/kg
Calcium	0.91mg/kg

bacteria. Test for presence of Siderophore was performed. CAS medium was prepared and spot inoculation was performed. Plates were incubated at 37°C for 24 hours and results were obtained (Miranda *et al.*, 2007).

### Cellulase assay

Freshly prepared Carboxy Methyl Cellulase (CMC) media was inoculated and incubated at 37°C for 24 hours. The media was flooded with 0.1% congo red

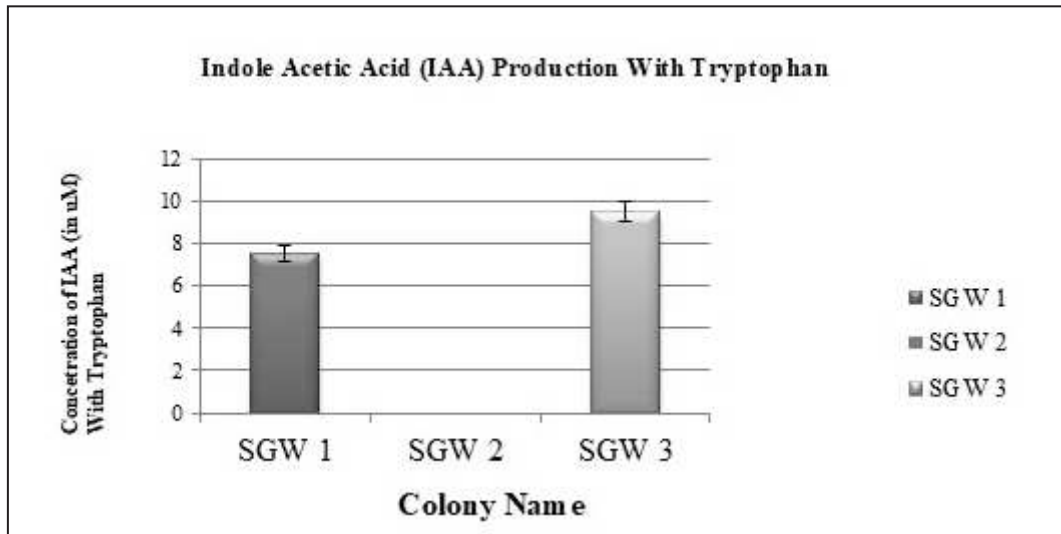


Fig. 4

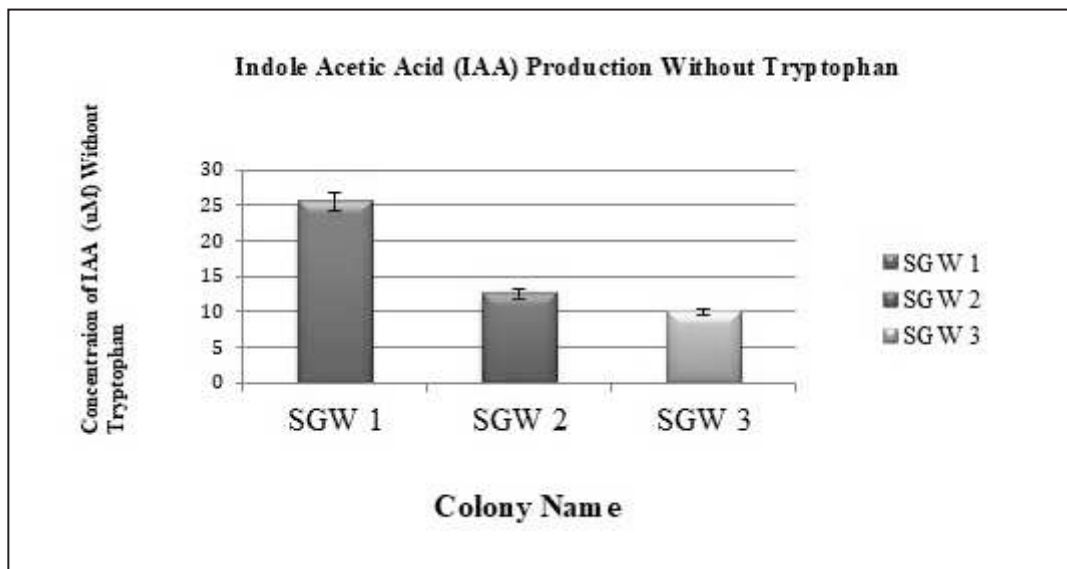


Fig. 5

dye. The excess reagent was discarded and the plate was washed with NaCl. This test checked if the bacteria present in the soil sample produced Cellulase enzyme (Islam *et al.*, 2018).

**Antibiotic disk diffusion assay**

Antibiotic tests for all the three bacteria were performed using Kirby- Bauer Disk Diffusion Susceptibility test using two antibiotics-

Cotrimoxazole and Cefataxime and observations were taken (Hudzicki *et al.*, 2009).

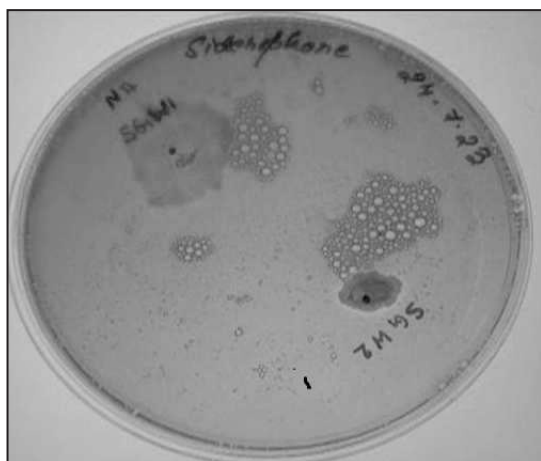
**RESULTS**

**Characterization of soil sample**

The physico-chemical analysis of the soil was carried out. The pH of the soil sample was 7.5 which was slightly alkaline. The macronutrients and the

**Table 2.** The table represents the characterization of the bacterial isolates from the soil sample.

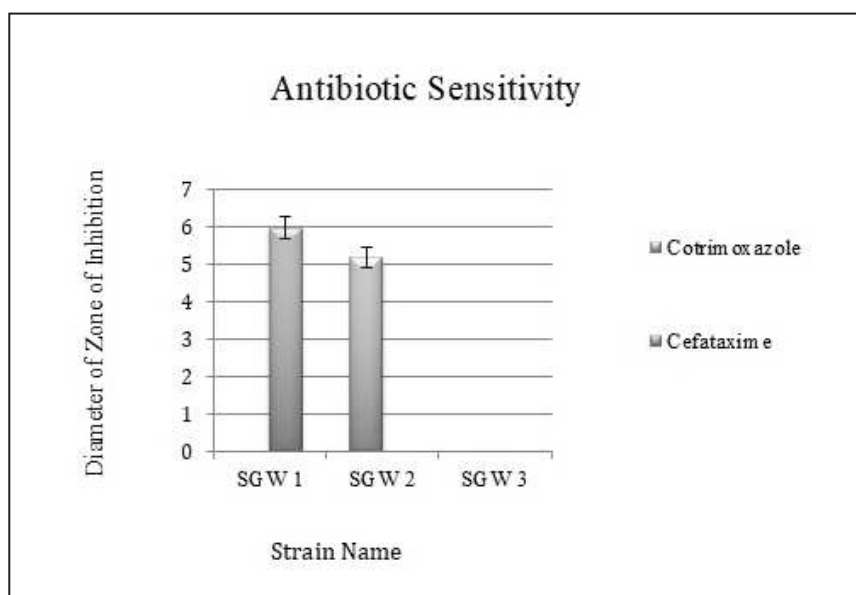
Colony Name	Colony Morphology	Gram character	Cellular Morphology	Hichrome Bacillus	Hichrome UTI
SGW 1	Translucent yellowish, white colony	Positive	Cocci	Whitish Pink Colonies	Off white creamy colony
SGW 2	White, small, round colonies	Positive	Oval shaped	Dark green colonies	Deep blue colonies
SGW 3	Golden yellow colonies	Positive	Cocci	Greenish yellow colonies turned media yellow	Pink colonies which have turned purple



**Fig. 6**



**Fig. 7**



**Fig. 8**

**Table 3.** The table represents characterization of the bacterial isolates on the basis of their nutrient sequestration, siderophore production and agriculturally important enzymes production.(where “+” = presence and “-” = absence of the character in the qualitative assay)

Name of colony	Nitrogen fixing	Phosphorous solubilisation assay	Potassium solubilisation assay	Zinc solubilisation assay	Siderophore assay	Cellulase assay
SGW 1	+	-	-	-	-	-
SGW 2	+	-	-	+	+	+
SGW 3	+	-	-	-	-	-

micronutrients were present in the rhizospheric soil. The data of the physico-chemical analysis of the soil sample has been provided in Table 1.

#### Enumeration and characterisation of bacterial isolates

The colony characteristics of the isolated bacterial strains indicated bacterial diversity. The bacterial load in the stock solution was estimated to be  $1.8 \times 10^6$  CFU per gram of soil. Pure culture of isolated bacterial strains (SGW1, SGW2, SGW3) were obtained by streak plate method (where SGW signify SuGarcane Waste/ bagasse mixed soil).

The characteristics of different colonies are given in Table 2. The isolated bacterial strains were Gram positive in nature Fig. 1. The cellular morphology of the bacterial isolates has been included in Table 2.

#### Hichrome Agar characterization of bacterial isolates

The hicrome agar characterization depends on enzymes produced by the bacterial isolates, which binds with the chromogenic substrate present in the media resulting in the formation of different colour as observed in Fig. 2 and Fig. 3. The colony characters have been included in Table 2.

#### Test for Nitrogen, Phosphate and Potassium (NPK) solubilizing bacteria

The three bacterial isolates SGW1, SGW2 and SGW3 indicated positive result by growing on Jensen agar medium. Only SGW2 tested positive for phosphate and potassium solubilization which was indicated by a halo around the colony (Table 3).

#### Test for zinc solubilizing bacteria

The bacterial strain SGW2 showed zinc solubilizing property after 24hrs by growing on zinc solubilizing agar medium (Table3).

#### Indole-acetic acid (IAA) assay

The IAA assay was carried out in both presence and absence of tryptophan. The results indicated that in presence of tryptophan SGW3 produced higher concentration of IAA than SGW1 (Fig. 4). In the absence of tryptophan all the three bacterial isolates produced IAA and SGW1 produce the highest concentration as compared to the other two bacterial isolates (Fig. 5).

#### Siderophore assay

Siderophore production helps the bacteria to readily uptake certain metals from the environment like iron which is needed for various metabolic activities as a cofactor. The bacterial strain SGW2 tested positive for

siderophore production (Table 3). A yellow halo was observed around the spot inoculation in the CAS media (Fig. 6).

### Cellulase assay

Cellulase is an agriculturally important enzyme that helps the bacterial isolate to break down cellulose. It is a lignocellulolytic enzyme that helps to maintain the soil nutrient by breaking down plant litter. The qualitative cellulase assay indicated cellulase production by SGW2 (Table 3). A clear halo was observed around the bacterial colony (Fig. 7).

### Antibiotic disk diffusion assay

The Kirby-Bauer Disk Diffusion Susceptibility test, indicated antibiotic sensitivity of the bacterial isolates SGW1 and SGW2 (Fig. 8).

## DISCUSSION

In our study, plant growth promoting activities have been observed in the rhizobacterial isolates (SGW 1, SGW 2 and SGW 3) from soil enriched with sugarcane waste. Recent studies have shown, the presence of plant growth promoting rhizobacteria in sugarcane bagasse deposited soil have improved plant growth and health. Here, a study has been carried out on the bacterial strains isolated from soil which is supplemented with sugarcane waste residues where various plant growth promoting characteristics have been reported. Physico-chemical results from soil showed a slightly alkaline pH and a considerate level of macronutrients and micronutrients in order to carry out microbial activity. Similar findings have been reported in the soils of Vidarbha area exhibiting favourable microbial activity (Dorlikar and Thengare, 2025). All strains here strongly promote nitrogen fixation. A recent study has showed that a particular strain of *Pseudomonas maltophilia* isolated from sugarcane stalks showed high nitrogenase activity, and therefore, considered as an endogenous nitrogen-fixing bacteria (Xing *et al.*, 2016). Furthermore, siderophore and zinc solubilization activities were also reported in our study where SGW 2 exhibited mineral solubilization like iron and zinc for plants. Similarly, another finding demonstrated plant growth-

promoting mechanisms in some rhizobacterial strains which were treated in sugarcane plants and induced nitrogen uptake, phosphate solubilization, phytohormones, and defense-related enzymes etc which are mainly contributed by rhizobacterial strains like *Pseudomonas* sp. (Singh *et al.*, 2024). Cellulose degradation ability has been observed in SGW 2 strain, isolated from soil enriched with sugarcane waste. Another finding indicated a rare abundant bacterium has been discovered that plays a crucial role in degradation of Lignocellulose from Sugarcane Biomass (Puentes-Télez *et al.*, 2020). Based on these results, microorganisms isolated from the soil can be considered as a good plant growth promoting rhizobacteria which aids in plant growth along with waste degrading ability.

## CONCLUSION

The present study of the bacterial isolates SGW1, SGW2, SGW3 obtained from the rhizospheric soil of sugarcane in Vidarbha region, India demonstrated their potential of plant growth promoting activities. All the three isolates exhibited positive nitrogen fixation ability, which indicates their possibility of improving the fertility of the soil as well as supporting the growth of the plants. Among these bacterial isolates, SGW2 showed positive results for siderophore production, zinc solubilization and cellulolytic activities suggesting their possible role in mobilization of various micronutrients, iron acquisition as well as degradation of agricultural wastes. Hence, the plant growth promoting activities observed in these isolates could serve a potential role in ensuring sustainable agriculture and a promising implementation in environmental and agricultural management practices.

## ACKNOWLEDGEMENT

We would like to thank our Principal Father Dominic Savio SJ and the Department of Microbiology, St Xavier's College (Autonomous) Kolkata, India for their constant support and guidance.

**DISCLAIMER**

The authors declared that there is no conflict of interest while performing the work and preparation of the manuscript.

**REFERENCE**

- Ben-David, A. and Davidson, C.E. 2014. Estimation method for serial dilution experiments. *Journal of Microbiological Methods*, **107**: 214-221.
- Dorlikar, A. and Thengare, M. 2025. Soil fertility and micronutrient analysis in different agroecosystems of Vidarbha region, Maharashtra, India. *Environment and Ecology*, **43**: 355-364. <https://doi.org/10.60151/envec/LGYX1381>.
- Gang, S., Sharma, S., Saraf, M., Buck, M. and Schumacher, J. 2019. Analysis of indole-3-acetic acid (IAA) production in *Klebsiella* by LC-MS/MS and the Salkowski method. *Bio-protocol*, **9**(9): e3230. <https://doi.org/10.21769/BioProtoc.3230>.
- Hudzicki, J. 2009. Kirby-Bauer disk diffusion susceptibility test protocol. *American Society for Microbiology*. [accessed 2 Jan, 2026].
- Islam, F and Roy, N. 2018. Screening, purification and characterization of cellulase from cellulase producing bacteria in molasses. *BMC Res Notes*, **11**(1): 1-6. <https://doi.org/10.1186/s13104-018-3558-4>
- Kamila, S., Mondal, S., Chatterjee, B., Roy, B. and Mitra, A.K. 2022. Isolation of saline tolerant PGPR (ST-PGPR) from sinking island of Ghoramara. *Journal of Environment and Sociobiology*, **19**(2): 125-135.
- Mehnaz, S. 2011. Plant growth-promoting bacteria associated with sugarcane. In: Maheshwari, D.K. (Ed.), *Bacteria in agrobiology: crop ecosystems* Berlin, Heidelberg: Springer, pp. 165-187.
- Pérez-Miranda, S., Cabirol, N., George-Téllez, R., Zamudio-Rivera, L.S. and Fernández, F.J. 2007. O-CAS, a fast and universal method for siderophore detection. *Journal of Microbiological Methods*, **70**(1): 127-131.
- Poopathi, S., Chinnasamy, M. and Rajeswari, G. 2013. Potential of sugarcane bagasse (agro-industrial waste) for the production of *Bacillus thuringiensis israelensis*. *Tropical Biomedicine*, **30**: 504-515.
- Santos, R.M.D., Diaz, P.A.E., Lobo, L.L.B. and Rigobelo, E.C. 2020. Use of plant growth-promoting rhizobacteria in maize and sugarcane: characteristics and applications. *Frontiers in Sustainable Food Systems*, **4**: 136. <https://doi.org/10.3389/fsufs.2020.00136>
- Sarker, A. and Al-Rashid, J. 2013. Analytical protocol for determination of indole-3-acetic acid (IAA) production by plant growth promoting bacteria (PGPB). Report No. 012, pp 1-5.
- Singh, R.V., Sharma, P. and Sambyal, K. 2022. Application of sugarcane bagasse in chemicals and food packaging industry: potential and challenges. *Circular Economy and Sustainability*, **2**(4): 1479-1500.
- Singh, P., Singh, R.K., Li, H.B., Guo, D.J., Sharma, A., Verma, K.K. and Li, Y.R. 2024. Nitrogen fixation and phytohormone stimulation of sugarcane plant through plant growth promoting diazotrophic *Pseudomonas*. *Biotechnology and Genetic Engineering Reviews*, **40**(1):15-35. <https://doi.org/10.1080/02648725.2023.2177814>
- Xing Y, Wei C, Mo Y, Yang L, Huang S, Li Y. 2016. Nitrogen-fixing and plant growth-promoting ability of two endophytic bacterial strains isolated from sugarcane stalks. *Sugar Tech*, **18**(4): 373-379.
- Zhang, T., Jian, Q., Yao, X., Guan, L., Li, L., Liu, F. and Lu, L. 2024. Plant growth-promoting rhizobacteria (PGPR) improve the growth and quality of several crops. *Heliyon*, **10**: e31553. <https://doi.org/10.1016/j.heliyon.2024.e31553>

---

**FULL LENGTH ARTICLE**

---

**Comparative effects of Arsenate (V) and Arsenite (III) on inducing oxidative stress and osmolyte accumulation in mungbean seedlings**

---

**Arpita Swarnakar\***

Department of Botany, Bangabasi College, University of Calcutta, Kolkata -700009, India.

---

Received : 11.05.2026

Accepted : 20.06.2026

Published : 30.06.2026

---

The effects of sodium arsenate ( $\text{Na}_2\text{HAsO}_4 \cdot 7\text{H}_2\text{O}$ ) and sodium arsenite ( $\text{NaAsO}_2$ ) on the growth and activity of a few oxidising enzymes of mungbean seedlings were investigated. It was found that among both arsenic species, sodium arsenite had drastic effects on growth and biochemical metabolism of germinating mungbean (*Vigna radiata* (L.) Wilczek cv. B-105) seedlings, in comparison to sodium arsenate. Inorganic arsenicals (arsenate as well as arsenite) imposed stress on the growth of mungbean seedlings. With the increase in concentration of sodium arsenate and sodium arsenite (0.5  $\mu\text{M}$ , 1  $\mu\text{M}$  and 2  $\mu\text{M}$ ), significant decrease in 5 day old seedling length *i.e.*, shoot and root length and fresh weight and dry weight of mung bean seedlings were observed. Under arsenate-induced oxidative stress, levels of osmolyte proline,  $\text{H}_2\text{O}_2$  and phenol content were found to be elevated. An appreciable increase in the activities of some reactive oxygen species (ROS) scavenging enzymes, *viz.*, catalase [EC 1.11.1.6], catechol peroxidase [EC 1.11.1.7], ascorbic acid oxidase [EC 1.10.3.3] and polyphenol oxidase [EC 1.10.3.3] were also observed, indicating oxidative stress. Arsenite was found to be more effective in inducing oxidative stress than arsenate.

**Keywords:** Sodium arsenate, Sodium arsenite, Antioxidants, Oxidative stress, Osmolytes, *Vigna radiata* (L.) Wilczek cv. B-105.

---

## INTRODUCTION

Arsenic contamination is a major global concern now. Arsenic (As) is a ubiquitous, carcinogenic trace metalloid (Pigna *et al.*, 2009) found in virtually all environmental media. It is released by geological activity, smelting operations, fossil fuel combustion and use in pesticides, herbicides, *etc.* (Pickering *et al.* 2000). It is a potential contaminant of groundwater, especially in Asian countries such as Bangladesh, India, China and Taiwan. In West Bengal, India, concentration of arsenic (As) in ground water of some places has been found to be above the maximum

permissible limit (recommended value by WHO and US EPA is 0.01 mg/l) in many districts. This is regarded as the biggest arsenic calamity in the world. Arsenic toxicity is a chronic problem and currently epidemic in West Bengal. Arsenic is a non essential metalloid that is toxic and harmful to agricultural production, as it reduces plant biomass and yield. It has become a global burden and a major environmental concern (Abbas *et al.*, 2018). Crop plants are also affected when irrigated in fields by arsenic-contaminated groundwater. Thus, arsenic has earned a place on the United States Environmental Protection Agency (USEPA) priority list as one of the most hazardous substances (ATSDR, 2022). The impact of this contaminated irrigation on mungbean is

---

\*Corresponding author : aswarnakar1975@gmail.com

important, as it is a major pulse crop and a source of dietary protein for poor people around the world.

Arsenic usually exists in the stable (As (III)) and (As (V)) valence states in which it exists naturally in the forms of oxyanions of arsenite (As(III)) and arsenate (As (V)). The two forms of inorganic arsenic-arsenate (AsV) and arsenite (AsIII), are easily taken up by the cells of the plant root. Phytotoxicity of As varies between and within plant species, As oxidation state, and edaphic conditions (Kashyap and Garg, 2018). As(III) combines with SH (sulfhydryl) groups, inactivating proteins, enzymes, and lipid peroxidation with consequent cellular damage causing fatality (Ullrich-Eberius *et al.*, 1989). During the detoxification of As in the plant, an oxidation–reduction reaction occurs due to valence variations leading to ROS production (Meharg and Hartley-Whitaker, 2002).

Elevated soil As levels resulting from long term use of arsenic contaminated groundwater for irrigation, inhibit rice seed germination and seedling establishment. Root tolerance index (RTI) and relative shoot height (RSH) for rice seedlings decreased with increasing concentrations of arsenate (Abedin and Meharg, 2002). Arsenic, also, has a profound role in inhibiting the activities of enzymes required for growth and metabolism. To mitigate heavy metal and metalloid-induced toxicities, plants have developed various stress tolerance mechanisms. The synthesis of osmolytes (proline and glycine betaine (GB) was reported to be enhanced in most plants under heavy metal toxicity, thereby protecting the cells from dehydration stress (Ahmad *et al.*, 2020). The enzymatic [superoxide dismutase (SOD), ascorbate peroxidase (APX), catalase (CAT), glutathione reductase (GR), monodehydroascorbate reductase (MDHAR) and dehydroascorbate reductase (DHAR)] as well as non-enzymatic antioxidants [ascorbic acid (AsA), glutathione (GSH),  $\alpha$ -tocopherols and phenolic compounds] can effectively diminish the production of ROS (Ahmad *et al.*, 2010). Biochemical responses of plants to toxic metals are complex and several defense strategies are adopted by the plants, one of which includes enzymatic anti-oxidative system [e.g. catalase (CAT), ascorbate peroxidase (APX), and glutathione reductase (GR)]

(Bhaduri and Fulekar, 2012).

Therefore, the present investigation was undertaken to examine the effect of different concentrations of sodium arsenate and sodium arsenite on the regulation of growth and development of mungbean seedlings and to study the altered metabolism of the seedlings due to oxidative stress induced by arsenic (As) toxicity.

## MATERIALS AND METHODS

### Plant material and arsenical treatments

Mungbean (*Vigna radiata* (L.) Wilczek cv. B -105) seeds, collected from Pulses and Oilseeds Research Station, Berhampore, Government of West Bengal, India were treated with 0.1% w/v HgCl<sub>2</sub> solution for 2 min for surface sterilization and washed repeatedly with distilled water. Two salts of arsenic *viz.*, Sodium arsenate (Na<sub>2</sub>HAsO<sub>4</sub>·7H<sub>2</sub>O) and Sodium arsenite (NaAsO<sub>2</sub>) (Merck) were used for arsenic treatment. Mungbean seeds were treated with arsenic salts at concentrations – 0.5 $\mu$ M, 1 $\mu$ M and 2 $\mu$ M (sub lethal doses) for 5 days. The seeds (about 20) were grown on petridishes lined with double layered filter paper (Whatman No. 2). Freshly prepared 10 ml of treatment solution was applied to respective petridishes after washing the previous solution daily. The seedlings were exposed to 14 hr photo period (260 $\mu$ molm<sup>-2</sup>s<sup>-1</sup> PFD). The petridishes were kept in climatic room under controlled conditions of temperature 25°C $\pm$ 2°C) and relative humidity (65%). The pH of the solution was 6.5 throughout. The seeds treated with only distilled water for 5 days served as control. The seedlings were harvested after 5 days for further studies. The above mentioned arsenate and arsenite concentrations are comparable to field soil conditions and are environmentally relevant.

### Morphological studies

After 5 days, arsenate and arsenite-induced damaging effects were observed and root length and shoot length of growing mungbean seedlings were measured in all the sets. Seedling length of 10 seedlings were determined after excising the cotyledons and

**Table 1.** Effect of different concentrations of sodium arsenate, As(V) and sodium arsenite, As(III) on shoot and root length as well as fresh and dry weight of 5 day old mungbean seedlings.

Figures in parentheses indicate % decrease (-) over control. C.D. - Critical Difference.

Treatment	Shoot length (cm)		Root length (cm)		Fresh weight (g)		Dry weight (g)	
	As(V)	As(III)	As(V)	As(III)	As(V)	As(III)	As(V)	As(III)
Control	12.5	12.5	4.5	4.5	3.29	3.29	0.40	0.40
0.5 $\mu$ M	7.0(-44)	5.8(-54)	1.5(-67)	0.8(-82)	2.7(-18)	2.45(-25)	0.29(-28)	0.22(-45)
1 $\mu$ M	4.7(-62)	3.6(-71)	0.8(-82)	0.5(-89)	1.32(-60)	1.25(-62)	0.22(-45)	0.18(-57)
2 $\mu$ M	2.4(-81)	1.5(-92)	0.4(-91)	0.3(-91)	0.9(-73)	0.7(-79)	0.17(-58)	0.14(-65)
S.E(mean)	0.3	0.31	0.1	0.1	0.03	0.02	0.02	0.02
C.D. (P=0.05)	0.44	0.46	0.21	0.2	0.27	0.28	0.032	0.030

averaged. Fresh weight and dry weight of 10 seedlings were determined after excising the cotyledons and averaged. For estimating dry weight, the seedlings were selected randomly from the same set and then averaged. The seedlings were allowed to dry in an oven at 70°C for 3 days. All the experiments were repeated thrice and analysed statistically.

### Quantitative estimations

The osmolyte proline content was estimated according to the method of Bates *et al.* (1973). The estimation of total phenolic compounds was done according to the method of Malik and Singh (1980). The estimation of total H<sub>2</sub>O<sub>2</sub> or hydrogen peroxide content of the seedlings were done according to Velikova *et al.* (2000). The H<sub>2</sub>O<sub>2</sub> content was determined using an extinction coefficient of 0.28  $\mu$ M<sup>-1</sup>cm<sup>-1</sup>.

### Enzyme assay

Assay of the activity of a few oxidising enzymes was done. Enzyme extraction process was carried out at 4°C. The 5 day old seedlings were homogenised in pre-chilled 0.05M phosphate buffer (pH 7.4) and centrifuged at 10,000 x g for 15 min. The supernatants were used for assay after making a definite volume in each set and the enzyme activity was expressed on fresh weight basis. Assay of catalase [EC1.11.1.6] was

carried out according to the method of Gasper and Lacoppe (1968). Catechol peroxidase [EC 1.11.1.7] activity was assayed following the method of Chance and Maehly (1955), with colorimetric determination of the colour intensity of oxidized catechol at 420nm. Ascorbic acid oxidase [EC 1.10.3.3] was assayed according to Olliver (1967). The polyphenol oxidase [EC 1.10.3.1] enzyme activity was assayed spectrophotometrically according to Mayer and Harel (1979) with some modifications.

### Statistical analysis

The experiments were carried out in a completely randomized design (CRD) with 3 replicates; each replica comprising a single petridish containing an average of 20 seeds. All the experiments were analyzed statistically using ANOVA analysis and expressed as Critical Difference at 5% level (taking p=0.05 as significant).

## RESULTS AND DISCUSSION

### Effect of arsenate and arsenite on growth of seedlings

From the present work, it is well established that both arsenic salts are very toxic for the growth of mung bean seedlings. These salts inhibited growth at very

**Table 2.** Effect of different concentrations of sodium arsenate, As(V) and sodium arsenite, As(III) on proline content, phenol content and H<sub>2</sub>O<sub>2</sub> contents of 5 day old mungbean seedlings.

Figures in parentheses indicate % promotion (+) over control. C.D. – Critical Difference.

Treatment	Proline content (mg/g f.wt.)		Phenol content (mg/g f.wt.)		H <sub>2</sub> O <sub>2</sub> content (mg/g f.wt.)	
	As(V)	As(III)	As(V)	As(III)	As(V)	As(III)
Control	0.04	0.04	0.68	0.68	0.045	0.045
0.5µM	0.06(+50)	0.09(+125)	0.81(+19)	1.10(+62)	0.057(+27)	0.07(+56)
1µM	0.08(+100)	0.13(+225)	0.92(+35)	1.16(+71)	0.068(+51)	0.078(+73)
2µM	0.12(+175)	0.17(+325)	1.14(+67)	1.32(+94)	0.079(+76)	0.09(+100)
S.E(mean)	0.01	0.01	0.02	0.02	0.01	0.01
C.D.(P=0.05)	0.002	0.002	0.064	0.064	0.004	0.004

small As concentrations such as 0.5µM (Table 1). Roots were characteristically stubby and brittle, and root tips gradually turned brown. In the present work, length of mung bean seedlings demonstrated an inverse relationship to the applied molar concentrations of sodium arsenite and arsenate. Inhibition of elongation of mung bean seedlings started at a concentration of 0.5µM and it was remarkably pronounced at 2µM. The reduction in seedling length increased with higher doses of As, the effect being more pronounced on root than shoot. The present investigation reveals that arsenic is more toxic for root growth than shoot growth, possibly because retention of As in the roots was higher than that in the stem. Similar reports regarding root growth inhibition were also noted in alfalfa, lettuce, wheat, rice and other plants due to As toxicity (Rofkar and Dwyer, 2011, Allevato *et al.*, 2019).

Treatment with sodium arsenate and arsenite resulted in progressive decline of average fresh and dry weight of 5 day old mung bean seedlings and the effect is concentration – dependent (Table 1). Greater reduction of fresh weight relative to the dry weight of the germinated seedlings, induced by As toxicity, is a common observation as drastic water loss takes place as an immediate effect of most of the abiotic and biotic

stresses imposed. It appears that marked dehydration of seedlings is one of the significant effects associated with growth inhibition. Reduction in fresh and dry weight due to As toxicity has also been reported in maize, mung bean (Stoeva *et al.*, 2005) and rice (Jung *et al.* 2017) plants. With higher concentration of As(V), the water content of the mung bean seedlings declined (Swarnakar, 2017). In the present investigation, arsenite was found to be more toxic for growth of the seedlings.

#### Effect of arsenate and arsenite on proline content of seedlings

In the present investigation, the total proline content of the mungbean seedlings were found to be elevated with the increase in the concentration of sodium arsenate and sodium arsenite which shows that the seedlings were oxidatively stressed (Table 2). Phenomenal accumulation of proline has been reported in plants subjected to stress conditions (Dashek and Erickson, 1981). Beside acting as a cytoplasmic osmoticum and osmolyte, proline may function as a scavenger of free radicals (Abbas *et al.*, 2018). Elevated level of proline has been reported to confer increased tolerance to hyperosmotic stress that

**Table 3.** Effect of different concentrations of sodium arsenate, As(V) and sodium arsenite, As(III) on the activity of catalase, catechol peroxidase, ascorbic acid oxidase and polyphenol oxidase enzymes in 5 day old mungbean seedlings.

Figures in parentheses indicate % promotion (+) of enzyme activity over control. C.D.- Critical Difference.

Treatment	Catalase (mg H <sub>2</sub> O <sub>2</sub> destroyed/h/g f. wt.)		Catechol peroxidase (Change in O.D. at 420 nm/min/gf. wt.)		Ascorbic acid oxidase (mg Ascorbic acid destroyed/h/g f. wt.)		Polyphenol oxidase (Change in O.D. at 480 nm/h/g f. wt.)	
	As(V)	As(III)	As(V)	As(III)	As(V)	As(III)	As(V)	As(III)
Control	97	97	0.12	0.12	7.2	7.2	0.38	0.38
0.5µM	109(+12)	130(+34)	0.19(+58)	0.24(+100)	10.1(+40)	12.4(+72)	0.41(+8)	0.46(+21)
1µM	130(+34)	142(+46)	0.24(+100)	0.37(+208)	14.2(+97)	18.1(+151)	0.47(+24)	0.58(+53)
2µM	143(+47)	158(+63)	0.36(+200)	0.48(+300)	19.1(+165)	25.2(+250)	0.64(+68)	0.79(+107)
S.E (mean)	5	5	0.1	0.1	0.3	0.3	0.1	0.1
C.D. (P=0.05)	3.9	3.9	0.100	0.100	3.1	3.1	0.022	0.022

might be the possible role of proline in stressed plants (Sadeghipour and Monem, 2021).

#### Effect of arsenate and arsenite on phenol content of seedlings

In the present research work, As stress resulted in an increase in phenol content of mung bean seedlings, the promotion being more in arsenite - treated seedlings than arsenate (Table 2). Phenolic compounds have been found to be associated with antioxidant activity (Larson, 1995) and are included under non-enzyme antioxidants (Shen *et al.*, 1997). It has been clarified that phenolic compounds have active ROS scavenging capacity (Yasuhisa *et al.*, 1993).

#### Effect of arsenate and arsenite on H<sub>2</sub>O<sub>2</sub> content of seedlings

Arsenicals induced oxidative stress led to an increased H<sub>2</sub>O<sub>2</sub> content in mung bean seedlings. Highest H<sub>2</sub>O<sub>2</sub> content was found in seedlings treated with the highest concentration of As used, *i.e.*, 2µM (Table 2). H<sub>2</sub>O<sub>2</sub> is one of the potent Reactive oxygen species (ROS) produced in plants. Rapid increase in ROS concentration in response to adverse environmental changes (stress) is called "Oxidative Burst" (Apostol

*et al.*, 1989). When the equilibrium between production and scavenging of ROS is perturbed by any abiotic stress factor or like arsenate here, the plant becomes hypersensitive to stress and thus H<sub>2</sub>O<sub>2</sub> level increases (Mukherji, 2009). During abiotic stress, H<sub>2</sub>O<sub>2</sub> serves as a signalling molecule to regulate biological processes and plays a dual role in plant defence. Also, H<sub>2</sub>O<sub>2</sub> effectively increases the activities of H<sub>2</sub>O<sub>2</sub> scavenging enzymes (Stone and Yang, 2006).

#### Effect of arsenate and arsenite on antioxidant enzyme activities of seedlings

In the present work, under arsenate and arsenite - induced stress, growth inhibition in mung bean seedlings was recorded with a simultaneous increase in activity of all the four oxidizing enzymes *viz.*, catalase, phenol or catechol peroxidase, ascorbic acid oxidase and polyphenol oxidase. (Table 3). Activity of these oxidizing enzymes have been found to be stimulated by toxic concentrations of heavy metals as well (Syta *et al.*, 2013). Roquejo and Tena (2005) have suggested that the induction of oxidative stress is a main process underlying arsenic toxicity in plants. Arsenic toxicity in plants is thought to be induced through an enhanced generation of reactive oxygen species, ROS (Wang *et al.*, 2007). Catalase and

peroxidase are important enzymatic defense systems of plants against free oxygen radicals. Therefore, increased activities of these enzymes, observed in the present work, can be considered as circumstantial evidence for enhanced production of ROS due to oxidative stress which might be one of the reasons for poor growth. The morphological traits like seedling growth are altered with a simultaneous aggravation in antioxidant activity under As stress (Khan *et al.*, 2024). The activities of the oxidizing enzymes were found greater in seedlings treated with sodium arsenite than sodium arsenate.

## CONCLUSION

Arsenic has marked inhibitory and toxic effect on growth and metabolism and thereby impairing productivity of plants. Arsenate and arsenite affect the early growth parameters of mungbean seedlings, including shoot and root length along with fresh and dry weight. Arsenic alters the morphological and physiological characters of the seedlings which ultimately lead to stunted growth and death of the seedlings. Arsenicals induced oxidative stress in the mungbean seedlings as evidenced by the increase in the osmolyte proline and simultaneous increase in ROS scavengers. The activities of all four enzymatic antioxidants, *viz.*, catalase, catechol peroxidase, ascorbic acid oxidase and polyphenol oxidase, were found to be elevated in order to save the cells from oxidative stress. In the present investigation, arsenite was found to induce more oxidative stress, in comparison to arsenate.

## DISCLAIMER

The authors declared that there is no conflict of interest while performing the work and preparation of the manuscript.

## REFERENCE

- Abbas, G., Murtaza, B., Bibi, I., Shahid, M., Niazi, N.K., Khan, M.I., Amjad, M., Hussain M. and Natasha. 2018. Arsenic Uptake, Toxicity, Detoxification and Speciation in Plants; Physiological, Biochemical and Molecular aspects. *Int. J. Environ. Res. Public Health*, **15**(1): 59.
- Abedin, M.J. and Meharg, A.A. 2002. Relative toxicity of arsenite and arsenate on germination and Early seedling growth of rice (*Oryza sativa* L.). *Plant and soil*, **243**(1): 57-66.
- Ahmad, P., Alam, P., Balawi, T.H., Altalayan, F.H., Ahanger, M.A. and Ashraf, M. 2020. Sodium nitroprusside (SNP) improves tolerance to arsenic (As) toxicity in *Vicia faba* through the modifications of biochemical attributes, antioxidants, ascorbate-glutathione cycle and glyoxalase cycle. *Chemosphere*, **244**: 125-480.
- Ahmad, P., Jaleel, C.A., Salem, M.A., Nabi, G. and Sharma, S. 2010. Roles of enzymatic and nonenzymatic antioxidants in plants during abiotic stress. *Crit. Rev. Biotechnol.*, **30**: 161-175.
- Allevato, E., Stazmi S.R., Marabottini, R. and D'Annibale, A. 2019. Mechanisms of arsenic assimilation by plants and counter measures to attenuate its accumulation in crops other than rice. *Ecotoxicology and Environmental Safety*, **185**: 109701.
- Apostol, I., Heinstejn, P.F. and Low, P.S. 1989. Rapid stimulation of an oxidative burst during elicitation of cultured plant cells. Role in defence and signal transduction. *Plant Physiol.*, **90**: 106-116.
- ATSDR (Agency for toxic substances and diseases registry). 2022. Substance Priority List. <https://www.atsdr.cdc.gov/spl/index.html#2022spl> [accessed 5 October, 2023].
- Bates, L.S., Waldren, R.P. and Treare, I.D. 1973. Rapid estimation of free Proline for water stress determination. *Plant and Soil*, **39**: 205-207.
- Bhaduri, A.M. and Fulekar, M.H. 2012. Antioxidant enzyme responses of plants to heavy metal stress. *Rev. Environ. Sci. Biotechnol.*, **11**: 55-69.
- Chance, B. and Maehly, A.C. 1955. Assay of catalases and peroxidases. In Colowick, S.P. and Kaplan, N.O. (Eds.), *Methods in Enzymology* New York: Academic Press, 764-765.
- Dashek, W.V. and Erickson, S.S. 1981. Isolation, assay, biosynthesis, metabolism, uptake and translocation and functions of proline in plant cell tissues. *Bot. Rev.*, **47**: 349-385.
- Gasper, T. and Lacoppe, J. 1968. The effect of CCC and AMO-1618 on growth, catalase, peroxidase, IAA oxidase activity of young barley seedlings. *Physiol. Pl.*, **2**: 1104-1109.
- Jung, H.I., Lee, J., Chae, M.J., Kong, M.S., Lee, C.H., Kang, S.S. and Kim, Y.H. 2017. Growth-inhibition

- patterns and transfer-factor profiles in arsenic-stressed rice (*Oryza sativa* L.). *Environ. Monit. Assess.*, **189**: 638.
- Kashyap, L. and Garg, N. 2018. Arsenic Toxicity in Crop Plants: Responses and Remediation Strategies. In Hasanuzzaman, M., Nahar Kand Fujita, M. (Eds.), *Mechanisms of Arsenic Toxicity and Tolerance in Plants*. Singapore : Springer.
- Khan, Z., Thounaojam, T.C., Rajkumari, J.D., Deka, B.K., Rahman, R. and Upadhyaya, H. 2024. Arsenic induced chromosomal aberrations, biochemical and morphological changes in *Vigna radiata* L. (Mungbean) seedlings and its amelioration by Curcumin, *Vegetos*, **37**: 1185-1194.
- Larson, R.A. 1995. Plant defences against oxidative stress. *Archives of Insect Bio-chemistry and Physiology*, **29**(2):175-186.
- Malik, C.P. and Singh, M.B.1980. *Plant Enzymology and Histochemistry*, India: Kalyani Publishers.
- Mayer, A.M. and Harel, E.1979. Polyphenol oxidase in plants. *Phytochemistry*, **18**:193-215.
- Meharg, A.A. and Hartley Whitaker, J. 2002. Arsenic uptake and metabolism in arsenic resistant and non resistant plant species, *New Phytologist*, **154**(1): 29-43.
- Mukherji, S. 2009. Reactive oxygen species (ROS): a dual role in plant biology. *J. Botan. Soc. Bengal*, **63**(1):1-12.
- Olliver, M.1967. Ascorbic acid estimation. In Sebrell, W.H. and Harris, R.S. (Eds.), *The Vitamins*. NewYork: Academic Press, 338.
- Pickering, I.J., Prince, R.C., George, M.J., Smith, R.D., George, G.N. and Salt, D.E. 2000. Reduction and coordination of Arsenic in Indian mustard. *Plant Physiol.*, **122**: 1171-1178.
- Pigna, M., Cozzolino, V., Violante, A. and Meharg, A.A. 2009. Influence of Phosphate on Arsenic uptake by Wheat (*Triticum durum* L.) irrigated with Arsenic Solutions at three different concentrations. *Water, Air and Soil Pollution*, **197**(1-4): 371-380.
- Rofker, R.J. and Dwyer, D.F. 2011. Effects of light regime, temperature and plant age on uptake of arsenic by *Spartina pectinata* and *Carex stricta*. *Int. J. Phyto.*, **13**: 528-537.
- Requejo, R. and Tena, M. 2005. Proteome analysis of maize roots reveals that oxidative stress is a main contributing factor to plant arsenic toxicity. *Phytochemistry*, **66**(13): 1519-1528.
- Sadeghipour, O. and Monem, R. 2021. Improving arsenic toxicity tolerance in mung bean [*Vigna radiata* (L.) Wilczek] by salicylic acid application. 2021, *Vegetos*, **34**: 663-670.
- Shen, B., Jensen, R.G. and Bohnert, H.J. 1997. Increased resistance to oxidative stress in transgenic Plants by targeting mannitol biosynthesis to chloroplast. *Plant Physiol.*, **113**:1177-1183.
- Stoeva, N., Berova, M. and Zlatev, Z. 2005. Effect of arsenic on some physiological parameters in bean plants. *Biologia Plantarum*, **49**(2): 293-296.
- Stone, J.R. and Yang, S. 2006. Hydrogen peroxide: A signaling messenger. *Antioxid. Redox Signal*, **8**(3-4): 243-70.
- Swarnakar, A. 2017. Enhancement Effect of Gibberellic Acid and Kinetin on Sucrose metabolism in mung bean seedlings under Arsenate toxicity. *American J. of Biosc. Bioengg.*, **5**(1): 50-55.
- Sytar, O., Kumar, A. and Latowski, D. 2013. Heavy metal-induced oxidative damage, defense reactions and detoxification mechanisms in plants. *Acta. Physiol. Plant*, **35**: 985-999.
- Ullrich-Eberius, C.I., Sanz, A. and Novacky, A.J. 1989. Evaluation of arsenate and vandate associated changes of electrical membrane potential and phosphate transport in *Lemna gibba* G1. *J. Exp. Bot.*, **40**(210): 119-128.
- Velikova, V., Yordanov, I. and Edreva, A. 2000. Oxidative stress and some antioxidant systems in acid rain-treated bean plants, *Plant Sci.*, **151**: 59.
- Wang, L.H., Meng, X.Y., Guo, B. and Duan, G.L. 2007. Reduction of arsenic oxidative toxicity by phosphate is not related to arsenate reductase activity in wheat plants. *J. Pl. Nutrition.*, **30**(12): 2105-2117.
- Yasuhisa, T., Hashizume, H. and Yamazaki, M.1993. Super oxidizeradical scavenging activity of phenolic compounds. *Int. J. Biochem.*, **25**(4): 491-494.

---

FULL LENGTH ARTICLE

---

## Palynofloristic and palynofacies analyses of the Permian sediments of Pachwara coalfield, Rajmahal Basin, India: Implications for age, depositional environment and palaeoecology

---

Apurba Mahanti<sup>1,2</sup>, Ashalata D'Rozario<sup>1</sup>, Madhab Naskar<sup>3</sup>, Subir Bera<sup>1\*</sup>

<sup>1</sup>Department of Botany, University of Calcutta, 35 Ballygunge Circular Road, Kolkata 700019, India

<sup>2</sup>Department of Botany, Narasinha Dutt College, Howrah 711101, India

<sup>3</sup>Department of Botany, Sonarpur Mahavidyalaya, Kolkata 700149, India

---

Received : 15.05.2026

Accepted : 12.06.2026

Published : 30.06.2026

---

Palynological and palynofacies investigations were carried out on thirty borecore samples from Pachwara Coalfield of the Rajmahal Basin, Jharkhand, India. The recovered palynoassemblage is represented by trilete, monolete spores, monosaccate, plicate, striate disaccate, non-striate disaccate pollen grains and organic walled microfossils (OWMs). The assemblage is dominated by non-striate disaccate pollen, *Scheuringipollenites*, followed by *Cyclogranisporites*, *Brevitriletes*, *Faunipollenites*, *Crescentipollenites*, *Primuspollenites*, *Rhizomaspora*, *Marsupipollenites* and *Laevigatosporites*. This composition closely corresponds to the *Scheuringipollenites* assemblage zone of the Barakar Formation and indicates an early Permian (Artinskian) age for the studied succession. Palynofacies analysis reveals two principal depositional phases. The first phase is characterized by dominance of structured terrestrial organic matter (ST), accompanied by subordinate charcoal/opaque phytoclasts (CH/OP), indicating low-energy forest-swamp conditions with abundant influx of woody debris. The second phase is dominated by CH/OP with subordinate ST matter, suggesting more oxidizing swampy to fluvio-deltaic environments influenced by periodic oxidation. The occurrence of freshwater organic-walled microfossils, supports deposition in a predominantly continental setting. The integrated palynological and palynofacies data indicate that the sediments belong to the Barakar Formation and were deposited within a fluvio-swampy environment under humid climatic conditions interrupted by episodic oxidation. The study contributes significantly to refining the palynostratigraphy and palaeoenvironmental reconstruction of the Lower Gondwana succession in the Pachwara coalfield in particular and Rajmahal Basin in general.

**Keywords:** Palynology, Palynofacies, Palaeoenvironment, Pachwara Coalfield, Rajmahal Basin, Early Permian.

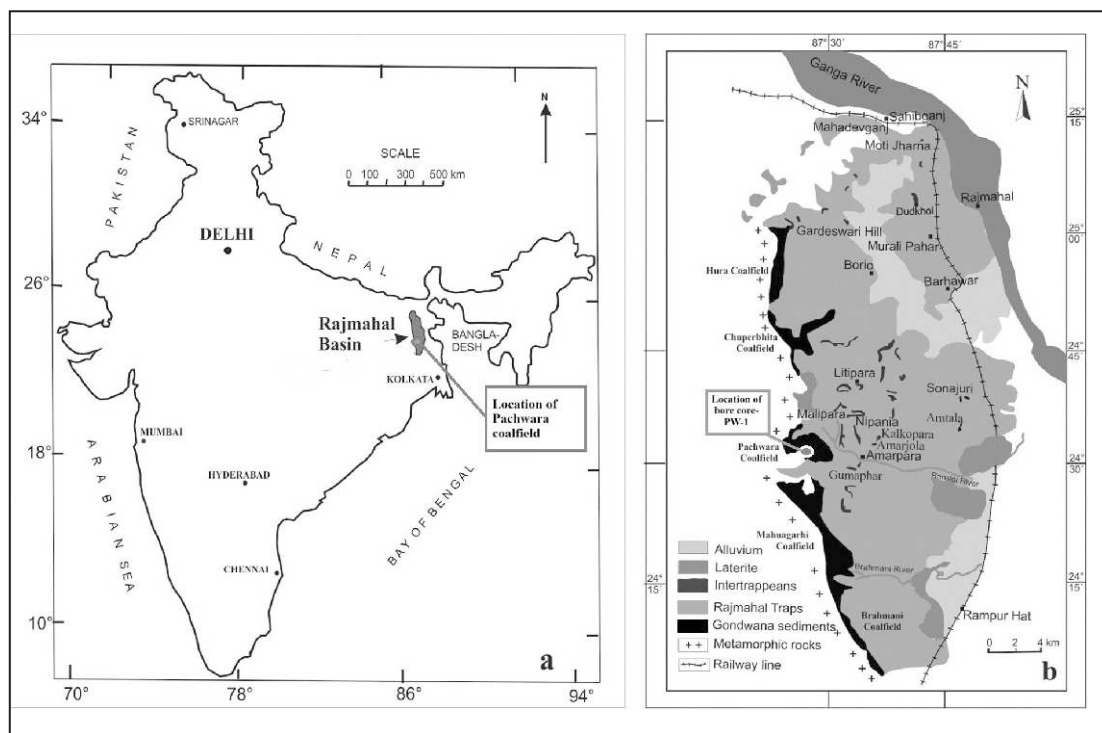
---

\*Corresponding author : [berasubir@yahoo.co.in](mailto:berasubir@yahoo.co.in)

## INTRODUCTION

The Gondwana Supergroup of peninsular India preserves one of the most complete continental sedimentary archives documenting environmental, climatic, and floral evolution from the Late Carboniferous to the Early Cretaceous. These successions occur within a series of fault-controlled intracratonic basins and contain extensive coal-bearing deposits that are of considerable economic and palaeobotanical significance. Among these basins, the Rajmahal Basin occupies a unique position along the northeastern margin of the Indian Gondwana realm. It contains coal deposits aligned in an NNW–SSE trending linear belt along the western flank of the Rajmahal hills and records a prolonged history of continental sedimentation and vegetation dynamics associated with the evolution of eastern Gondwanaland. This belt extends from north to south as Hura, Chuperbhita, Pachwara, Mahuagarhi and Brahmani coalfields. The Pachwara coalfield lies in the central part of Rajmahal Basin (Figs. 1a & 1b).

The Lower Gondwana succession of the Rajmahal Basin is represented primarily by the Talchir and Barakar formations, whereas the Upper Gondwana succession comprises the Dubrajpur and Rajmahal formations. The general stratigraphic succession is given in Table 1 (Raja Rao, 1987; Tiwari and Tripathi, 1995; Tripathi, 2008). The coal-bearing Barakar Formation constitutes one of the most productive stratigraphic units within the basin and preserves abundant palynological records that provide crucial information regarding floral composition, age, palaeoclimate and depositional environments. Owing to the scarcity of age-diagnostic macrofossils in many continental deposits, dispersed spores and pollen grains serve as one of the most reliable tools for biostratigraphic correlation and stratigraphic subdivision of Gondwana sediments (Traverse, 2007). Extensive palynological investigations have been conducted from various Lower and Upper Gondwana sequences of the Rajmahal Basin. In Lower Gondwana formations investigations done in different coalfields (Maheshwari, 1967; Srivastava and



**Fig.1a & 1b.** Map showing location of collection site

**Table 1.** General Stratigraphic Succession in Rajmahal Basin (Raja Rao, 1987, Tiwari and Tripathi 1995; Tripathi 2008).

Age	Group	Formation	Lithotype
Recent/ Quaternary		Soil/ Alluvium	Yellow to maroon sandy, pebbly soil and clay
----- Unconformity (Overlap) -----			
Early Cretaceous to Late Jurassic	Upper Gondwana	Rajmahal Formation	Basic volcanics and intertrappeans (medium to fine –grained sandstone, dark grey claystone , grey shale and siltstone with oolites)
----- Unconformity (Overlap) -----			
Jurassic to Late Triassic	Upper Gondwana	Dubrajpur Formation	Medium–grained sandstone, pebbly sandstone, grey siltstone, mottled shale and claystone
----- Unconformity (Overlap) -----			
Early Permian	Lower Gondwana	Barakar Formation	Coarse–grained to pebbly sandstone, very fine to medium –grained feldspathic sandstone, grey shale, carbonaceous shale and coal seams
Early Permian to Late Carboniferous	Lower Gondwana	Talchir Formation	Conglomerate and pebbly sandstone, greenish fine–grained sandstone, olive - green shale and siltstone
----- Unconformity -----			
Precambrian		Chhotanagpur Gneissic Complex	Granite gneiss, chlorite biotite

Maheshwari, 1974; Ghosh *et al.*, 1984; Banerjee and D'Rozario, 1988, 1990; Murthy *et al.*, 2018, 2020, 2021; Pillai *et al.*, 2020) and in Upper Gondwana sediments works include (Rao, 1936, 1943; Vishnu Mittre, 1953, 1954; Tiwari *et al.*, 1984; Tripathi *et al.*, 1990, 2013; Bakshi *et al.*, 1992; Tiwari and Tripathi, 1995; Tripathi, 2004, 2008; Tripathi and Ray, 2006; Murthy *et al.*, 2018, 2020).

These studies were primarily based on palynological investigation and recently on the combined study of

palynology and palynofacies analyses. Previous investigations from the Rajmahal Basin have primarily focused on taxonomic characterization and age determination on the basis of palynoassemblages. Comparatively fewer studies have integrated palynological data with palynofacies analyses to reconstruct depositional environments and palaeoecological conditions. Palynofacies analysis has emerged as a powerful complementary tool because it enables the assessment of terrestrial versus aquatic organic matter input, oxidation levels,

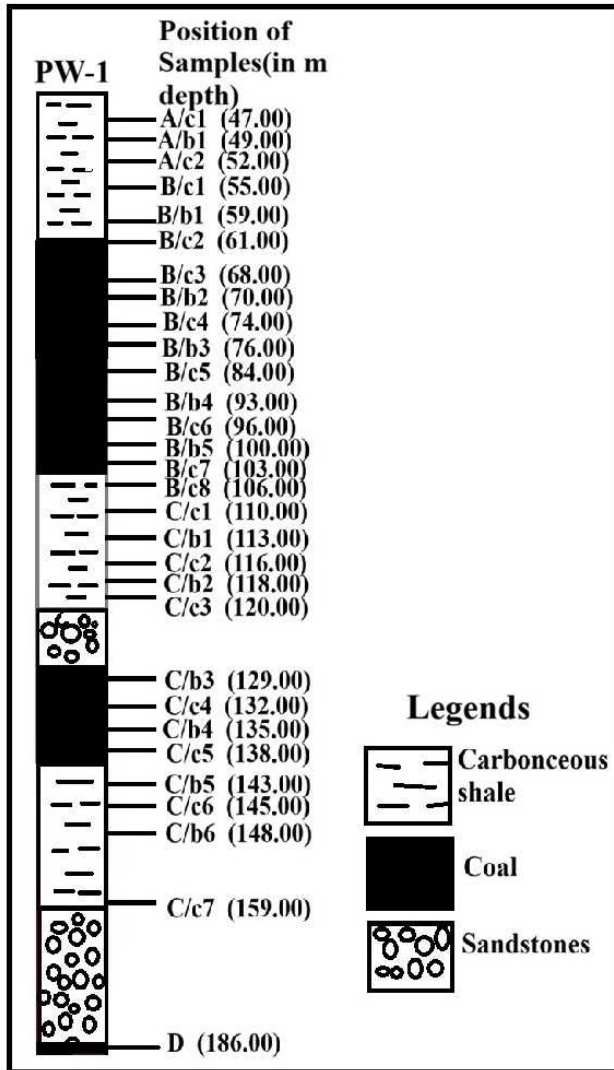


Fig.2. Lithostratigraphic log of bore core PW-1

transport mechanisms, and depositional energy regimes (Tyson, 1995). The relative abundance of structured terrestrial debris, amorphous organic matter, degraded organic matter, charcoal particles, and spore-pollens provides valuable insights into peat-forming environments and broader palaeoenvironmental changes. Furthermore, recent studies have demonstrated that charcoal-rich palynofacies assemblages can be used as indicators of palaeowildfire activity, oxygen availability, and hydrological fluctuations within Gondwanan coal-forming ecosystems (Murthy *et al.*, 2021; Wheeler and Götz, 2016; Nhamutole *et al.*, 2023). Consequently,

integrating palynological and palynofacies datasets offer an opportunity to reconstruct both vegetation history and depositional dynamics with greater precision than either approach alone. Nevertheless, significant gaps remain in the palynological documentation of several sectors of the basin, particularly within the Pachwara Coalfield, where detailed integrated palynofloristic and palynofacies studies remain comparatively limited.

The present study aims to investigate the palynological and palynofacies characteristics of Lower Gondwana sediments from the Pachwara Coalfield in order to: (i) establish the age of the studied succession based on palynostratigraphically significant taxa; (ii) correlate the recovered assemblage with equivalent Gondwana palynozones of India; (iii) reconstruct the depositional environment and palaeoecological conditions through palynofacies analysis; and (iv) evaluate the significance of organic matter distribution patterns using ternary palynofacies modelling. The study provides new information on the early Permian palaeoenvironmental evolution of the Rajmahal Basin and contributes to a more comprehensive understanding of Lower Gondwana coal-forming ecosystems in eastern India.

Table 2. Geological succession in Pachwara coalfield (Tripathi *et al.*, 2010)

Age		Formation
Recent to Sub-Recent		Alluvium
Unconformity		
E.Cretaceous		Rajmahal Formation
Unconformity		
E.Triassic to E.Cretaceous		Dubrajpur Formation
Unconformity		
Early Permian		Barakar Formation
Unconformity		
Early Permian		Talchir Formation
Unconformity		

## MATERIALS AND METHODS

### Geological setting and sample collection

The Pachwara coalfield lies in the central part of Rajmahal Basin. The coal measure representing Barakar Formation rests directly on Precambrian rocks and are overlain by Dubrajpur Formation or Rajmahal Traps. The generalized geological succession in Pachwara Coalfield is given in Table 2. The present investigation is based on borecore samples (PW-1), collected from Pachwara Coalfield (24°30'-24°36': 87°23'-87°36') of the Rajmahal Basin, Jharkhand (Fig. 1). Thirty samples representing coal, shaly coal, shale, carbonaceous shale, and fine-grained sandstone were collected from different depths of the borecore for palynological and palynofacies analyses. The lithological succession and sampling horizons are shown in (Fig. 2).

### Sample preparation and analysis

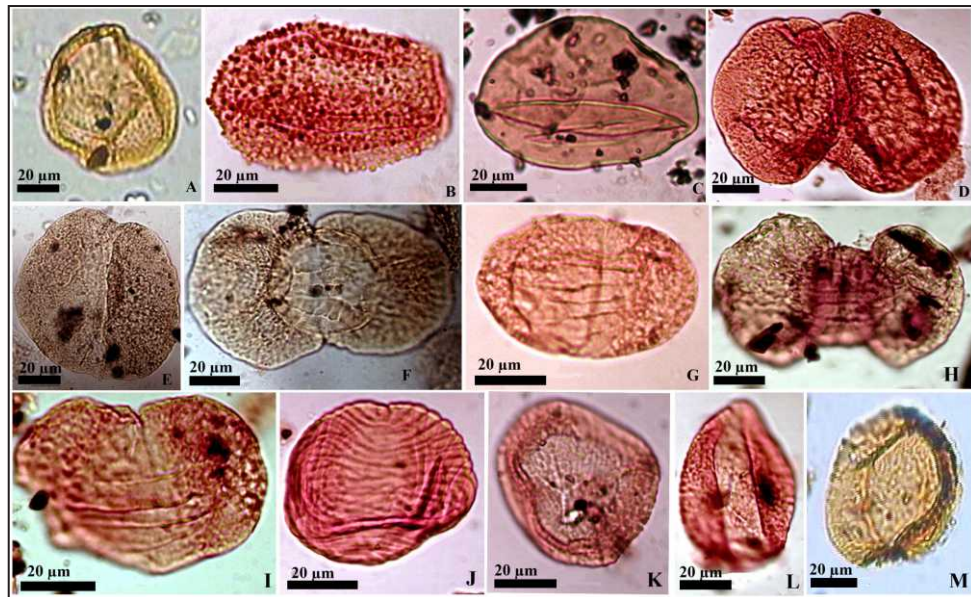
Approximately 50 g of each sample was crushed into small fragments of 2-5 mm size and processed using standard palynological maceration techniques following Traverse (2007). Samples were initially treated with 40% hydrofluoric acid (HF) to dissolve silicate minerals, followed by oxidation using concentrated nitric acid (HNO<sub>3</sub>). The residues were subsequently treated with 5% potassium hydroxide (KOH) to remove humic substances and improve palynomorph visibility. Thorough washing with distilled water was carried out after each step of chemical treatment. The final residues were preserved in 50% glycerine and slides were prepared using glycerine jelly. Microscopic examination was performed using a Zeiss Axioscope-2 microscope equipped with a Panasonic digital imaging system. Photomicrographs were obtained using 10× and 40× objectives with a 10× eyepiece. Quantitative palynological analysis was conducted by counting a minimum of 300 palynomorphs from each productive sample. Relative abundance percentages were calculated for all identified taxa. Taxonomic identification was based on published Gondwana palynological literature and Potonié 1970. For palynofacies analysis palynological slides were used.

Quantitative palynofacies analysis was based on 500 organic matter particles. Recovered palynofacies components have been grouped under five major categories of organic constituents following Aggarwal *et al.*, 2017, 2019, Batten, 1996; Hart, 1986; Joshi *et al.*, 2024; Pocock *et al.*, 1987; Tyson, 1995; Svobova and Sarkar, 2024. These categories are: **Structured Terrestrial (ST)**: which includes cuticles, tracheids, woody tissues, and other recognizable plant fragments. **Charcoal/Opaque Phytoclasts (CH/OP)**: consisting of black to dark-brown opaque organic particles produced through oxidation and/or charring of plant tissues. **Amorphous Organic Matter (AOM)**: which includes structureless organic material derived from microbial degradation, bacterial activity, resins, and highly altered plant tissues. **Degraded Organic Matter (DOM)**: consisting of partially decomposed terrestrial organic particles exhibiting indistinct cellular organization. **Spore-Pollen (SP)**: includes spores, pollen grains, and other palynomorphs. The materials and processed samples and slides are deposited in the Palaeobotany and Palynology Laboratory, Department of Botany, University of Calcutta, India.

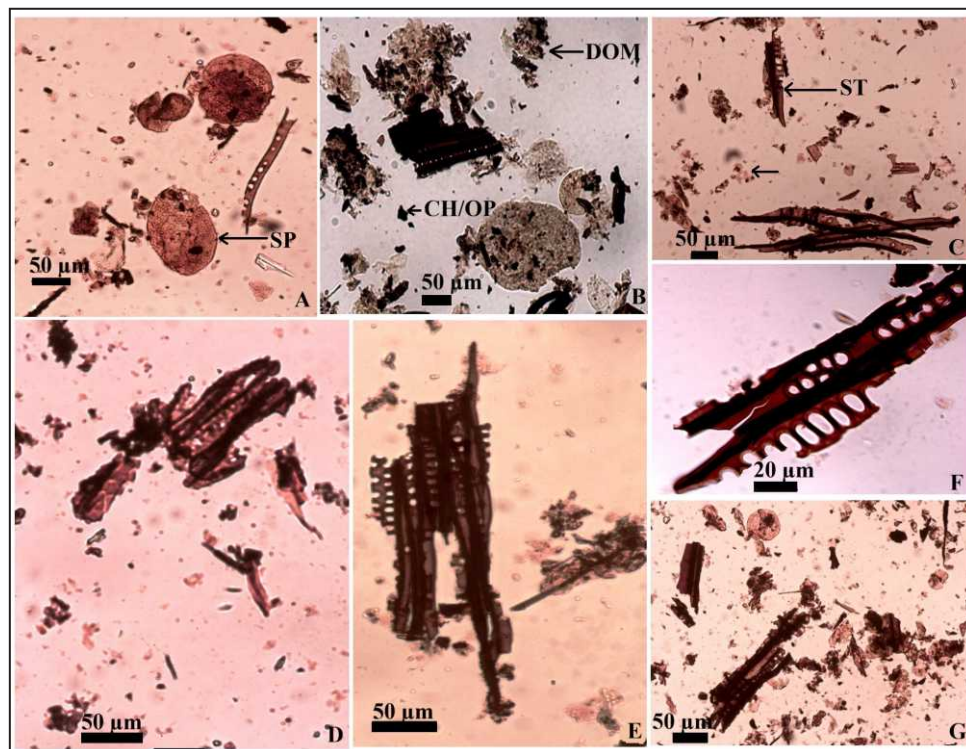
## RESULTS

### Palynological analysis

Palynological investigation of thirty samples from borecore PW-1 revealed a rich and diverse palynoflora. Of the thirty processed samples, fifteen produced abundant and well-preserved palynomorphs, whereas the remaining fifteen samples yielded only sparse and poorly preserved palynomorphs. A total of forty-three palynomorph taxa were identified, representing trilete, monolete spores, monosaccate, non-striate disaccate, striate disaccate, plicate pollen grains, and organic-walled microfossils (OWMs) (Figs. 3, 4). The recovered assemblage is dominated by non-striate disaccate pollen grains, which constitute the principal component of the productive samples (Fig. 3). Among them, *Scheuringipollenites* is the most abundant and consistently represented taxon throughout the productive horizons. Other significant non-striate disaccate pollen grains include *Alisporites*, *Cuneatisporites* and *Corisaccites*. Monosaccates are



**Fig.3.** Selected palynomorphs recovered from the bore core. A. *Cyclogranisporites gondwanensis* B. *Cyclobaculisporites indicus*, C. *Laevigatosporites colliensis*, D. *Scheuringipollenites barakarensis*, E. *Scheuringipollenites maximus*, F. *Rhizomaspora indica* G. *Faunipollenites singrauliensis*, H. *Striatites notus*, I. *Striatopodocarpites magnificus*, J. *Vittatina africana*, K. & L. *Marsupipollenites triradiatus*, M. *Peltacystia venosa*



**Fig. 5.** (A,B,C,D,E and G) - Different types of recovered palynofacies components, (F) - Enlarged view of single ST component

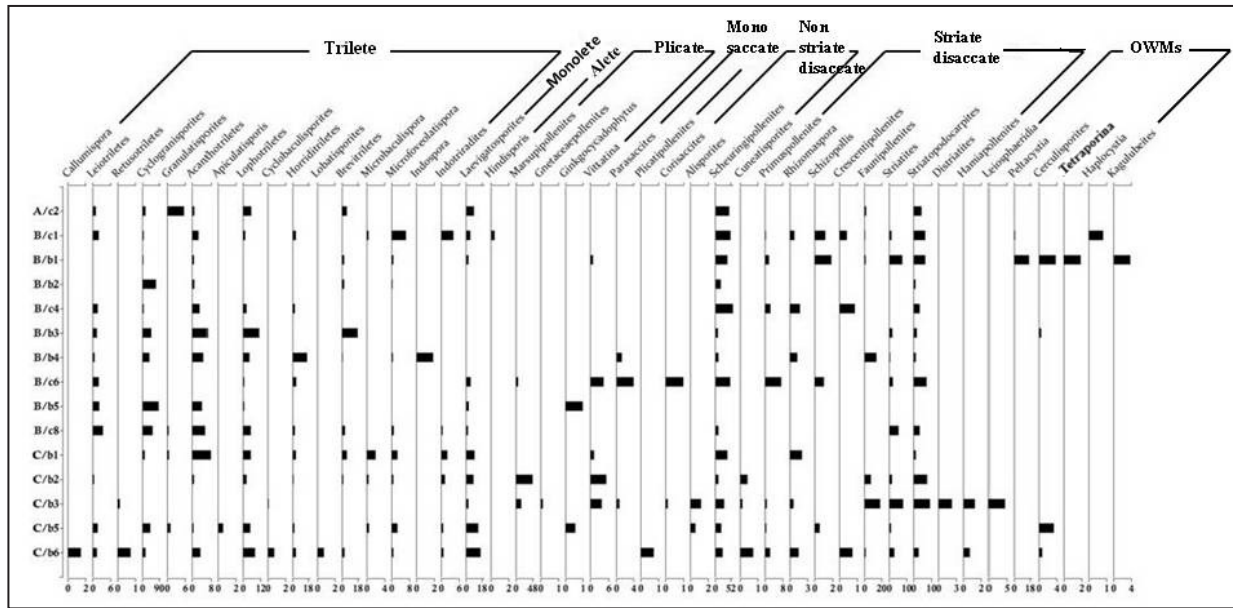


Fig.4. Relative abundance of various palynomorphs in bore core PW-1

represented by *Parasaccites* and *Plicatipollenites*. Striate disaccates form an important subordinate component and are represented chiefly by *Faunipollenites*, *Crescentipollenites*, *Primuspollenites*, *Rhizomasporea*, *Striatites*, *Striatopodocarpites*, *Distriatites* and *Hamiapollenites*. Trilete spores constitute a secondary but significant element of the assemblage and include *Cyclogranisporites*, *Horriditriletes*, *Acanthotriletes*, *Leiotriletes*, *Brevitriletes*, *Lophotriletes* and *Indotriradites* and many other types. Monolete spores are represented mainly by *Laevigatosporites*. Plicate pollen grains such as *Marsupipollenites*, *Vittatina*, *Ginkgocycadophytus*, and *Gnetaceapollenites* occur sporadically. *Marsupipollenites* however occupies the dominant position in one of the samples. The OWMs are represented by *Peltacystia*, *Circulisporites*, *Kagulubeites*, *Leiosphaeridia*, *Hindisporis* and *Tetraporina* (Barua *et al.*, 2026). The entire succession of deposition is characterized by the dominance of the non-striate disaccate pollen grain *Scheuringipollenites* accompanied by subdominance of the trilete genus *Cyclogranisporites* at certain stratigraphic levels. Whereas in other cases *Cyclogranisporites* gains dominance over *Scheuringipollenites* (Fig. 3).

**Palynofacies analysis**

Eighteen samples yielded rich and diverse particulate organic matter for palynofacies analysis. The frequency distribution of palynofacies components reveals the predominance of terrestrial organic matter throughout the studied succession (Figs. 5, 6). ST constitutes the dominant palynofacies component in fourteen of the eighteen productive samples. Within these ST dominated samples, twelve samples exhibit CH/OP as the subdominant constituent, whereas the remaining two samples show AOM as the subdominant component. In contrast, four samples are characterized by the dominance of CH/OP, accompanied by ST matter as the principal subordinate component. These samples contain comparatively lower proportions of AOM, DOM and SP. AOM occurs in low to moderate frequencies and rarely exceeds the abundance of ST particles. DOM is consistently represented in minor amounts, indicating limited organic degradation. The SP fraction constitutes only a small proportion of the total particulate organic matter, despite the palynological richness observed in several samples. The ternary palynofacies distribution also reveals the predominance of ST and CH/OP (Fig. 7).

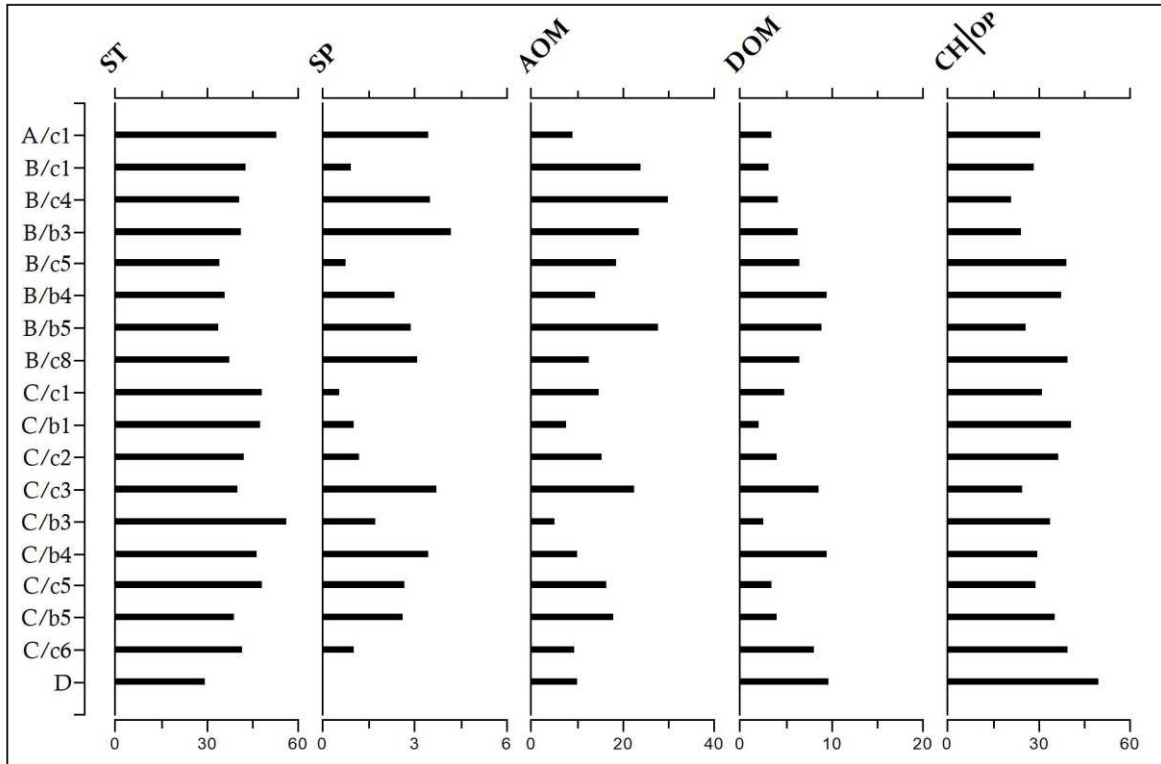


Fig. 6. Relative abundance of various palynofacies components in bore core PW-1.

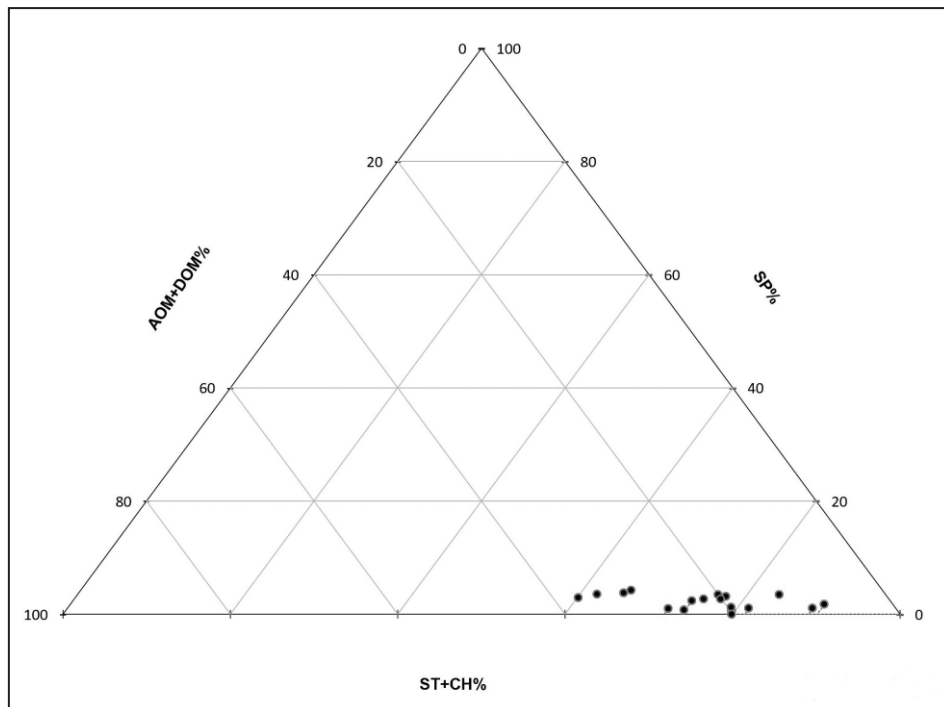


Fig. 7. Ternary diagram showing the distribution of various palynofacies components.

**Table 3.** List of recovered palynotaxa in bore core PW-1 and their botanical affinities (Balme 1995; Hochuliet *et al.*, 2010; Lindström and McLoughlin, 2007; Mishra and Jha, 2017; Mishra and Singh 2018; Di Pasquo and Grader, 2012 and Mishra *et al.*, 2017).

Palynotaxa	Botanical Affinity Order/ family/group
<i>Callumispora</i> sp.	Filicales
<i>Leiotriletes</i> sp.	Filicales
<i>Retusotriletes</i> sp.	Rhyniophyte
<i>Cyclogranisporites</i> sp.	Filicales
<i>Granulatisporites</i> sp.	Filicales
<i>Acanthotriletes</i> sp.	Filicales
<i>Apiculatisporis</i> sp.	
<i>Lophotriletes</i> sp.	Filicales
<i>Cyclobaculispora</i> sp.	
<i>Horriditriletes</i> sp.	Filicales
<i>Lobatisporites</i> sp.	Filicales
<i>Brevitriletes</i> sp.	Filicales
<i>Microbaculispora</i> sp.	Filicales
<i>Microfoveolatispora</i> sp.	Filicales
<i>Indospora</i> sp.	Lycopsidales
<i>Indotriradites</i> sp.	
<i>Laevigatosporites</i> sp.	Filicales, Marratiales
<i>Hindisporis</i> sp.	
<i>Plicatipollenites</i> sp.	Cordaitales
<i>Parasaccites</i> sp.	Cordaitales, Coniferales
<i>Corisaccites</i> sp.	Coniferales
<i>Alisporites</i> sp.	Corystospermales
<i>Scheuringipollenites</i> sp.	Glossopteridales
<i>Cuneatisporites</i> sp.	
<i>Primuspollenites</i> sp.	?Peltaspermales
<i>Rhizomaspora</i> sp.	
<i>Schizopollis</i> sp.	
<i>Crescentipollenites</i> sp.	Glossopteridales/ Coniferales
<i>Faunipollenites</i> sp.	Glossopteridales
<i>Striatites</i> sp.	Glossopteridales, Coniferales
<i>Striatopodocarpites</i> sp.	Glossopteridales
<i>Distriatites</i> sp.	
<i>Hamiapollenites</i> sp.	Coniferales
<i>Marsupipollenites</i> sp.	
<i>Gnetaceapollenites</i> sp.	
<i>Vittatina</i> sp.	Glossopteridales
<i>Ginkgocycadophytus</i> sp.	
<i>Peltacystia</i> sp.	Zygnemataceae
<i>Circulisporites</i> sp.	Zygnemataceae
<i>Haplocystia</i> sp.	
<i>Tetraporina</i> sp.	
<i>Kagulubeites</i> sp.	Zygnemataceae
<i>Leiosphaeridia</i> sp.	Chlorophyta

## DISCUSSION

### Palynostratigraphic significance and age assessment

The present assemblage shows prevalence of non-striate disaccate pollen *Scheuringipollenites*, along with other trilete, monolete and striate disaccate genera. The overwhelming dominance of *Scheuringipollenites* is particularly significant because this taxon serves as the principal marker of the *Scheuringipollenites barakarensis* Assemblage Zone, which has been extensively documented from the Damodar, Wardha-Godavari, Son-Mahanadi, Satpura, Talcher, and Rajmahal basins. The present assemblage exhibits strong similarity to the *Scheuringipollenites-Faunipollenites* association reported from the lower and middle parts of the Barakar Formation in several Indian Lower Gondwana coalfields (Tiwari and Tripathi, 1992; Jha and Aggarwal, 2012, 2015). The assemblage also compares closely with Palynoassemblage-II of borecore RT-4 from the Raniganj Coalfield (Murthy *et al.*, 2010) and Palynoassemblage-III of borecore MBKW-3 from the Mand-Raigarh Coalfield (Murthy *et al.*, 2014), both of which are assigned to the late Early Permian. Similar assemblages have been documented from the Johilla, Pathakhera, Wardha, Talcher, and Sohagpur coalfields, further reinforcing the regional consistency of the recovered palynoflora. *Scheuringipollenites* dominated assemblages are also known from Rahmahal basin (Bharadwaj and Srivastava, 1986; Banerjee and D'Rozario, 1988, 1990; Murty *et al.*, 2023).

Dominance of *Cyclogranisporites* is observed in the middle Barakar assemblages recovered from Seam II of Talcher coalfield (Srivastava, 1984), assemblage B of Talcher coalfield (Bharadwaj and Srivastava, 1969) and from lower Barakar sediments of Hura and Chuparbhitia coalfields of Rahmahal Basin (Banerjee and D'Rozario, 1988, 1990).

Collectively, the palynological evidence firmly supports assignment of the studied succession to the Barakar Formation and indicates an early Permian (Artinskian) age for the sedimentary sequence penetrated by borecore.

### Palaeovegetation and palaeoclimate

The recovered palynoflora provides valuable information regarding the composition of the Permian vegetation that occupied the Rajmahal Basin. The dominance of non-striate and striate bisaccate pollen grains indicate that glossopterid gymnosperms formed the principal component of the regional vegetation. Glossopterids are widely regarded as the dominant peat-forming plants throughout Gondwana during the early Permian and were particularly successful in humid, lowland swamp environments. The associated occurrence of trilete spores, including *Cyclogranisporites*, *Brevitriletes*, *Leiotriletes*, and *Lophotriletes*, suggests the presence of diverse pteridophytic communities occupying moist habitats adjacent to the peat-forming swamps (Table 3). The abundance of glossopterid-derived pollen, together with the extensive coal-bearing intervals encountered in the borehole, suggests a humid climatic regime capable of sustaining extensive mire development. Such climatic conditions are consistent with palaeoclimatic reconstructions from other Gondwana basins during the Artinskian, when widespread peat accumulation occurred across large parts of peninsular India. Dominance of *Scheuringipollenites*, suggest temperate climate with humid condition (Gautam *et al.*, 2022).

### Palynofacies and depositional environment

Analysis of palynofacies data reveal two depositional phases. One phase is dominated by ST components which is regionally, similar with Palynofacies-I of the Chintalapudi sub-basin in the Godavari Valley Coalfield (Joshi *et al.*, 2024), distinguished only by a notably lower frequency of SP in the present study. Globally, it is comparable with Permian sediments from the Sydney and Bowen basins (Michaelsen *et al.*, 2000; Wheeler *et al.*, 2020). The other phase is characterized by dominance of CH/OP and subdominance of ST components along with moderate occurrence of AOM, and sparse presence of DOM and SP. This signature closely correlates with the lower Gondwana records across India (Pocock *et al.*, 1987; Tyson, 1995; Closas *et al.*, 2005; Carvalho *et al.*, 2013; Pienkowski and Waksmundzka, 2009; Aggarwal *et al.*, 2019; Joshi *et al.*, 2024; Mishra *et al.*, 2025).

CH/OP frequencies serve as proxies for depositional polarity, transport distance, and high sediment oxygenation (Carvalho *et al.*, 2013; Joshi *et al.*, 2024). Specifically, the assemblage mirrors the CH/OP dominant, SP depleted character of the Auranga Basin, though it retains a higher frequency of ST elements than observed there (Mishra *et al.*, 2025). Such opaque-rich configurations are diagnostic of strongly oxic environments, placing the depositional setting within stable oxic swamps, fluvial channels, or prodeltaic to delta-front complexes (Closas *et al.*, 2005; Pieńkowski and Waksmundzka, 2009).

Beyond the Indian subcontinent, the dual-phase organic signature aligns closely with high-latitude Gondwanan depositional systems. The primary Charcoal (CH)-heavy assemblage, backed by subdominant Structured Terrestrial (ST) fragments, finds strong equivalents in the Permian Karoo Supergroup, indicating persistent paleowildfire activity and highly oxidizing conditions within coal-forming mires (Ruckwied *et al.*, 2014; Wheeler *et al.*, 2016; Nhamutole *et al.*, 2023). Conversely, periods of ST dominance mirror successions in the Sydney and Bowen basins, reflecting shifting environmental states to low-energy fluvial systems that efficiently transported well-preserved woody debris across Glossopteris-dominated floodplains (Michaelsen *et al.*, 2000; Wheeler *et al.*, 2020).

Overall, the palynofacies assemblage is characterized by the dominance of ST plant debris and CH/OP particles, indicating a strong terrestrial influence and substantial contribution from arborescent vegetation. The ternary palynofacies distribution (Fig. 7) further supports the interpretation of a predominantly terrestrial depositional system. The concentration of samples near the ST+CH apex indicates that sedimentation was largely controlled by the influx of woody-plant debris and charcoaled phytoclasts derived from adjacent woody vegetation. The very low proportions of AOM+DOM suggest limited preservation of amorphous organic matter and restricted development of persistently reducing conditions, whereas the low spore-pollen component is most likely attributable to dilution by abundant phytoclasts. The close clustering of samples further indicates relatively stable depositional conditions

throughout much of the studied interval, despite minor fluctuations in oxidation intensity reflected by variations in charcoal abundance.

### Palaeoecological consideration of OWMs

The palynological assemblage is dominated by terrestrial spores and pollen grains and lacks unequivocal marine palynomorphs such as marine dinoflagellate cysts. The occasional occurrence of freshwater organic-walled microfossils like *Peltacystia*, *Circulisporites* suggests freshwater conditions (Mays *et al.*, 2021). Presence of *Leiosphaeridia* suggests shallow marine environment with decreased salinity during the Permian-Triassic interval (van Soelen *et al.*, 2018) to non-marine fluvial and lacustrine set-up towards Lower Triassic (Mays *et al.*, 2020). Occurrence of *Peltacystia*, *Circulisporites* suggest affinity to class Zygnematophytaceae (Division Charophyta) (Mays *et al.*, 2021) *Leiosphaeridia* shows polyphyletic similarity with phycmata of pyramimonadalean prasinophytes and vegetative cells of Class Trebouxiophyceae (Division Chlorophyta) (Moczydlowska, 2011; Mays *et al.* 2021; Barua *et al.*, 2026).

### CONCLUSION

The present palynological and palynofacies investigations of borecore PW-1 from the Pachwara Coalfield provide important insights into the age, depositional environment and palaeoecology of the Lower Gondwana succession in the Rajmahal Basin. Palynological analyses indicate that the studied succession belongs to the Barakar Formation and is of late early Permian (Artinskian) age. The dominance of the *Scheuringipollenites* palynoassemblage, together with its close resemblance to coeval assemblages from other Indian Gondwana basins, provides a reliable basis for regional stratigraphic correlation. The palynofacies composition reflects deposition within a terrestrial fluvio-swamp system characterized by abundant input from arborescent vegetation. Variations in the relative abundance of structured terrestrial matter and charcoal/opaque phytoclasts suggest alternating peat-forming and oxidizing phases. The abundance of glossopterid-derived pollen indicates the widespread development of

*Glossopteris*-dominated vegetation under humid climatic conditions favourable for coal formation. Collectively, these findings refine the palynostratigraphic framework of the Rajmahal Basin and contribute to a better understanding of the depositional history and palaeoecology of the early Permian Gondwana landscapes of eastern India.

### ACKNOWLEDGEMENT

The authors are grateful to DST FIST and DBT Builders programs, Department of Botany, University of Calcutta for providing necessary facilities. Sincere thanks are due to the Regional Coal Survey Laboratory, Raniganj for granting permission to collect core samples and providing facilities and information during field investigations.

### DISCLAIMER

The authors declare that there is no conflict of interest.

### REFERENCE

- Aggarwal, N., Agrawal, S. and Thakur, B. 2019. Palynofloral, palynofacies and carbon isotope characteristics of Permian coal deposits from the Godavari Valley Coalfield, South India: Insights into age, palaeovegetation and palaeoclimate. *International Journal of Coal Geology*, **214**: 1-22.
- Aggarwal, N., Carvalho, M., Jha, N. and Thakur, B. 2017. Palynology and palynofacies of the Permian strata in the Kothagudem Sub-basin, Andhra Pradesh, Southern India. *Journal of the Palaeontological Society of India*, **62**(2): 175-186.
- Baksi, A.K., Tiwari, R.S., Tripathi, A. and Farrar, E. 1992. Geochemical, geochronological and palynological observations on Lower Cretaceous lavas in the Rajmahal Basin. In *National Symposium on Mesozoic Magmatism of the Eastern Margin of India* (pp. 16-17).
- Balme, B.E. 1995 Fossil in situ spores and pollen grains: an annotated catalogue. *Rev. Palaeobot. Palynol.*, **87**(2-4): 323.
- Banerjee, M. and D'Rozario, A. 1988. Biostratigraphy and environment of deposition in the Lower Gondwana sediments of Chuperbhita Coalfield, Rajmahal Hills. *Journal of the Palaeontological Society of India*, **33**: 73-90.

- Banerjee, M. and D'Rozario, A. 1990. Palynostratigraphic correlation of Lower Gondwana sediments in the Chuperbhita and Hura Basins, Rajmahal Hills, Eastern India. *Review of Palaeobotany and Palynology*, **65**: 239-255.
- Barua, A., D'Rozario, A., Mahanti, A. and Bera, S. 2026. Organic-walled microfossils of algal affinity from the Permian of West Bengal, India and their palaeoecological considerations. *Geophytology*, **56**(1): 23-36.
- Batten, D.J. 1996. Palynofacies and palaeoenvironmental interpretation. In: Jansonius, J., and McGregor, D.C. (Eds.), *Palynology: Principles and Applications*, 3:1011-1064.
- Bharadwaj, D.C. and Srivastava, A.K. 1986. Palynological dating of bottom seam in Gomani River section, Chuperbhita Coalfield, Santhal Parganas, Bihar. *National Seminar on Coal Resources of India*, Banaras.
- Bharadwaj, D.C. and Srivastava, S.C. 1969. Palynological correlation of coal seams in Talcher Coalfield, Orissa, India. *Palaeobotanist*, **17**(2): 152-156.
- Carvalho, M.A., Ramos, R.R.C., Crud, M.B., Witovisk, L., Kellner, A.W.A., Silva, H.P., Grillo, O.N., Riff, D. and Romano, P.S.R. 2013. Palynofacies as indicators of palaeoenvironmental changes in a Cretaceous succession from the Larsen Basin, James Ross Island, Antarctica. *Sedimentary Geology*, **295**: 53-66.
- Closas, M.C., Permanyer, A. and Vila, M.J. 2005. Palynofacies distribution in a lacustrine basin. *Geobios*, **38**: 197-210.
- Di Pasquo, M.M. and Grader, G. 2012. The palynology of the lower permian (Asselian- ?Artinskian) copacabana formation of apillapampa, cochabamba, Bolivia. *Palynol.*, **36**: 264-276.
- Gautam, S., Mendhe, V.A., Murthy, S., Mishra, D.P. and Mishra, V.K. 2022. Palynoassemblages and depositional environment of the subsurface Permian sediments in Raniganj Coal Belt, Damodar Basin, West Bengal, India *Journal of Earth Science*, **131**(4): 224.
- Ghosh, A.K., Roy, S.P. and Laskar, T. 1984. Biostratigraphy and some anomalous petrological properties of Chuperbhita coals, Rajmahal Coalfield, Bihar. In *Evolutionary Botany and Biostratigraphy* (pp. 323-330).
- Hart, G.F. 1986. A review of the use of palynology in palaeoenvironmental analysis. *Geological Society Special Publication*, **32**: 1-15.
- Hochuli, P. A., Hermann, E., Vigran, J.O., Bucher, H. and Weissert, H. 2010. Rapid demise and recovery of plant ecosystem across the end-Permian extinction event. *Global and Planetary Change*, **74**: 144-155.
- Jha, N., & Aggarwal, N. 2012. Palynostratigraphy of the Mailaram area, Godavari Basin. *Geophytology*, **42**: 1-12.
- Jha, N. and Aggarwal, N. 2015. Palynological investigations in the Kachinapalli area, Godavari Basin. *Journal of Earth System Science*, **124**: 1023-1035.
- Joshi, H., Aggarwal, N. and Jha, N. 2024. Palynofloral, palaeovegetational and palaeoenvironmental investigations in the Lower Kamthi Formation of South India. *Journal of Palaeosciences*, **73**: 45-65.
- Lindström, S. and McLoughlin, S. 2007. Synchronous palynofloristic extinction and recovery after the end-Permian event in the Prince Charles Mountains, Antarctica: Implications for palynofloristic turnover across Gondwana. *Review of Palaeobotany and Palynology*, **145**: 89-122.
- Maheshwari, H.K. 1967. Studies in the Glossopteris flora of India—29. Miospore assemblage from the Lower Gondwana exposures along Bansloi River in Rajmahal Hills, Bihar. *Palaeobotanist*, **15**(3):258–280.
- Mays, C., Vajda V., Frank, T.D., Fielding, C.R., Nicoll, R.S., Tevyaw, A.P. and McLoughlin, S. 2020. Refined Permian–Triassic floristic timeline reveals early collapse and delayed recovery of south polar terrestrial ecosystems. *GSA Bulletin*, **132**(7-8): 1489-1513.
- Mays, C., Vajda, V. and McLoughlin, S. 2021. Permian-Triassic non-marine algae of Gondwana—Distributions, natural affinities and ecological implications. *Earth-Science Reviews*, **212**: 1-29.
- Michaelsen, P., Henderson, R.A., Crosdale, P.J., Mikkelsen, S.O., 2000. Facies architecture and depositional dynamics of the Upper Permian Rangel coal measures, Bowen Basin, Australia. *Journal of Sedimentary Research*, **70**(4): 879-895.
- Mishra, S. and Jha, N. 2017. Early permian (asselian-sakmari) palynoflora from Chintalapudi area, godavari graben, south india and its Palaeoenvironmental implications. *Journal of the*

- Palaeontological Society of India*, **62**(2), December 31: 157-174.
- Mishra, S. and Singh, V.P. 2018. Palynology, palynofacies, and taphonomical studies of Kamthi Formation, (Godavari Graben), southern India: Implications to biostratigraphy, palaeoecology, and depositional environment 2018. *International Journal of Coal Geology*, **195**:102-124.
- Mishra, S., Aggarwal, N., Jha, N., 2017. Palaeoenvironmental change across the Permian-triassic boundary inferred from palynomorph assemblages (Godavari Graben, South India). *Palaeobio, Palaeoenv.*, **98** (2): 177-204.
- Mishra, S., Aggarwal, N. and Verma, A.K. 2025. Palaeodepositional consequences for hydrocarbon generation using geochemistry and palynology: example from Auranga coalfield in India. *Journal of Petroleum Exploration and Production Technology* **15**: 177. <https://doi.org/10.1007/s13202-025-02095-4>.
- Moczydłowska, M. 2011. The early Cambrian phytoplankton radiation: acritarch evidence from the Lukati Formation, Estonia. *Palynology* **35**(1): 103-145.
- Murthy, S., Agnihotri, D., Uhl, D., Jasper, A. and Singh, R.K. 2023. Palaeoenvironmental and stratigraphical implications of the palynoflora and macro-charcoal from the early Permian of the Chuperbhita Coalfield, Rajmahal Basin, Jharkhand, India *Journal of Palaeosciences*, **72**: 141-151. <https://doi.org/10.54991/jop.2023.1865>
- Murthy, S., Chakraborti, B. and Roy, M.D. 2010. Palynodating of subsurface sediments, Raniganj coalfield, Damodar Basin, West Bengal. *Journal of Earth System Sciences*, **119**(5): 701-710.
- Murthy, S., Kavali, P.S., Di Pasquo, M. and Chakraborti, B. 2018. Late Pennsylvanian and Early Cisuralian palynofloras from the Rajmahal Basin, eastern India. *Historical Biology*, **32**: 143-159.
- Murthy, S., Mendhe, V.A., Uhl, D., Mathews, R.P., Mishra, V.K. and Gautam, S. 2021. Palaeobotanical and biomarker evidence for Early Permian wildfire in the Rajmahal Basin, India. *Journal of Palaeogeography*, **10**(5): 1-21.
- Murthy, S., Ram Awatar and Gautam, S. 2014. Palynostratigraphy of Permian succession in the Mand-Raigarh coalfield, Chhattisgarh, India. *Journal of Earth System Science*, **123** (8): 1879-1893.
- Murthy, S., Saxena, A. and Chakraborti, B. 2020. Palynostratigraphy of Permian and Mesozoic subsurface sediments of Brahmani Coalfield, Rajmahal Basin, India. *Journal of the Palaeontological Society of India*, **65**(2): 149-161.
- Nhamutole, N., Bamford, M., Souza, P. and Carmo, D. 2023. Palynofacies analysis of the JOG16N-8 borehole, Maniamba Basin, Mozambique. *Journal of African Earth Sciences*, **205**:104997.
- Pieńkowski, G. and Waksmundzka, M. 2009. Palynofacies in Lower Jurassic epicontinental deposits of Poland. *Episodes*, **32**: 21-32.
- Pillai, S.S.K., Mathews, R.P., Murthy, S., Goswami, S., Agarwal, S., Sahoo, M. and Singh, R.K. 2020. Palaeofloral investigation from Lalmatia Coal Mine, Rajmahal Basin. *Journal of the Geological Society of India*, **96**: 43-57.
- Pocock, S.A.J., Jansonius, J. and McGregor, D.C. 1987. Palynofacies and depositional environments. *AAPG Studies in Geology*, **23**:45-67.
- Potonié, R., 1970. Synopsis der Gattungen der sporae dispersae. Pt. V. Nachtrage Zu allen Gruppen (Turmae). *Beih. Geol. Jb.*, **87**: 1-87.
- Raja Rao, C.S. 1987. Coal resources of Bihar (excluding Dhanbad District). *Bulletin Geological Survey India Series*, **45**(IV): 300-322.
- Rao, A.R. 1936. Winged pollen from the Jurassic of India. Proceedings of 23rd Indian Science Congress Association, Indore **34**.
- Rao, A.R. 1943. Jurassic spores and sporangia from the Rajmahal Hills, Bihar. *Proceedings of National Academy Sciences, India* (B) **13**(6): 181-197.
- Ruckwied, K., Götz, A.E. and Jones, P. 2014. Palynological records of the Permian Ecca Group (South Africa). *Palaeogeography, Palaeoclimatology, Palaeoecology*, **413**: 167-172.
- Srivastava, S.C. 1984. Palynological succession in Lower Gondwana sediments of Talcher Coalfield, Orissa. In *Proceedings of the Fifth Indian Geophytological Conference*: 119-128.
- Srivastava, S.C. and Maheshwari, H.K. 1974. Palynostratigraphy of the Damuda Group in the Brahmani Coalfield, Rajmahal hills, Bihar. *Geophytology*, **4**(1): 35-45.
- Svobodová, M. and Sarkar, S. 2024 Palynology and palynofacies analysis of the Subathu Formation

- (Early Ypresian-Middle Lutetian) of Morni Hills, Haryana, India *Journal of Palaeosciences*, **73**: 27-44. DOI: 10.54991/jop.2024.1868
- Tiwari, R.S., Kumar, P. and Tripathi, A. 1984. Palynodating of Dubrajpur and Intertrappean beds in subsurface strata of the north eastern Rajmahal Basin. *In*: Tiwari, R.S. *et al.* (Editors) – Proceedings of Vth Indian Geophytological Conference, Lucknow 1983 Special publication: The Palaeobotanical Society: 207-225.
- Tiwari, R.S. and Tripathi, A. 1992. Marker assemblages of Permian and Triassic miospores in India. *Palaeobotanist*, **40**: 194-236.
- Tiwari, R.S. and Tripathi, A. 1995. Palynological assemblages and absolute age relationship of Intertrappean beds in the Rajmahal Basin, India. *Cretaceous Research*, **16**: 53-72.
- Traverse, A. 2007. *Paleopalynology (2nd ed.)*. Springer, Dordrecht, 813 pp.
- Tripathi, A. 2004. Palynology evidences of hitherto unrecognized Jurassic sedimentation in Rajmahal Basin, India. *Rivista Italiana di Paleontologiae Stratigrafia*, **110**: 35-42.
- Tripathi, A. 2008. Palynochronology of Lower Cretaceous volcanosedimentary succession of the Rajmahal formation in the Rajmahal Basin, India. *Cretaceous Research*, **29**: 913-924.
- Tripathi, A. and Ray, A. 2006. Palynology of the Dubrajpur Formation (Early Triassic to Early Cretaceous) of the Rajmahal Basin, India. *Palynology*, **30**: 133-149.
- Tripathi, A., Jana, B.N., Verma, O., Singh, R.K. and Singh, A.K. 2013. Early Cretaceous palynomorphs, dinoflagellates and plant megafossils from the Rajmahal Basin, Jharkhand, India. *Journal of Palaeontological Society of India*, **58**: 125-134.
- Tripathi, A., Tiwari, R.S. and Kumar, P. 1990. Spores dispersae and their distributional pattern in subsurface Mesozoic sediments of Rajmahal Basin, Bihar, India. *Palaeobotanist*, **37**: 367-388.
- Tripathi, A., Murthy, S. and Singh, R.K. 2010. Palynodating of coal-bearing strata near Kunda Pahari, Pachwara coalfield, Rajmahal basin, Jharkhand, India. *Journal of palaeontological society of India*, **55**(1): 29-35.
- Tyson, R.V. 1995. *Sedimentary Organic Matter: Organic Facies and Palynofacies*. Chapman & Hall, London.
- van Soelen, E.E., Twitchett, R.J. and Kürschner, W.M. 2018. Salinity changes and anoxia resulting from enhanced run-off during the late Permian global warming and mass extinction event. *Climate of the Past*, **14**: 441-453.
- Vishnu Mittre 1953. Microfossils from the Jurassic of Rajmahal Hills, Bihar. Proceedings of 40th Indian Science Congress Association. Lucknow, pt. III. **112**.
- Vishnu Mittre 1954. Petrified spores and pollen grains from the Jurassic of the Rajmahal Hills, Bihar. *Palaeobotanist*, **2**: 117-127.
- Wheeler, A. and Götz, A.E. 2016. Palynofacies patterns of the Highveld coal deposits (Karoo Basin, South Africa). *Acta Palaeobotanica*, **56**: 3-15.
- Wheeler, A., Van de Wetering, N., Esterle, J.S. and Götz, A.E. 2020. Paleoenvironmental changes in the palynology and palynofacies of a Late Permian marker mudstone, Galilee Basin, Australia. *Palaeoworld*, **29**: 439-452.

---

**SHORT COMMUNICATION**

---

**Conservation of *Androsace umbellata* (Primulaceae), a threatened species in plains of West Bengal**

---

**Shramona Chaudhuri, Firdousi Rahaman, Camellia Nandi and Shuvadeep Majumdar\***

Department of Botany, Scottish Church College, 1 & 3 Urquhart Square, Kolkata-700006, West Bengal, India

---

Received : 18.02.2026

Accepted : 20.03.2026

Published : 30.06.2026

---

*Androsace umbellata* is considered as threatened and conserved in a restricted area in the Scottish Church College, Kolkata, West Bengal.

**Keywords:** *Androsace umbellata*, Conservation, Scottish Church College, Threatened.

---

**INTRODUCTION**

While working on the restoration of herbarium in Scottish Church College, Kolkata, authors came across a curious plant of Primulaceae. Mishandled for years the herbarium sheet was not in the proper condition but the field data revealed that the plant was collected from the college premises in the year 2015. In the year 2023, the species had been found to grow in the college campus and after a continuous monitoring of the habitat from January to early March (2023-2025) and with the help of literature the taxon was identified as *Androsace umbellata* (Lour.) Merr. of the family Primulaceae. This is one of the significant findings of the occurrence of the taxon from the plains of West Bengal (6 m).

According to Tiwari and Dash (2020), the genus *Androsace* L. is represented by 38 species, one subspecies and a variety in India. Barik *et al.* (2018)

has listed the taxon in the threatened list of India. *Androsace umbellata* mostly occurs in the temperate regions of West Bengal (Aitken, 1999), but here it thrives well in an isolated small patch of land in Scottish Church College garden. Prain (1903) recorded this species as *A. saxifragaefolia* Bunge (= *A. umbellata*) from North and Central Bengal. According to Ghosh (2016) the genus *Androsace* is represented by only one species i.e. *A. umbellata* in West Bengal and he mentioned the occurrence of the taxon as "Throughout the State", but actually it occurs in the colder areas of the state. No previous collection and reports are found elsewhere.

Understanding the importance of conservation of the plant we have demarcated the area for safe growth. Continuous assessment for last three years, revealed that the diversity calculated by quadrat method shows that the taxon has significantly increased each year from 2023 (40), 2024 (45) and 2025 (92) considering the conservation strategies enforced by the authorities (see Table 1).

---

\*Corresponding author : smbotn@scottishchurch.ac.in

Another plant of Primulaceae also growing in the garden is *Lysimachia arvensis* (L.) U.Manns & Anderb.  $\equiv$  *Anagallis arvensis* L.

#### MATERIALS AND METHODS

Continuous monitoring of the plant for three years from January to early March (2023-2025) was done in the college garden and quadrat method was performed year wise. Identification was carried out following standard protocol.

#### Taxonomic treatment

*Androsace umbellata* (Lour.) Merr., Philipp. J. Sci. 15(3): 237. 1920 (1919); R.B. Ghosh in V. Ranjan, P. Lakshminarasimhan, S.S. Das & H.J. Chowdhery

(eds.), Fl. West Bengal 3: 324. 2016. *Drosera umbellata* Lour., Fl. Cochinch.: 186. 1790. *Androsace saxifragifolia* Bunge in Enum. Pl. China Bor. 53. 1833 (as 'saxifragaefolia'); Hook. f., Fl. Brit. India 3: 496. 1882; Prain, Bengal Pl. 1: 640. 1903. (Fig.1).

Annual herbs, bearing stolons with slender branches, up to 6 cm high; leaves simple, petioles 0.4–2.8 cm long, pubescent; lamina broadly ovate, orbicular or suborbicular 0.6–1.8 cm in diameter, base cordate, margin crenate, apex obtuse, pubescent on both surfaces; umbels 3–6-flowered; peduncles single to several per rosette, flowers 2–2.5 mm, pubescent; pedicels 3–8 mm long; bracts lanceolate, 2–3.2 mm long, base, apex, pubescent; calyx 2.5–4 mm long, (4–)5 lobed, gamosepalous, divided almost to base, pubescent, lobes ovate to elliptic, 2–3 × 1–2 mm,



**Fig. 1.** A, B. *Androsace umbellata* (Lour.) Merr.; C, D. *Lysimachia arvensis* (L.) U.Manns & Anderb.

**Table 1.**

CALCULATION OF QUADRAT OF <i>Androsace umbellata</i>																								
YEAR	Q1	Q2	Q3	Q4	Q5	Q6	Q7	Q8	Q9	Q10	Q11	Q12	Q13	Q14	Q15	Q16	Q17	Q18	Q19	Q20	TOTAL INDIVIDUAL SPECIES	PERCENTAGE FREQUENCY	DENSITY	ABUNDANCE
2023	0	0	1	2	6	3	3	7	6	6	3	2	1	0	0	0	0	0	0	0	40	55%	2	3.636
2024	0	0	0	2	8	3	3	9	8	7	3	2	0	0	0	0	0	0	0	0	45	45%	2.25	5
2025	0	0	2	8	5	4	7	9	13	20	8	5	4	2	2	1	1	1	0	0	92	80%	4.6	5.75

acute, much spreading in fruit; corolla white with yellow mark in the center, 2–3 mm in diameter; lobes ovate to oblong, entire; capsules subglobose, c.3 mm in diameter.

*Specimen Examined:* India, West Bengal, Kolkata, Scottish Church College, 22.587883°N, 88.369897°E, alt. 6 m, 10.02.2025, *S. Majumdar SCC/01/2025* (Herbarium, Scottish Church College).

*Habitat & Ecology:* Terrestrial, growing in shady places.

*Flowering and fruiting:* January–March.

*Distribution in India:* Delhi, Haryana, Himachal Pradesh, Jammu & Kashmir, Madhya Pradesh, Odisha, Punjab, Sikkim, Uttarakhand, Uttar Pradesh, West Bengal (Tiwari and Dash, 2020).

According to Flora of Bhutan (1999) “there is an unlocalised Hooker specimen labeled 'Sikkim' which is probably from the Darjeeling terai”.

The percentage frequency, density and abundance of *A. umbellata* calculated for the year 2023 is 55%, 2 and 3.636 respectively; for the year 2024 is 45%, 2.25 and 5 and 80%, 4.6 and 5.75 for the year 2025 (see Table 1). We feel ecstatic to locate, conserve and ensuring its survivality and multiplication each year through the valiant effort of gardeners and college authorities.

#### ACKNOWLEDGEMENT

Authors thank Principal, Scottish Church College for encouragement and providing facilities. Authors are

also grateful to anonymous reviewers for positive comments and improvement of the manuscript. Authors acknowledges Scottish Church College for providing financial assistance (Grant no. RDC-SCCFRG/2023/03). Authors are indebted to dissertation students for their help in various ways.

#### DISCLAIMER

The authors declared that there is no conflict of interest while performing the work and preparation of the manuscript.

#### REFERENCE

- Aitken, E. 1999. *Androsace*. In: Grierson AJC, Long DG. (Eds.) *Flora of Bhutan*. Royal Botanic Garden, Edinburgh. 2(2): 555-564.
- Barik, S.K., Tiwari, O.N., Adhikari, D., Singh, P.P., Tiwari, R. and Barua, S. 2018. Geographic distribution pattern of threatened plants of India and steps taken for their conservation. *Curr. Sci.*, **114**(3): 470-503.
- Ghosh, R.B. 2016. Primulaceae. In: Ranjan V, Lakshminarasimhan P, Dash SS, Chowdhery HJ. (Eds.) *Flora of West Bengal III*. Botanical Survey of India, Bhubaneswar. 1-493.
- Prain, D. 1903. Bengal Plants I. Calcutta. 1-680.
- Tiwari, U.K. and Dash, S.S. 2020. Primulaceae. In: Dash SS, Mao AA. (Eds.) *Flowering Plants of India An Annotated checklist (Dicotyledons) II*. Botanical Survey of India, Bhubaneswar. 1-566.

## Erratum

“Thajuddin N. and Suseela M.R. 2025. Algal blooms: a mystery of nature. Journal of the Botanical Society of Bengal. 79(2): 53-76.”

Author correction: The review article entitled 'Algal blooms: a mystery of nature' published in volume 79(2): 53-76, December, (2025) requires an author correction to few errors in text. Necessary corrections are as follows

Page 55 Right side 1st para line 4: The first author of the article – to correct as – the second author of this review article

Page 56 left side last para: First author of the article – to correct as – the second author of this review article

Page 62 right side first line: First author – to correct as – second author

Page 73 – Acknowledgement 1st line: First author – to correct as – second author

6th line: Second author – to correct as – first author

## Tribute to Professor Subhendu Mukherji (1937-2026)



Professor Subhendu Mukherji, Retired Professor and Ex-Head of the Department of Botany (1988-90), Calcutta University passed away on April 17, 2026 leaving behind his wife, two daughters and many students. Born in 1937 at Bhadrakali, Hooghly he passed his Matriculation examination in 1952 from Mitra Institution, Kolkata and Pre-University examination in 1953 from Presidency College, standing 6th in position and acquired gold medal for scoring highest marks in Sanskrit. He graduated with honours in Botany from Presidency College in 1956. After passing the MSc examination in Botany from Calcutta University in 1958, Prof. Mukherji started his research work in the Department of Botany, C.U. under the supervision of Prof. S.M. Sircar in a project "Role of mineral nutrition on the physiology of lodging habit in rice", sponsored by the ICAR, New Delhi. He was awarded the Ph.D. degree in Botany from the Calcutta University in 1966 on the thesis concerned with the lodging habit of rice plant under heavy fertilizer application in relation to grain yield response and mineral uptake.

He also worked as a Research Officer in Plant Physiology Laboratory from 1964-68 in a PL 480 project offered to Prof. S.M. Sircar by the United States.

Professor Mukherji joined the Department of Botany, University of Calcutta as Lecturer in Botany in 1968, became Reader in 1976 and Professor of Botany in 1983. He was the Head of the Department for the period from 1988 to 1990. He was incharge of Plant Physiology and Biochemistry section till his retirement in 2002. Professor Mukherji implemented several research projects funded by the ICAR, CSIR and UGC. The major areas of research interest of Dr. Mukherji were (a) Characterization of heavy metal and metalloid toxicity in higher plants and algae (b) Influence of water and salinity stress on growth, metabolism and productivity of crop plants (c) Growth regulating properties of penicillin in higher plants (d) Environmental pollution in general with special reference on impact of automobile exhaust on road side plants. He and his associates published 140 research papers and several review articles in reputed PR reviewed journals. 40 research students obtained their PhD degree from the Calcutta University under his guidance. He was one of the authors of a Plant Physiology and Biochemistry text book written for UG and PG students.

He was elected fellow of Indian Society for Plant Physiology, Life Member of Indian Science Congress Association and Indian Society for Plant Physiology. He served the Botanical Society of Bengal as Secretary, Treasurer, Vice President and President. Prof. Mukherji was founder member and Ex-President, Plant Physiology Forum, Kolkata.

Professor Mukherji will be remembered as a beloved mentor and enduring source of inspiration to generations of students. Admired for his warm personality and dedication to cultural life he was held in deep affection by students, research scholars and faculty members. For more than three decades he graced the stage in the department's annual reunion play, a cherished tradition that reflected his spirit and commitment to the community. His legacy lives on through the countless students and scholars he guided. He will be deeply missed, yet fondly remembered by all whose lives he touched.

**Asok K. Biswas**  
Secretary, Alumni Association  
Department of Botany, C.U.



## INSTRUCTIONS TO AUTHORS

Manuscript should be typed in 'Times New Roman' font with ~ 25 mm margins, one and a half spaced and mailed to the Editor at editorjbsb@gmail.com in the following formats: Microsoft Word for text and JPG/TIF format for figures and tables, in separate files. Do *not* submit PDFs, DTP files or LaTeX files. All pages should be numbered sequentially. Each line of the text should also be numbered, with the top line of each page being line 1. [Ensure the "Language" is "English (U.K)"]. Use of Large Language Models (LLMs) such as ChatGPT is not permitted.

*Preparation of the manuscript:* The manuscript should have a brief and informative full title followed by the names of all authors. A running title, not exceeding 75 characters, including spaces, should be provided. Each name of author should have an identifying superscript number (<sup>1, 2, 3</sup> etc.) associated with the relevant institutional address, to be entered further down the page. The corresponding author's name should have a superscript asterisk\*. The institutional address (es) of each author should be listed next, being preceded by the relevant superscript number. The e-mail address of the corresponding author should also be provided

The *second page* will include the ABSTRACT written within 300 words without citation of references, to be followed by three to ten KEY WORDS that include the full botanical name(s) of any relevant plant material. If many species are involved, broad species groups or taxa may be mentioned instead. Core terms used in the title should be included in the key words, to make digital searches more effective. The Title, Abstract and Key words should be self-explanatory.

The *third and subsequent pages* will comprise the *text file* written in a lucid language. 'FULL LENGTH ARTICLES' will usually be structured into INTRODUCTION, MATERIALS AND METHODS, RESULTS, DISCUSSION, ACKNOWLEDGEMENTS, DECLARATIONS and REFERENCES. Mention of specialized items of equipment mentioned in MATERIALS AND METHODS section, should be followed by details of the model, manufacturer, city and country of origin. There should be no repetition of data in both tabular and graphical forms, in the RESULTS section. For other descriptive items including literature reviews, other kinds of subdivisions in the text are allowed. For SHORT COMMUNICATIONS, there is no abstract. REVIEW ARTICLES are generally commissioned by the journal. Unsolicited review articles may be considered for publication at the sole discretion of the Editor.

Numbers up to and including ten should be spelt out unless they are measurements. All numbers above ten are to be in numerals except at the beginning of sentences. Appropriate position of tables and figures should be indicated in the text. The journal style prohibits the use of footnotes within articles. If required, such notes may be merged parenthetically in the text, or as a separate paragraph.

*Abbreviations* should be used sparingly and should be spelt out on first use, with the abbreviation in parenthesis. Measurements should be given in SI or SI-derived units. [See the box item]. Standard chemical symbols, names of chemicals (CO<sub>2</sub>, ATP), procedures (SEM, UV, PCR, UPGMA), molecular terminology (SDS-PAGE, bp) or statistical terms (s.d., s.e., t-test, ANOVA) are accepted. Tables and figures should be numbered in Indo-Arabic (Figure 1, Table 2 etc).

*Mathematical equations* are to be used in proper symbolic form; word equations are not accepted. Symbols and equations may be typed directly into MS Word wherever possible. In other cases, use of the MathType software is recommended for display of inline equations, or sometimes the Equation Editor or Microsoft's Insert → Equation function, may be used. However, in running text, do not use MathType, Equation Editor, or the Insert → Equation function to insert single variables, Greek/ other symbols [like Δ, λ or ' (prime)], or mathematical operators (e.g. ±, ≥, γ). Also, these should not be used for only a part of the equation, and equations should not be a mix of different equation tools or appear in "hybrid" forms (part text - part MathType or part MathType - part Equation Editor).

*Figures:* A list of captions and legends to the figures should be submitted in a separate page. Photographs may be minimized to fit one column. If a plate has more than one photograph, they should all be clear and have the same resolution. If necessary, hand-drawing with India ink, on a Bristol board may be made. An 8-10 pt Microsoft Sans Serif font may be used for text labelling of figures. Use scale bars (instead of magnification factors) and error bars in the figures wherever necessary. For keys to figures, use *verbal cues* (e.g. open circle, closed red circle). Use of an appropriate statistical measure of central tendency (median/average) and error bars is advised, wherever appropriate. Indicate the sample size (*n* number), the test statistic and the *P* value. In calculating the degree of reduction of the figures, authors should keep in mind the column-size (7.5 cm) as well the page-size (16.25 cm x 20 cm) of the journal.

*Tables:* The tables should come in sequence at the end of the main text (article) file, in JPG/TIF format, and *not* inserted as an image/picture. Tables with statistical analyses should indicate the standard of errors and ranges in the table legend. For tables that feature chemical structures, the native ChemDraw file(s) need to be submitted separately as .cdx files. Tables related to experiments should have brief legends describing the experiments, so that data are intelligible.

*Nomenclature of plants, genes and sequences:* *Plant names* must be written out in full binomial form in the main text for

each organism at first mention, and duly italicized. Later, genus initial may be used followed by species name. The author citation is generally desired. *The International Plant Names Index* and *The Plant Book: a portable dictionary of plants, their classification and uses*, 4<sup>th</sup> ed., by D.J. Mabberley (Cambridge: Cambridge University Press, 2017) may be used for guidance to correct usage. Any cultivar or variety should also be stated where appropriate, using the ISHS *International Code of Nomenclature for Cultivated Plants* (2004), Eds., C.D. Brickell *et al* (ISBN 3-906166-16-3) for guidance. However, once defined in full, the plants may be named in their common vernacular or quasi-scientific forms without italics or uppercase letters (e.g. arabidopsis, sunflower, tomato), wherever convenient.

For gene nomenclature, authors should adhere to standard rules for nomenclature of genes and their encoded proteins. Species-specific gene nomenclature rules are available for arabidopsis, maize, rice and wheat. The names of genes or gene-families should be spelled out at first mention.

If authors intend to publish novel nucleotide or protein sequences, those should first be submitted in electronic form, at one of the major data repositories -- EMBL Nucleotide Sequence Database, GenBank, or the DNA Data Bank of Japan (for nucleotides) and UniProt or SWISS-Prot (for amino acid sequences). The accession number obtained is to be submitted. The sequence matrices may be presented in the paper only if their alignment is crucial to the core message of the publication. For chemical, biochemical and molecular biological nomenclature, the rules of the *International Union of Pure and Applied Chemistry (IUPAC)* and the *International Union of Biochemistry and Molecular Biology (IUBMB)* need to be followed.

Very large files may be submitted electronically as SUPPLEMENTARY INFORMATION.

*Text citation:* The author's last name and the year of publication for the source should appear in the text within parentheses - such as (Sharma and Sharma, 1994) or (Sharma and Sharma, 1994, a,b,c) to distinguish between papers of the same authors published in the same year.

**Reference styles** with examples.

The references are to be given after the ACKNOWLEDGEMENTS and DECLARATIONS section.

a) Journal articles

- with 1 author:

1] Chakraborty HL. 1954. Morphology of the staminate flowers of Cucurbitaceae with special reference to the evolution of stamens. *Bull Bot Soc Bengal* **8**:186-213.

- with 2 authors:

2] Becker B, Marin B. 2009. Streptophyte algae and the origin of embryophytes. *Ann Bot* **103**: 999–004.

- with 7 authors or more: write the names of the first three authors followed by et al.

3] Rhie A, Nurk S, Cechova M *et al*. 2023. The complete sequence of a human Y chromosome. *Nature* **121**: 344–54.

b) Books and book chapters

**i) An authored book**

4] Sharma AK, Sharma A. 1994. *Chromosome Techniques: A manual*. Reading, UK: Harwood Academic Publishers.

**ii) An edited book**

5] Samajpati N, Chattopadhyay SB. 1984. (Eds.) *Interaction of plant pathogens in the host*. Calcutta: Oxford & IBH.

**iii) A chapter in an edited book**

6] Arora RK. 1981. Native food plants of north-eastern India. In Jain SK (Ed.), *Glimpses of Indian ethnobotany* New Delhi: Oxford & IBH, 91-106.

c) Doctoral dissertation

7] Ghosh M 1964. Cytogenetical and embryocultural work in rice (*O. sativa* L.) and related species. PhD thesis. University of Calcutta (unpublished).

d) Dataset with persistent identifier

8] Bennett MD, Leitch IJ. 2012. Plant DNA C-values database. (Release 6.0, Dec 2012) <http://data.kew.org/cvalues> [accessed 8 July, 2017].

e) Online-only journals

9] Behera PK, Kumar V, Sharma SS, Lenka SK, Panda D. 2023. Genotypic diversity and abiotic stress response profiling of short-grain aromatic landraces of rice (*Oryza sativa* L. *indica*). *Current Plant Biology* **33**: 100269 <https://doi.org/10.1016/j.cpb.2022.100269>.

f) Pre-prints

10] Dolzhenko E, English A, Dashnow H *et al*. 2023. Resolving the unsolved: comprehensive assessment of tandem repeats at scale. Preprint at *BioRxiv*. doi: <https://doi.org/10.1101/2023.05.12.540470>.

g) Web links or URLs should come *directly in the main text* and not in the Reference section.

## h) Scientific &amp; Technical Reports:

11] Tomato Genome Consortium. 2012. The tomato genome sequence provides insights into fleshy fruit evolution. *Nature* 485: 635-641.

12] Cohen JT, Duggar K, Gray GM, *et al.* 2001. Evaluation of the potential for bovine spongiform encephalopathy in the United States. Boston: Harvard School of Public Health, Center for Risk Analysis, Report No. PB2002-108684, p.116. Supported by the US Department of Agriculture.

## i) Software:

13] Felsenstein J. 2022. PHYLIP, v3.698, Dep. Genome Sciences & Dep. Biology, University of Washington <https://doi.org/10.12345/ABC000999>

A current issue of the journal or the *World List of the Scientific Periodicals* may be consulted, if required.

'Personal Communications' will not feature in the reference list, but it may be cited in the text.

**Declarations :**

Apart from Acknowledgements, all manuscripts should include the following (where relevant), under the heading 'Declarations': individual authors' contributions, statement on competing interests, statement on funding, consent for publication, information on availability of data and materials, and additional authors' information. Manuscripts reporting studies involving animals must include a statement on *ethics approval*, the name of the committee that approved the study, and its reference number if appropriate.

Proofs of the articles if sent to the authors, must be returned to the Editor within seven days of receiving the proofs. Corrections at the proof stage involving deviations from the text are not allowed and are chargeable to the authors. Only e-reprints will be provided to the corresponding author with effect from January 1, 2020.

**Publication :** Journal of the Botanical Society of Bengal is a peer reviewed journal and published bi-annually and issued usually during June and December of each year.

**Editor-in-Chief:** Professor Subir Bera, Department of Botany, University of Calcutta.

Cheques and bank drafts issued should be drawn in favour of **Botanical Society of Bengal**.

Name of Account Holder : Botanical Society of Bengal  
 Name of the Bank : UCO Bank  
 Branch Name : Ballygunge Circular Road  
 Branch Code : 0837  
 Bank A/c No. : 08370100001762  
 IFSC Code : UCBA0000837

**Contents :** The Editors will be glad to consider all types of the scientific communications and Book Reviews in Botany, Plant Biology and allied subjects.

**Processing & printing charges:** The rate will be ₹ 600.00 per page (wef. January 1, 2022). Extra charges will be levied on printing of coloured plates @ ₹ 4000.00 per plate.

**Membership :** Membership of the Botanical Society of Bengal is open to all persons interested in Botany. Membership forms are available from the Office of the Society, Department of Botany, University of Calcutta, Kolkata 700019. It can also be downloaded from the society website. The Botanical Society of Bengal is pleased to provide opportunities to students and research scholars to enrol as Student Members with an amount of ₹ 3000/ for M.Sc. students and ₹ 4000/ for research scholars. The status will be upgraded on a par with other members, after completion of their courses. The life membership will remain unchanged at ₹ 6000/.

Mail all your orders including back volumes and special issues to : Secretary, Botanical Society of Bengal, 35, Ballygunge Circular Road, Kolkata 700 019, West Bengal, India.

Twelve and half per cent discount are allowed to Book Sellers and Purchasers only.

Postage and packing charges extra.

### Abbreviations and units of measurement to be used

Abbreviations ought to be spelled out at first mention. Use of the minus index to indicate 'per' (e.g.  $\text{m}^{-2}$ ,  $\text{L}^{-1}$ ,  $\text{h}^{-1}$ ) is preferred, except in such cases as 'per plant', 'per field' etc.

Wherever possible, use the *Système international d'unités* (SI units). Use of non-SI unit of protein mass such as Dalton (Da), or kilodaltons (kDa), is permitted.

Units of volume may be expressed in terms of cubic metre (e.g.  $8 \times 10^{-9} \text{ m}^3$ ,  $8 \times 10^{-6} \text{ m}^3$  or  $8 \times 10^{-3} \text{ m}^3$ ) or litre (e.g. 8  $\mu\text{L}$ , 8 mL, 8 L), but this use must be consistent in the manuscript. Concentrations may be expressed typically as 8  $\text{mmol m}^{-3}$ , 8  $\mu\text{M}$  (for 8  $\mu\text{mol L}^{-1}$ ), or 40 $\text{mg L}^{-1}$ .

<b>Common prefixes</b>		<b>Units of mass</b>		<b>Units of concentration</b>	
tera ( $10^{12}$ )	T	kilogram	kg	molar	M
giga ( $10^9$ )	G	gram	g	millimolar	mM
mega ( $10^6$ )	M	milligram	mg	micromolar	$\mu\text{M}$
kilo ( $10^3$ )	k	microgram	$\mu\text{g}$	parts per million	ppm
deca (10)	da				
deci ( $10^{-1}$ )	d	<b>Units of time</b>		<b>Units of temperature</b>	
centi ( $10^{-2}$ )	c	hour	h	Kelvin	K
milli ( $10^{-3}$ )	m	minute	min	Celsius	$^{\circ}\text{C}$
micro ( $10^{-6}$ )	$\mu$	second	s		
nano ( $10^{-9}$ )	n	day	day		
pico ( $10^{-12}$ )	p	month	month		
femto ( $10^{-15}$ )	f	year	yr		
atto ( $10^{-18}$ )	a				
<b>Units of volume</b>		<b>Units of length</b>			
litre	L	metre	m		
millilitre	mL	centimetre	cm		
microlitres	$\mu\text{L}$	millimeter	mm		
		micrometer	$\mu\text{m}$		
		nanometer	nm		

Rates for back volumes are as follows. (Vols. 1, 7, 10, 31, 33 are out of print)						
Vol. 1 (1947)	to	Vol. 13 (1959)	=	₹ 100.00	US \$ 10.00	
Vol. 14 (1960)	to	Vol. 33 (1985)	=	₹ 75.00	US \$ 8.00	
Vol. 40 (1986)	to	Vol. 55 (2002)	=	₹ 200.00	US \$ 35.00	
Vol. 57 (2003)	to	Vol. 75 (2021)	=	₹ 1000.00	US \$140.00	

Journal Title is covered in *Biological Abstract*, *Review of Plant Pathology*, *Agricola Database*, *BIOSIS*, *CABS*, *Cambridge Scientific Abstracts*, *Current Literature in Plant Science*, and *Indian Science Abstract*.

*Journal of the Botanical Society of Bengal for June 2026 (Vol. 80 No. 1) was issued on 30 June, 2026.*

## Executive Council for the 89th session (2025-2028)

### President

Prabir Kumar Saha

### Vice-Presidents

Radhanath Mukhopadhyay  
Aloke Bhattacharjee

### Hony. Secretary

Santanu Paul

### Editor of Publication

Subir Bera

### Hony. Treasurer

Ashalata D'Rozario

### Business Manager

Madhab Naskar

### Librarian

Asis Kumar Pal

### Members of the Council

Biswanath Chakraborty  
Shyamal Kr Chakraborty  
Binay Chaubey  
Krishendu Acharya  
Sushovan Bera  
Sudha Gupta  
Dipak Kumar Paruya

Dipu Samanta  
Shreyasi Basak  
Amrita Pal Basak  
Amitava Nayak  
Anirban Chouini  
Biplab Bandyopadhyay (Co-opted)  
Rashmi Mukherjee (Co-opted)

### Form IV (See Rule 8)

1. Place of Publication : Kolkata
2. Periodicity of its Publication : Bi-annual (June and December)
3. Printer : Mrs. Shyamali Das  
Nationality : Indian  
Address : 2, P. C. Das Lane, Serampore, Hooghly,  
Pin - 712204
4. Publisher : Ashalata D'Rozario  
Nationality : Indian  
Address : Botanical Society of Bengal,  
Department of Botany, University of Calcutta,  
Kolkata 700019, India
5. Editor-in-Chief : Subir Bera  
Nationality : Indian  
Address : Botanical Society of Bengal,  
Department of Botany, University of Calcutta,  
Kolkata 700019, India
6. Names and address of individuals : Botanical Society of Bengal  
who own the newspapers and Partners  
or Shareholders holding more than one  
per cent of the total capital

I, Ashalata D'Rozario, hereby declare that the particulars given above are true to the best of my knowledge and belief.

June 30, 2026

Sd/ Ashalata D'Rozario  
Signature of Publisher

**JOURNAL OF THE BOTANICAL SOCIETY OF BENGAL**

*(The Journal follows suggestive parameters of UGC for peer reviewed journals; NAAS score : 3.02)*

**VOLUME 80 NUMBER 1, JUNE 2026**

**CONTENTS**

<b>EDITORIAL : Santanu Paul</b>	i
<b>REVIEW ARTICLE</b>	
<b>Kaushal Agarwal, Dhruvkumar H. Wankawala, Giridhar Raveendar, Sudha Gupta and Pranab Kumar Mondal : Microfluidics in plant science: emerging technologies and applications</b>	1
<b>FULL LENGTH ARTICLE</b>	
<b>Subodh Hansda, Sourav Gorai, Ankit Kumar Ghorai and Subrata Raha : Effect of vermicompost on growth and yield of four selected ornamental flowering plants in relation to its taxonomic significance</b>	16
<b>Mithu Biswas, Anusree Das, Srabanti Rana, Swastik Guha : Chitosan and Aloe leaf gel extract based composite biofilm production using bagasse - microcrystalline cellulose as reinforcement (West Bengal) for preservation of traditional knowledge</b>	31
<b>A. Banerjee, S. Maity, S. Roy, S. Chandra, B. Chatterjee and A.K. Mitra : Characterization of plant growth promoting bacteria from sugarcane Rhizosphere in Vidarbha Region, India</b>	46
<b>Arpita Swarnakar : Comparative effects of Arsenate (V) and Arsenite (III) on inducing oxidative stress and osmolyte accumulation in mungbean seedlings</b>	54
<b>Apurba Mahanti, Ashalata D'Rozario, Madhab Naskar, Subir Bera : Palynofloristic and palynofacies analyses of the Permian sediments of Pachwara coalfield, Rajmahal Basin, India: Implications for age, depositional environment and palaeoecology</b>	61
<b>SHORT COMMUNICATION</b>	
<b>Shramona Chaudhuri, Firdousi Rahaman, Camellia Nandi and Shuvadeep Majumdar : Conservation of <i>Androsace umbellata</i> (Primulaceae), a threatened species in plains of West Bengal</b>	75
<b>ERRATUM</b>	78
<b>TRIBUTE : Professor Subhendu Mukherji (1937-2026) by Asok K. Biswas</b>	79

---

**© BOTANICAL SOCIETY OF BENGAL**

Department of Botany, University of Calcutta,

Tarakanath Palit Siksha Prangan,

35, Ballygunge Circular Road, Kolkata 700 019, India

**Website: [www.botansocbengal.org](http://www.botansocbengal.org)**

**E-mail: [secbsbengal1935@gmail.com](mailto:secbsbengal1935@gmail.com)**

---